

Chemistry and Characterization of Coal Macerals

A C S S Y M P O S I U M S E R I E S **252**

Chemistry and Characterization of Coal Macerals

Randall E. Winans, EDITOR
Argonne National Laboratory

John C. Crelling, EDITOR
*Southern Illinois University
at Carbondale*

Based on a symposium sponsored by
the Division of Fuel Chemistry
at the 185th Meeting
of the American Chemical Society,
Seattle, Washington,
March 20–25, 1983



American Chemical Society, Washington, D.C. 1984



Library of Congress Cataloging in Publication Data

Chemistry and characterization of coal macerals.
(ACS symposium series, ISSN 0097-6156; 252)

Bibliography: p.
Includes indexes.

I. Maceral—Congresses.

I. Winans, Randall E., 1949- . II. Crelling, John
C. III. American Chemical Society. Division of Fuel
Chemistry. IV. Series.

TP325.C4416 1984 662.6'2 84-6260
ISBN 0-8412-0838-7

Copyright © 1984

American Chemical Society

All Rights Reserved. The appearance of the code at the bottom of the first page of each chapter in this volume indicates the copyright owner's consent that reprographic copies of the chapter may be made for personal or internal use or for the personal or internal use of specific clients. This consent is given on the condition, however, that the copier pay the stated per copy fee through the Copyright Clearance Center, Inc., 21 Congress Street, Salem, MA 01970, for copying beyond that permitted by Sections 107 or 108 of the U.S. Copyright Law. This consent does not extend to copying or transmission by any means—graphic or electronic—for any other purpose, such as for general distribution, for advertising or promotional purposes, for creating a new collective work, for resale, or for information storage and retrieval systems. The copying fee for each chapter is indicated in the code at the bottom of the first page of the chapter.

The citation of trade names and/or names of manufacturers in this publication is not to be construed as an endorsement or as approval by ACS of the commercial products or services referenced herein; nor should the mere reference herein to any drawing, specification, chemical process, or other data be regarded as a license or as a conveyance of any right or permission, to the holder, reader, or any other person or corporation, to manufacture, reproduce, use, or sell any patented invention or copyrighted work that may in any way be related thereto. Registered names, trademarks, etc., used in this publication, even without specific indication thereof, are not to be considered unprotected by law.

PRINTED IN THE UNITED STATES OF AMERICA

**American Chemical
Society Library**
1155 16th St., N.W.
Washington, D.C. 20036

ACS Symposium Series

M. Joan Comstock, *Series Editor*

Advisory Board

Robert Baker
U.S. Geological Survey

Martin L. Gorbaty
Exxon Research and Engineering Co.

Herbert D. Kaesz
University of California— Los Angeles

Rudolph J. Marcus
Office of Naval Research

Marvin Margoshes
Technicon Instruments Corporation

Donald E. Moreland
USDA, Agricultural Research Service

W. H. Norton
J. T. Baker Chemical Company

Robert Ory
USDA, Southern Regional
Research Center

Geoffrey D. Parfitt
Carnegie Mellon University

Theodore Provder
Glidden Coatings and Resins

James C. Randall
Phillips Petroleum Company

Charles N. Satterfield
Massachusetts Institute of Technology

Dennis Schuetzle
Ford Motor Company
Research Laboratory

Davis L. Temple, Jr.
Mead Johnson

Charles S. Tuesday
General Motors Research Laboratory

C. Grant Willson
IBM Research Department

FOREWORD

The ACS SYMPOSIUM SERIES was founded in 1974 to provide a medium for publishing symposia quickly in book form. The format of the Series parallels that of the continuing ADVANCES IN CHEMISTRY SERIES except that in order to save time the papers are not typeset but are reproduced as they are submitted by the authors in camera-ready form. Papers are reviewed under the supervision of the Editors with the assistance of the Series Advisory Board and are selected to maintain the integrity of the symposia; however, verbatim reproductions of previously published papers are not accepted. Both reviews and reports of research are acceptable since symposia may embrace both types of presentation.

PREFACE

COAL IS AN EXTREMELY COMPLEX, heterogeneous material that is difficult to characterize. It is a rock formed by geological processes and composed of a number of distinct organic substances called macerals and of lesser amounts of inorganic entities called minerals. Each coal maceral and mineral has a unique set of physical and chemical properties that contributes to the overall behavior of coal. Although much is known about the mineral properties of coal, surprisingly little is known about the properties of the individual macerals.

This volume covers a wide range of fundamental topics in coal maceral science that varies from the biological origin of macerals to their chemical reactivity. Several chapters report novel applications of instrumental techniques for maceral characterization. These new approaches include solid ^{13}C NMR, electron spin resonance, IR spectroscopy, fluorescence microscopy, and mass spectrometry. A recently developed method for maceral separation is also presented; many of the new instrumental approaches have been applied to macerals separated by this new method. The contributions in this volume present a sampling of the new directions being taken in the study of coal macerals to further our knowledge of coal petrology and coal chemistry.

RANDALL E. WINANS
Argonne National Laboratory

JOHN C. CRELLING
Southern Illinois University at Carbondale

January 23, 1984

Chemistry and Characterization of Coal Macerals: Overview

RANDALL E. WINANS

Chemistry Division, Argonne National Laboratory, Argonne, IL 60439

JOHN C. CRELLING

Department of Geology, Southern Illinois University at Carbondale, Carbondale, IL 62901

The Maceral Concept

All of the papers in this book deal with the chemistry and characterization of coal macerals and, as such, recognize the heterogeneous nature of coal. Coal is, in fact, a rock derived from a variety of plant materials which have undergone a variety of physical and chemical transformations. While a number of chemical studies of coal have found the concept of a single "coal molecule" useful, the papers in this book are aimed at characterizing in some way the various macromolecules that comprise the many kinds of coal macerals.

Although the heterogeneous nature of coal has long been recognized in microscopical studies, for example by White and Thiessen in 1913 (1) and in 1920 (2), the term "maceral" was introduced only in 1935 by Marie C. Stopes (3). In this paper (page 11) she says:

"I now propose the new word "Maceral" (from the Latin macerare, to macerate) as a distinctive and comprehensive word tallying with the word "mineral". Its derivation from the Latin word to "macerate" appears to make it peculiarly applicable to coal, for whatever the original nature of the coals, they now all consist of the macerated fragments of vegetation, accumulated under water."

The concept behind the word "macerals" is that the complex of biological units represented by a forest tree which crashed into a watery swamp and there partly decomposed and was macerated in the process of coal formation, did not in that process become uniform throughout but still retains delimited regions optically differing under the

microscope, which may or may not have different chemical formulae and properties. These organic units, composing the coal mass I proposed to call macerals, and they are the descriptive equivalent of the inorganic units composing rock masses and universally called minerals, and to which petrologists are well accustomed to give distinctive names."

The concept was well received and the term maceral is now recognized around the world. Today, many coal scientists, especially those outside of North America, regard coal macerals as the smallest microscopically recognizable unit present in a sample. However, in 1958 Spackman (4) presented a concept of macerals that is significantly different and more useful in the chemical aspects of coal science:

". . . macerals are organic substances, or optically homogeneous aggregates of organic substances, possessing distinctive physical and chemical properties, and occurring naturally in the sedimentary, metamorphic, and igneous materials of the earth."

The essence of this concept is that macerals are distinguished by their physical and chemical properties and not necessarily by their petrographic form; thus, even though two substances may be derived from the same kind of plant tissue, for example, cell wall material, and have a similar petrographic appearance, they would be different macerals if they had different chemical or physical properties.

Maceral Characterization

Two serious problems confront the coal scientist trying to characterize coal macerals. First, the macerals are very difficult to separate from the coal matrix and it is, therefore, rare to have a pure maceral concentrate to study. For this reason much of the maceral characterization has been done in situ with petrographic methods including reflectance and fluorescence analysis. The second problem is that coal is, in truth, a metamorphic rock; any given coal sample is part of a metamorphic (rank) series ranging from peat through lignite, sub-bituminous coal, bituminous coal, to anthracite. As the rank of coal increases, the physical and chemical properties of the coal change, and therefore, the various macerals change also. The nature of this change is poorly understood; for example, it may be a continuous change analogous to solid solution in minerals, or it may be discontinuous in some way. The inescapable constraint of the rank property of coal macerals is that in any

study of maceral properties, the coal rank must always be determined and included in maceral characterization. Even in studies of similar macerals in the same coal seam, variation in coal rank can occur and, therefore, cause differences in maceral properties.

Development of Petrographic Characterization

The development of the petrographic characterization of coal macerals closely followed the development of petrographic techniques. Some of the earliest petrographic characterization of coal macerals used mainly transmitted light techniques and examples can be found in the papers of Cady (5), Marshall (6), and Parks and O'Donnell (7). Although the technique of reflected light microscopy was also used elsewhere, it was developed and used extensively in Germany (8-10). Also, during the late 1940's Hoffmann and Jenkner (11) developed the use of optical reflectance measurements to characterize some coal macerals.

In the late 1950's and early 1960's the reflectance characterization of coal macerals was used with great success in carbonization studies. For example, it was shown by Spackman *et al.* (12) that the properties of the various coal macerals controlled the carbonization behavior of coal. Based on this work and that of Ammosov *et al.* (13) methods were developed to predict the carbonization properties of single coals and coal blends (14-17). These methods use a maceral point count analysis to give the maceral distribution and a reflectance analysis to characterize the thermal properties of the macerals.

The most recent petrographic method used to characterize coal macerals is quantitative fluorescence analysis. In this method the macerals are excited by incident ultraviolet light and the spectrum of the resulting fluorescent light is used to characterize the macerals. This technique has led to the discovery of new macerals (18), the quantitative discrimination between certain macerals in a given coal (19), and the correlation of the fluorescence properties of macerals to the rank, and technological properties of coal (20-22).

Previous Petrographic Characterization

As Stopes seems to have anticipated, a large number of macerals have been identified and named. All macerals, however, can be conveniently grouped into three major subdivisions - vitrinite, liptinite, and inertinite. The vitrinite group of macerals are derived from plant cell wall material (woody tissue) and usually make up 50-90% of most North American coals. Although there are a large number of named varieties of

vitronite macerals, it is interesting to note that most researchers studying the vitronite macerals divide them into two general groups. The terms telecollinite and desmocolinite are used in many cases to distinguish these two groups. Brown *et al.* (23) used the term vitronite A to separate a homogeneous higher reflectance variety from a duller, finely laminated, matrix variety (vitronite B). Taylor (24) used transmission electron microscopy (TEM) to show that at high magnification vitronite A was homogeneous while vitronite B contained inclusions of other macerals. Alpern (25) distinguished homocolinite and heterocolinite along the same lines. In carbonization studies Benedict *et al.* (26) found a less reactive variety, pseudovitronite, characterized by a higher reflectance and a more homogeneous nature than normal vitronite. Although the terms are not strictly synonymous, pseudovitronite, homocolinite, vitronite A, and telecollinite, have the coincident properties of higher reflectance, greater homogeneity, and lower carbonization reactivity than normal vitronite, heterocolinite, vitronite B, and desmocolinite. The appearance of pseudovitronite under reflected white light is shown in Figure 1A. It also should be noted that it is pseudovitronite that tends to occur in homogeneous vitreous layers in coal seams and, therefore, the material collected in the hand picking of these layers tends to be pseudovitronite and not, in fact, the more abundant normal vitronite.

The liptinite group of macerals is derived from the resinous and waxy parts of plants such as resin, spores, and pollen. This group makes up 5-15% of most North American coals and is the most aliphatic and hydrogen rich group of macerals. The most common varieties of liptinite macerals are sporinite, cutinite, and resinite. Sporinite is usually the most abundant variety and the study of sporinite in coal and other rocks is the essence of the science of palynology in which the various sporinite morphologies are examined to discern both age and botanical relationships. A good collection of papers on sporinite is found in Sporopollenin (27). Cutinite is derived from cuticle, the waxy coating on leaves, roots, and stems. Cutinite is quite resistant to weathering and is sometimes concentrated as "paper coal" or "leaf coal" where it can be easily extracted and characterized. One such occurrence in Indiana has been studied by Neavel *et al.* (28-30).

The resinite macerals are in some ways the most varied group. They are derived from both the wound resins (terpenes) of plants and various other plant fats and waxes making up the lipid resins. The terpene-derived resinites are the most abundant type and they are found in most North American coals as ovoid masses. However, in some coals, especially in the western USA the resinite occurs mainly as a secondary form showing

evidence of having been mobilized (see Figure 1B). This form is of considerable interest because it can be commercially exploited and marketed as a chemical raw material (31,32). The occurrence and infrared spectral properties of various resinites have been well studied by Murchison and Jones (33-36). Teichmüller has reported on the origin and fluorescence properties of secondary resinites (20).

The inertinite group of macerals is derived from degraded woody tissue and usually makes up 5-40% of most North American coals, although in some western Canadian, and all southern hemisphere coals, it can make up a greater percentage. The inertinite macerals have the highest reflectance, as seen in Figure 1A and C, and carbon content in any given coal and are usually divided into five general types. Fusinite and semi-fusinite are characterized by well-defined cell texture with fusinite having the highest reflectance (see Figure 1D). Semi-fusinite is the most abundant inertinite maceral type and has the largest range of reflectance - between vitrinite and fusinite. Macrinite and semi-macrinite are similar in reflectance to fusinite and semi-fusinite, respectively, but without the presence of cell texture. The processes of both forest-fire charring and biochemical degradation (composting) have both been thought to be involved in the origin of all of these maceral types (37-39). The fifth inertinite variety, micrinite, is a granular high-reflectance material that may be both highly reactive and of secondary origin (18,40,41).

In the first half of this introductory chapter the maceral concept has been discussed and the main maceral groups and their important maceral types described. Emphasis has been placed on in situ characterization techniques which rely mostly on microscopy. The rest of this chapter will examine other techniques used for chemical characterization and examine the reactivity of coal macerals in thermal processes. The availability of separated maceral concentrates was a necessary component of the studies which will be described.

Separations

The preparation of maceral concentrates for study has been achieved by one of two approaches, either by hand picking or by a variety of techniques which exploit the variation in density between the various maceral groups. The first level of hand picking is the judicious sampling of lithotypes. This term is used to identify the various layers found in a coal seam. For humic coals there are four main designations of lithotypes: vitrain, clarain, durain, and fusain (42). Vitrain bands are sources of fairly pure vitrinite group macerals while fusinite and semi-fusinite can be obtained from fusain. These are the

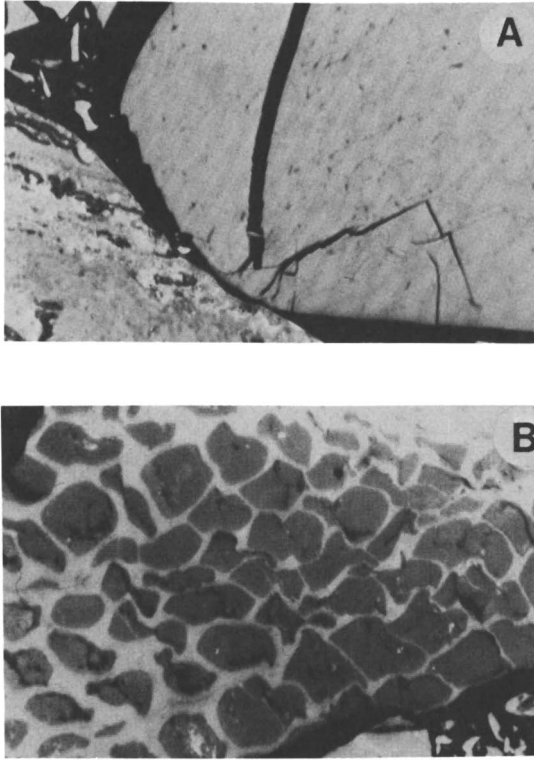
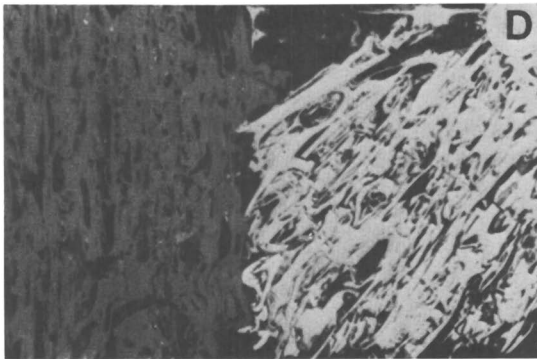
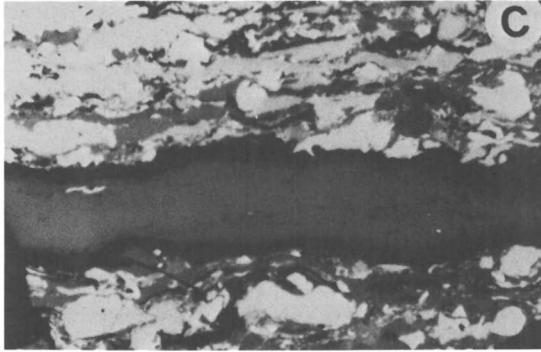


Figure 1. Photomicrographs of coal macerals from the Elkhorn No. 3 seam Eastern Kentucky - hvA bituminous rank. Reflected light in oil, diameter of field, 300 microns, crushed particle pellets.

- A. Large particle of pseudovitrinite at right showing serrated edges and well-developed cell texture. Particle at left is normal vitrinite with inclusions of sporinite (dark gray) and inertinite (white).
- B. Particles of vitrinite with cell-fillings of dark resinite.



- C. Particle made up of inertinite fragments in a vitrinite matrix with a zone of vitrinite running from left to right in the middle of the particle. Dark zones at boundaries of vitrinite are cutinite.
- D. Inertinite macerals, semi-fusinite at left and fusinite at right.

typical macerals which are concentrated by hand picking in addition to, in some cases, resinites (43). The other liptinites and the inertinite, micrinite, tend to be well dispersed among the other macerals which makes hand picking very difficult.

Due to the variation in chemical make up of coal macerals, their densities are different and this property has been exploited to produce maceral concentrates. Early studies in this area have been reviewed by Golouskin (44). Typically the macerals are fractionated by the float-sink technique using heavy liquids ranging in density from 1.2-1.5 g/cc. Kröger and coworkers (45) used mixtures of CCl_4 -toluene to fractionate each of four Ruhr coals into three groups. They found that liptinites fell in the range $\rho=1.20-1.25$, vitrinites $\rho=1.30-1.35$ and inertinites which they claimed were mostly micrinite $\rho=1.40-1.45$. A problem with using CCl_4 is that it cannot be completely removed from the maceral fractions after separation (46). Also, a portion of the coal can be solubilized in these solvent mixtures. Others have used aqueous salt solutions. An example is the technique used by van Krevelen and coworkers where coals crushed to $\sim 10 \mu\text{m}$ were fractionated in aqueous ZnCl_2 (47). A problem with aqueous solutions is the tendency for coal particles to agglomerate, a tendency that increases as the size of the particles decreases. Polar solvents have been added to the aqueous solutions to disperse the coal particles. Normally, the float-sink method is accelerated by centrifuging the solutions. Kröger developed a continuous flow centrifugation method for maceral group separation (45). Flotation methods for maceral separation have up to now yielded limited results, however, in one study it has been found that exinites could be concentrated (48).

Recently, a new approach for exploiting the density variation in macerals to achieve separation has been developed. Dyrkacz and coworkers (49,50) have applied density gradient centrifugation (DGC) to divide coals into narrow density fractions which can yield maceral concentrates of very high purity. The multi-step technique requires a two-stage grinding procedure to produce a fairly uniform particle size distribution of 3 microns, first by ball milling and second by grinding with high-velocity nitrogen gas in a fluid-energy mill. Next, the coal is demineralized by HCl and HF under nitrogen and finally separated in an aqueous CsCl_2 gradient with a non-ionic surfactant to disperse the particles. Demineralization has been found to be necessary to achieve high-resolution separations. In the past, it was thought that 3 micron particles were too small for petrographic identification. Dyrkacz has shown that although difficult, it is possible to distinguish the three main groups especially with the use of fluorescence microscopy for the liptinites. In fact, sporinite and alginite can be separated

with the DGC technique and distinguished petrographically (50). Five of the chapters in this book describe studies of macerals concentrated by this technique.

Two other sets of separated macerals have been studied fairly extensively including the samples prepared by Fenton and Smith (51) which have been termed the "British Macerals" and more recently a set obtained by Allan (52) separated by either hand picking or by a modified van Krevelen method (47). Characterization of these samples will be described in the next section.

Characterization

Early studies on separated macerals were done by Kröger (45,48,53-58), van Krevelen (47,59), and Given (60,61). Kröger and coworkers characterized their set of macerals from composition parameters (53), heats of wetting (54), pyrolysis (55,56) x-ray diffraction (57) and by process behavior such as carbonization (53,58). In a single paper, Dormans, Huntjens, and van Krevelen presented a significant amount of information on their set of macerals which is further discussed in van Krevelen's book (59). They proposed a method of presenting elemental analysis data which is now referred to as a van Krevelen plot and used extensively by organic geochemists. An example of such a plot is shown in Figure 2 with the typical distribution for the three main maceral groups. The plot shows the differences between macerals, the variation within macerals and the changes in their composition with increasing coalification.

Given and coworkers studying the "British Macerals" took more of an organic chemist's approach to characterization. The macerals were subjected to solvent extraction, lithium reduction, hydroxyl determination, oxidation, and reaction with various reagents. N-bromosuccinimide (NBS) was used to brominate aliphatic carbons which in the case for four macerals from an Aldwarke Silkstone coal yielded per 100 carbon atoms the following distribution of hydrogen which is replaced by bromine (61): vitrinite 16, exinite 25 1/2, micrinite 12, and fusinite 6. These values were similar to those obtained by the catalytic dehydrogenation (62) of hvA bituminous coal macerals which yielded in atoms of hydrogen per 100 carbons: vitrinite 25, exinite 31, micrinite 18, and fusinite 5. Such results would suggest that vitrinites and exinites should be more reactive in thermal processes and indeed this has been found to be true and will be discussed in the section on reactivity.

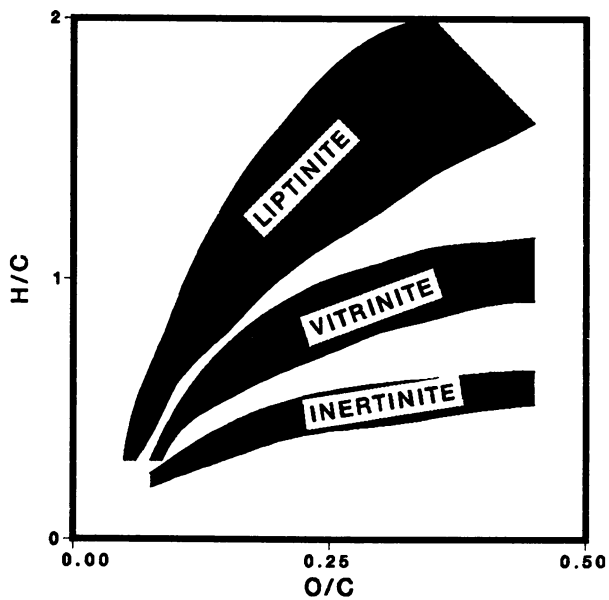


Figure 2. A van Krevelen plot showing approximate bands for the three main maceral groups.

Given determined hydroxyl groups in the separated macerals by acetylation (60,61). Acidic hydroxyl group abundance decreased from vitrinite > exinite > fusinite. The percentages of oxygen as OH in fusinites were low, averaging about 12% and were independent of rank. Both vitrinite and exinite hydroxyl content decrease with rank after passing through a maximum. Kröger and Bürger (63) presented data which differ from that reported by Given perhaps because of variations in the samples.

Aromaticity. One characteristic that describes coal macerals which has received much attention is the fraction of aromatic carbons (f_a). In an early study, van Krevelen used a densimetric technique to estimate the f_a values for a series of macerals (47). In general, the f_a values were found to increase from liptinite < vitrinite < inertinite for any given coal. Using broad line proton NMR Ladner and Stacey estimated hydrogen distributions and f_a 's for a set of "British Macerals" (64). Again, the data indicated that liptinites and vitrinites contain a significant amount of hydroaromatics. Broad line NMR data on ill-defined "dull coal" macerals have been reported (65).

The advent of solid ^{13}C NMR has resulted in an increased interest in this area. Retcofsky and Vanderhart (66) report f_a values for macerals from a Hernshaw hvA bituminous coal using cross polarization (CP). Zilm et al. (67) used a combination of CP and magic angle spinning (MAS) to examine some of Allan's macerals. Analyses of the Hernshaw samples have been repeated using CP/MAS (68) and in the paper the authors concluded that macerals although more homogenous than whole coals, are still quite complex. Recently the f_a values of macerals separated by density gradient centrifugation have been reported (69,70). Selected values from these studies are presented in Table I. The general trend first noted by van Krevelen is evident, but total agreement between different studies is not evident. The variation may be due to the techniques used or to variations in samples.

Free Radicals in Macerals. Electron spin resonance (ESR) has been used to study carbon free radicals in coals, and to some extent, separated macerals. The technique provides information on radical density and the environment of the radicals. The resonance position, termed the g-value, is dependent on the structure of the molecule which contains the free electron. The line width is also sensitive to the environment of the unpaired electron. In an early study, Kröger (71) reported that the spin concentration varied between maceral groups with liptinite < vitrinite << inertinite. For this limited set of samples the spin concentration increases with rank for liptinites and vitrinites and decreases for the micrinite samples. On the other hand, van Krevelen (72) found the same general results except

Table I. Aromaticities (f_a) of Separated Macerals

Maceral Group	Maceral	Sample	%C	Technique	f_a	Ref.	
Inertinite	Micrinite	Average	87.2	Densimetric	0.92	47	
	"	Hernshaw	85.9	CP	0.85	66	
	"	"	85.9	CP/MAS	0.78	68	
	Fusinite	"	91.5	CP	0.94	66	
	"	"	91.5	CP/MAS	0.92	68	
	"	Markham Main	91.6	CP/MAS	0.82	70	
	"	"	91.6	Broadline H NMR	0.92	64	
	"	Ohio No. 5	80.2	CP/MAS	0.75	69	
	Liptinite	"	Average	85.7	Densimetric	0.73	47
		"	Hernshaw	86.2	CP	0.66	66
"		"	86.2	CP/MAS	0.67	68	
"		Markham Main	82.6	CP/MAS	0.45	70	
"		"	82.6	Broadline H NMR	0.46	64	
"		Ohio No. 5	80.2	CP/MAS	0.45	69	
"		"	81.6	CP/MAS	0.18	69	
"		Silkstone	87.1	CP/MAS	0.51	67	
"		Torbane Hill	82.8	CP/MAS	0.13	67	
Vitrinite		"	Average	85.0	Densimetric	0.85	47
	"	Hernshaw	85.2	CP	0.85	66	
	"	"	85.2	CP/MAS	0.78	68	
	"	Markham Main	82.6	CP/MAS	0.76	70	
	"	"	82.6	Broadline H NMR	0.61	64	
	"	Ohio No. 5	78.4	CP/MAS	0.68	69	
"	Silkstone	86.6	CP/MAS	0.66	67		

that spin density for micrinities increased with rank. It is possible that the macerals termed micrinite in these studies were actually other low reflectance inertinites. In later studies, it was shown that at least for the inertinite, fusinite, spin concentration is fairly independent of rank (73,74). Austen *et al.* (73) found that vitrinites and liptinites exhibited similar esr linewidths which were rank dependent and decreased in samples with a carbon content greater than ~82%, while fusinite had narrower linewidths which were rank independent. Upon pyrolysis, the free spin concentration for vitrain increased while their linewidths decreased. Furthermore little change was observed for fusains up to about 650°C. These results have been recently confirmed (75). The authors concluded that fusinites are formed prior to incorporation into the sediment (73). Retcofsky (74) found higher g-values for lower rank vitrains which is probably due to the heteroatom content which decreases with increasing rank.

Organic Structural Analysis. Several approaches have been taken to obtain more detailed information on the variation of organic structures found in macerals. A widely used technique is pyrolysis (Py) combined with either gas chromatography (GC), mass spectrometry (MS) or GCMS. Another method which has been used extensively with whole coals and only to a limited extent with coal macerals is selective oxidative degradation. Recent studies include a series of papers by Allan (52). GC was used to examine the variations in hydrocarbon distributions between extracts of vitrinites and sporinites of various ranks (76,77) and alginites (78) and Py-GCMS to characterize all three sets of whole macerals (79). Triterpanes were found in all the extracts and it is interesting to note that the amount of n-alkanes for vitrinites and sporinites increased with rank. n-Alkanes were more abundant in the sporinites and were longer in chain length (77). Larter and Douglas (79) demonstrated that Py-GCMS has potential as a chemical fingerprinting method for coal macerals. More recently, Allan and Larter (80) have proposed that similarities observed for sporinite and vitrinites of the same rank may be due to "different molecular combinations of similar unit structures". Recently, Philp and Saxby have characterized a set of Australian macerals by Curie-point Py-GCMS (81).

Another rapid technique for characterizing non-volatile materials which has been applied to coal macerals is pyrolysis mass spectrometry (Py-MS) (82-84). The evaluation of the complex data produced by this technique has been aided by the use of statistical analysis. Homologous series of molecules can be identified and variation between the various maceral groups is quite evident.

Direct Characterization Techniques. The in situ analysis of elemental composition of coals by ion microprobe was first demonstrated by Dutcher et al. (85). Raymond (86) has applied this technique to examine the variation in composition of coal macerals which has been especially effective for looking at sulfur distribution. An example of the organic sulfur distribution for two bituminous coals is shown in Table II which is taken from reference (86). Note that the liptinites contain the

Table II. Distribution of Organic Sulfur in Bituminous Coal Macerals (86)

<u>U. Elkhorn hvAb Coal</u>								
	V	Pv	F	Sf	Ma	Mi	S	R
wt% of sample	38.9	2.2	7.1	5.3	13.2	13.3	17.6	2.4
wt% S ₀	0.73	0.45	0.30	0.38	0.64	0.60	0.94	1.03
<u>Ohio #4 hvBb Coal</u>								
	V	Pv	F	Sf	Ma	Mi	S	
wt% of sample	72.0	3.0	3.9	5.7	0.3	7.8	7.3	
wt% S ₀	2.93	2.56	0.73	1.51	0.92	2.90	3.89	

(All wt% on dmmf basis) V = vitrinite, Pv = pseudovitrinite, F = fusinite, Sf = semi-fusinite, Ma = macrinite, Mi = micrinite, S = sporinite, R = resinite.

greatest concentration of sulfur while the fusinites and semi-fusinites have the least amount. Also, Raymond has found that typically the sulfur content in vitrinite is close to the average value for whole coal even when vitrinite is not the major component. An initial study on the use of secondary ion mass spectrometry (SIMS) to analyze macerals has been reported (87) and appears to have potential as a characterization technique. The classic IR paper on coal macerals was published by Bent and Brown (88). They examined the variation in aliphatic and aromatic hydrocarbons for a set of the "British Macerals". In the conclusions they noted that the differences between "exinite" and vitrinite is in the "degree of aromaticity rather than of kind" and that with increasing rank this difference disappears.

Reactivity of Macerals in Conversion Processes

The behavior of coal macerals in processes other than coking has received limited attention. Neavel (89) reviewed some of the important work in relation to coal coking gasification, combustion, and pyrolysis. The reactivity of macerals in liquefaction has recently received more attention. Early work was done at the U.S. Bureau of Mines and has been reviewed by Davis *et al.* (90) and Given *et al.* (91). In these reviews, the authors noted that there is a difficulty in comparing this early work to recent studies due to the difference in how the macerals are identified. However, this early work does indicate that inertinites are less reactive in liquefaction. More recently, batch autoclave runs using tetralin as a solvent (90) demonstrated that vitrinites and exinites (sporinite and cutinite) are quite reactive. In two papers (91,92) it has been noted that Utah resinites are greatly solubilized. However, the question of actual resinite reactivity is still unclear since at least the Utah resinites tend to be naturally very soluble in organic solvents.

Liquefaction of inertinites is not always as poor as the name would imply. Table III shows some conversion data taken from Ref. (91), where conversion is defined as ethyl acetate solubles plus gases. The low reflecting Australian fusinites and semi-fusinites are reactive compared to the Illinois samples. This has been confirmed by a recent study on Australian inertinites (93) where it has been found that at higher temperatures (450°C) up to 54% of the inertinite was calculated to be converted. This difference between the Australian and North American inertinites has also been observed in carbonization reactions (94).

Product characterization from liquefaction has not been extensive. Philp and Russell (95) have examined products by Py-GCMS from metal halide catalyzed hydrogenation of a vitrinite, alginite, and inertinite, each from a different source. They were able to correlate Py-GCMS results with reaction temperature. King, *et al.* (96) examined the short contact time liquefaction of macerals separated by DGC from a single hvB bituminous coal. They found correlations between density and reactivity and composition of the products.

Conclusions

This introduction is intended to highlight the past research on coal macerals which has led to many of the studies presented in this book. Coal science is a very complex field, but it is important to recognize that the study of macerals

either in situ or after separation is a big step in the direction of reducing the complexity of the science.

Acknowledgments

R.E.W. acknowledges the support of the Office of Basic Energy Sciences, Division of Chemical Sciences, U.S. Department of Energy under contract W-31-109-ENG-38. J.C.C. would like to acknowledge support by the Gas Research Institute.

Table III. Liquefaction of Fusinite and Semi-Fusinite (91)

	Maceral Per Cent				$R_{0\max}$ (F+SF)	Conversion % daf
	V	F	SF	I		
PSOC 303 Callide Seam Australia	15	4	73	3	1.26	40
PSOC 304 Big seam Australia	31	14	44	9	1.49	41
PSOC 261, Fusain Illinois No. 6	21	65	12	2	3.50	25
PSOC 261A, Fusain Illinois No. 6	17	68	14	0	3.52	15
PSOC 262, Fusain Illinois No. 6 Williamson Co., IL	16	69	14	0	4.18	21
PSOC 263, Fusain Illinois No. 6 Peoria Co., IL	8	48	44	0	3.05	13.5
PSOC 264, Fusain Colchester No. 2 Fulton Co., IL	10	62	27	0	4.23	12

V = vitrinite; F = fusinite; SF = semi-fusinite; I = other inertinites $R_{0\max}$ = reflectance.

Literature Cited

1. White, D.; Thiessen, R. U.S. Bur. Mines Bull. No. 38 1913, 390 pp.

2. Thiessen, R. U.S. Bur. Mines Bull. No. 117 1920, 296 pp.
3. Stopes, Marie C. Fuel 1935, 14, 4-13.
4. Spackman, W. Trans N.Y. Acad. Sci. 1958, 20, No. 4, 411-423.
5. Cady, G.H. Jour. Geol. 1942, 50, 337-356.
6. Marshall, C.E. Econ. Geol. 1955, 50th Anniv. Vol. 757-834.
7. Parks, B.C.; O'Donnell, H.J. U.S. Bur. Mines Bull. No. 344 1956, 193 pp.
8. Stach, E. Lehrbuch der Kohlenmikroskopie Gluckauf, Kettwig, 1949, 285 pp.
9. Abramski, C.; Mackowsky, M.T.; Mantel, W.; and Stach, E. "Atlas für Angewandte Steinkohlenpetrographie"; Gluckauf:Essen 1951, 329 pp.
10. Freund, H. "Handbuch der Mikroskopie in der Technik"; Umschau Verlag:Frankfurt am Main, 2, 1952, 759 pp.
11. Hoffmann, E.; Jenkner, A. Gluckauf 1932, 68, 81-88.
12. Spackman, W.; Berry, W.F.; Dutcher, R.R.; Brisse, A.H. Yearbook Am. Iron and Steel Inst. 1960, 403-449.
13. Ammosov, I.I.; Eremin, I.V.; Sukhenko, S.F.; and Oshurkova, L.S. Koks i Khim 1957, 12, 9-12.
14. Schapiro, W.; Gray, R.J.; Eusner, G.R. Blast Furnace, Coke Oven, and Raw Materials Proc., A.I.M.E. 1961, 20, 89-112.
15. Schapiro, N.; Gray, R.J. Fuel 1964, 11, 234-242.
16. Benedict, L.G.; Thompson, R.R.; Wenger, R.O. Blast Furnace and Steel Plant 1968, 56, 217.
17. Benedict, L.G.; Thompson, R.R. Ironmaking Proc. A.I.M.E. 1976, 35, 276-288.
18. Teichmüller, M. Fortschr. Geol. Rheinld. u. Westf. 1974, 24, 37-64.
19. Crelling, J.C. Jour. Microscopy 1983, 132, pt. 3, 251-266.
20. Teichmüller, M. Fortschr. Geol. Rheinld u. Westf. 1974, 24, 65-112.
21. Ottenjann, K.; Teichmüller, M.; Wolf, M. in "Petrographic Organique et Potential Petrolier"; Alpern, B., Ed.; C.N.R.S.:Paris, 1975, 49-65.
22. Teichmüller, M.; Durand, B. Int. Jour. Coal. Geol. 1983, 2, 197-230.
23. Brown, H.R.; Cook, A.C.; Taylor, G.H. Fuel 1964, 43, 111-124.
24. Taylor, G.H. in "Coal Science"; Given, P.H.; Advances in Chemistry Series 55, Am. Chem. Soc.:Washington, D.C., 1966, 274-283.
25. Alpern, B. in "Adv. Org. Geochem. 1964"; Pergamon Press:Oxford, 1966, 129-145.
26. Benedict, L.G.; Thompson, R.R.; Shigo, J.J.; Aikman, R.P. Fuel 1968, 47, 125-143.
27. Brooks, J.; Grant, P.R.; Muir, M.D.; van Gijzel, P.; Shaw, G. "Sporopollenin"; Academic Press:New York, 1971; 718 pp.
28. Guennel, G.K.; Neavel, R.C. Science 1959, 129, 1671-1672.

29. Neavel, R.C.; Guannel, G.K. Jour. Sed. Pet. 1960, 30, 241-248.
30. Neavel, R.C.; Miller, L.V. Fuel 1960, 39, 217-222.
31. White, D. U.S. Geol. Sur. Prof. Paper 85-E. 1914, 65-96.
32. Crelling, J.C.; Dutcher, R.R.; Lange, R.V. Utah Geol. and Min. Sur. Bull. 118 1982, 187-191.
33. Jones, J.M.; Murchison, D.G. Econ. Geol. 1963, 58, 263-273.
34. Murchison, D.G., and Jones, J.M. in "Adv. in Organic Geochem. 1962"; Pergamon Press:London, 1964; 1-21.
35. Murchison, D.G.; Jones, J.M. in "Coal Science"; Given, P.H.; Advances in Chemistry Series No. 55, American Chemical Society:Washington, D.C., 1966; 307-331.
36. Murchison, D.G. Fuel 1976, 55, 79-83.
37. Marshall, C.E. Fuel 1954, 33, 134-144.
38. Skolnick, H. Bull. A.A.P.G. 1958, 42, 2223-2236.
39. Nandi, B.N.; Montgomery, D.S. Fuel 1975, 54, 193-196.
40. McCartney, J.T. Fuel 1970, 59, 409-414.
41. Shibaoka, M. Fuel 1978, 57, 73-77.
42. Stach, E. in "Textbook of Coal Petrology" 3rd Ed; Stach, E. Ed.; Gebruder Borntraeger:Berlin, 1982; p. 172.
43. Murchison, D.G.; Jones, J.M. Fuel 1963, 42, 141.
44. Golouskin, N.S. J. Appl. Chem. USSR 1959, 32, 2016.
45. Kröger, C.; Pohl, A.; Kuthe, F. Gluckauf 1957, 93, 122.
46. Horton, L. Fuel 1952, 31, 341.
47. Dormans, H.N.M.; Huntjens, F.J.; van Krevelen, D.W. Fuel 1957, 36, 321.
48. Kröger, C.; Bade, E. Gluckauf 1960, 96, 741.
49. Dyrkacz, G.R.; Bloomquist, C.A.A.; Horwitz, E.P. Sep. Sci. Technol. 1981, 16, 1571.
50. Dyrkacz, G.R.; Horwitz, E.P. Fuel 1982, 61, 3.
51. Fenton, G.W.; Smith, A.K. Gas World 1959, 54, 81.
52. Allan, J. Ph.D. Thesis U. of Newcastle, England, 1975.
53. Kröger, C.; Pohl, A.; Kuthe, Fr.; Hovesatadt, H.; Burger, H. Brennstoff-Chem. 1957, 38, 33.
54. Kröger, C.; Bukenecker, J. Brennstoff-Chem. 1957, 38, 82.
55. Kröger, C.; Pohl, A. Brennstoff-Chem. 1957, 38, 102.
56. Kröger, C.; Bruecker, R. Brennstoff-Chem. 1961, 42, 305.
57. Kröger, C.; Ruland, W. Brennstoff-Chem. 1958, 39, 1.
58. Kröger, C.; Gondermann, H. Brennstoff-Chem. 1957, 38, 231.
59. van Krevelen, D.W. "Coal"; Elsevier:Amsterdam, 1961.
60. Given, P.H.; Peover, M.E.; Wyss, W.F. Fuel 1960, 39, 323.
61. Given, P.H.; Peover, M.E.; Wyss, W.F. Fuel 1965, 44, 425.
62. Reggel, L.; Wender, I.; Raymond, R. Fuel 1970, 49, 281.
63. Kröger, C.; Burger, H. Brennstoff-Chem. 1959, 40, 76.
64. Ladner, W.R.; Stacey, A.E. Fuel 1963, 42, 75.
65. Tschamler, H.; DeRuiter, E. in "Coal Science"; Given, P.H., Ed.; Adv. in Chem. Series No. 55, American Chemical Society:Washington, D.C., 1966, p. 332.
66. Retcofsky, H.L.; Vanderhart, D.L. Fuel 1978, 57, 421.

67. Zilm, K.W.; Pugmire, R.J.; Larter, S.R.; Allan, J.; Grant, D.M. Fuel 1981, 60, 717.
68. Maciel, G.E.; Sullivan, M.J.; Petrakis, L.; Grandy, D.W. Fuel 1982, 61, 411.
69. Pugmire, R.J.; Zilm, K.W.; Woolfenden, W.R.; Grant, D.M.; Dyrkacz, G.R.; Bloomquist, C.A.A.; Horwitz, E.P. Org. Geochem. 1982, 4, 79.
70. Pugmire, R.J.; Woolfenden, W.R.; Mayne, C.L.; Karas, J.; Grant, D.M. This Volume, Chapter 6.
71. Kröger, C. Brenstoff-Chem. 1958, 39, 62.
72. Ref. (59), p. 395
73. Austen, D.E.G.; Ingram, D.J.E.; Given, P.H.; Binder, C.R.; Hill, L.W. in "Coal Science"; Given, P.H., Ed.; Adv. in Chem. Series No. 55, American Chemical Society:Washington, D.C. 1966; p. 344.
74. Retcofsky, H.L.; Thompson, G.P.; Hough, M.; Friedel, R.A. in "Organic Chemistry of Coal"; Larsen, J.W., Ed.; Symp. Series No. 71, American Chemical Society:Washington, D.C., 1978; p. 142.
75. Petrakis, L.; Grandy, D.W. Fuel 1981, 60, 115.
76. Allan, J.; Bjørøy, M.; Douglas, A.G. in "Advances in Organic Geochemistry 1975"; Campos, R.; Goni, J., Eds.; Pergamon:Oxford, 1977, p. 633.
77. Allan, J.; Douglas, A.G. Geochim. Cosmochim. Acta 1977, 41, 1223.
78. Allan, J.; Bjørøy, M.; Douglas, A.G. in "Advances in Organic Geochemistry 1979"; Douglas, A.G.; Maxwell, J.R., Eds.; Pergamon:Oxford, 1980; p. 599.
79. Larter, S.; Douglas, A.G. in "Environmental Biogeochemistry and Geomicrobiology"; Krumbein, W.E., Ed.; Ann Arbor: 1978; Vol. 1 p. 373.
80. Allan, J.; Larter, S.R. "Advances in Organic Geochemistry 1981"; Bjørøy, M., Ed., Pergamon:Oxford, 1983, p. 534.
81. Philp, R.P.; Saxby, J.D. "Advances in Organic Geochemistry 1979"; Douglas, A.G.,; Maxwell, J.R., Eds.; Pergamon:Oxford 1981; p. 639.
82. van Graas, G.; de Leeuw, J.W.; Schenck, P.A. in "Advances in Organic Geochemistry 1979"; Douglas, A.G.; Maxwell, J.R., Eds.; Pergamon Press:Oxford 1980, p. 485.
83. Winans, R.E.; Dyrkacz, G.R.; McBeth, R.L.; Scott, R.G.; Hayatsu, R. Proceedings Inter. Conf. Coal Sci. 1981 p. 22.
84. Meuzelaar, H.L.C.; Harper, A.M.; Pugmire, R.J. Preprint Div. of Fuel Chemistry, ACS 1983, 28(1), 97.
85. Dutcher, R.R.; White, E.W.; Spackman, W. Proc. 22nd Iron-making Conf., Iron and Steel Div., Metall. Soc. AIME, N.Y. 1964, 463.
86. Raymond, R. in "Coal and Coal Products: Analytical Characterization Techniques"; Fuller, E.L., Ed.; ACS Symposium Series No. 205, American Chemical Society:Washington, D.C., 1982; p. 191.

87. Wolf, M.; Migeon, H.N.; Butterworth, M.; Gaines, A.F.; Owen, N.; Page, F.M. Int. J. Mass Spectrom. Ion Phys. 1983, 46, 487.
88. Bent, R.; Brown, J.K. Fuel 1961, 40, 47.
89. Neavel, R.C. in "Chemistry of Coal Utilization, 2nd Suppl. Vol."; Elliot, M.A., Ed.; Wiley:N.Y. 1981, p. 91.
90. Davis, A.; Spackman, W.; Given, P.H. Energy Sources 1976, 3(1), 55.
91. Given, P.H.; Spackman, W.; Davis, A.; Jenkins, R.G. in "Coal Liquefaction Fundamentals"; Whitehurst, D.D., Ed.; ACS Symp. Series No. 139, American Chemical Society:Washington, D.C., 1980; pp. 3-34.
92. Petrakis, L.; Grandy, D.W. Fuel 1981, 60, 120.
93. Heng, S.; Shibaoka, M. Fuel 1983, 62, 610.
94. Diessel, C.F.K. Fuel 1983, 62, 883.
95. Philp, R.D.; Russell, N.J. in "Advances in Organic Geochemistry 1979"; Douglas, A.G.; Maxwell, J.R., Eds.; Pergamon:Oxford 1981; p. 653.
96. King, H.H.; Dyrkacz, G.R.; Winans, R.E. Fuel (in press).

RECEIVED January 23, 1984

Premaceral Contents of Peats Correlated with Proximate and Ultimate Analyses

A. D. COHEN and M. J. ANDREJKO¹

Earth and Space Sciences Division, MS D462, Los Alamos National Laboratory, Los Alamos, NM 87545

Proportions of premacerals and botanical constituents composing selected peat samples from Minnesota, Maine, North Carolina, and Georgia were determined by microscopic analysis of oriented microtome thin sections. These results were compared with proximate and ultimate analyses of the same samples. Peats with the highest proportions of birefringent premacerals tended to have the highest volatile matter (and H, O, and N contents). Peats with a dominance of premacerals in the light yellow to red range tended to be higher in volatile matter (and lower in fixed carbon) than those with a significant component of brown to black ingredients (preinertinites). Volatile matter also tended to increase as root content increased and to decrease as stem content increased. On the other hand, BTU tended to correlate more with ash content than with premaceral composition.

In a number of publications, peat types have been defined petrographically by their botanical and "premaceral" compositions (1-4). "Premacerals" are the organic components in the peats which, due to their color, opacity, shape, and fluorescence, can be projected as the probable progenitors of particular corresponding macerals in coals. Although the petrographic characterization of peats constitutes an important "first step" in understanding the origin and in predicting the general composition of the resultant coals, it is important that premaceral types and amounts in peats be correlated with various coal-quality tests (such as "proximate" and "ultimate" analyses). With these results it then becomes possible to develop a series of models

¹Current address: Department of Geology, Washington State University, Pullman, WA 99164-2812

with which to predict more precisely the chemical and physical composition of the resulting theoretical coals. These predictive characterizations can be applied not only to the projected seam-wide variability in coal quality for coals produced in similar depositional settings as that of the studied peats, but also to the prediction of the variations in industrial properties of the peats themselves, such as for gasification, liquifaction, soil conditioning, organic chemical production and so forth.

It is for these reasons that we have initiated this correlative study of peat petrography and peat industrial-chemical (coal quality) properties. Note that the information reported herein represents preliminary results based on a limited number of different types of peats that were analyzed for only a few "coal quality tests" (i.e., proximate analysis, ultimate analysis, and BTU content). Future studies will involve measurement of other petrographic parameters and include other industrial analyses (such as, gas and liquid yields, physical properties, organic chemical yields, and so forth).

Objectives

The objectives of this study are to:

1. Determine the variations in premaceral types and proportions within a wide variety of peat types.
2. Correlate premaceral contents with corresponding proximate (fixed carbon, moisture, ash, volatile matter), ultimate (C, H, O, N, S) and heating value (BTU) analyses.
3. Predict the probable variations in the proximate and ultimate makeup and BTU levels for coals which formed in similar vegetational and depositional settings to those of the peats studied in this project.

Methods

Carefully extracted samples of peat were slowly dehydrated in a series of alcohol solutions and then embedded in paraffin. After embedding, thin-sections (15 microns in thickness) were cut from these samples with a sliding microtome and mounted in Canada Balsam. Details of the procedure for the embedding and sectioning of peats have previously been described by Cohen.^(2,3)

Premaceral identification was made in transmitted white light, in polarized light (birefringence) and blue light fluorescence. Premaceral proportions were determined by area point-counting at 200 X. Proximate and ultimate analyses and BTU were obtained from commercial testing laboratories and also from the Department of Energy's Energy Technology Center at Grand Forks, North Dakota.

Results and Discussion

Botanical Composition. Figure 1a shows the relative abundances of plant groups observed in microtome sections of the peats. Note that these peats varied considerably in their botanical compositions. The Minnesota peat consisted predominantly of Sphagnum (peat moss) debris with some grasses and conifers. The Maine peat was composed mostly of algal material with some Sphagnum and Nymphaea (water lily) debris. The North Carolina peat was dominated by bay tree (Magnolia, Persea, Gordonia) and gum tree (Nyssa) debris; while the Georgia Nymphaea peat consisted predominantly of Nymphaea debris.

Figure 1b shows the abundance of plant organs comprising the peat. Again the differences between peat types are pronounced. The Minnesota peat is dominated by roots but with lesser but equal amounts of stem and leaf debris. On the other hand, the Maine peat has the highest concentration of leaves; the North Carolina peat has the highest wood content (stems) and lowest leaf content, while the Georgia (Nymphaea) peat has the highest proportion of roots.

Premaceral Types and Proportions. One simplified but useful means of displaying petrographic composition of peats in thin section is by graphing the area percentages of ingredients of different colors. Figure 2 shows such a point-count for four representative types of peat from this study. Note that the Minnesota Sphagnum and Georgia Nymphaea peats have approximately the same range of colors (peaking between light-yellow and light-brown) but that the Maine peat peaked in the clear to light-yellow range while that of the North Carolina peat had peaks in the light-yellow to red-brown range and also in the dark-brown and black categories.

The Georgia Nymphaea and Minnesota Sphagnum peats tended to have the highest previtrinites while the North Carolina and Georgia Taxodium peat (not shown) had the highest prephlobaphenites (and precorcollinites) and also the highest preinertinites (premicrinites, prefusinites, and presclerotinites).

Figures 3 and 4 give the area percentages of birefringent premacerals found in the samples studied. Since birefringence has been equated with cellulose content, it might therefore be expected that birefringence would decrease with depth in a deposit as a result of cellulose decomposition. However, as can be seen in Figure 3 (representing two cores from the Okefenokee Swamp of Georgia), birefringence may increase or decrease with depth depending on successions of peat types and moisture conditions during initial deposition. Figure 4 shows that Georgia Nymphaea and Minnesota Sphagnum peats have the highest proportions of birefringent constituents.

The concentration of fluorescent premacerals tended to correlate slightly with the proportion of birefringent premacerals.

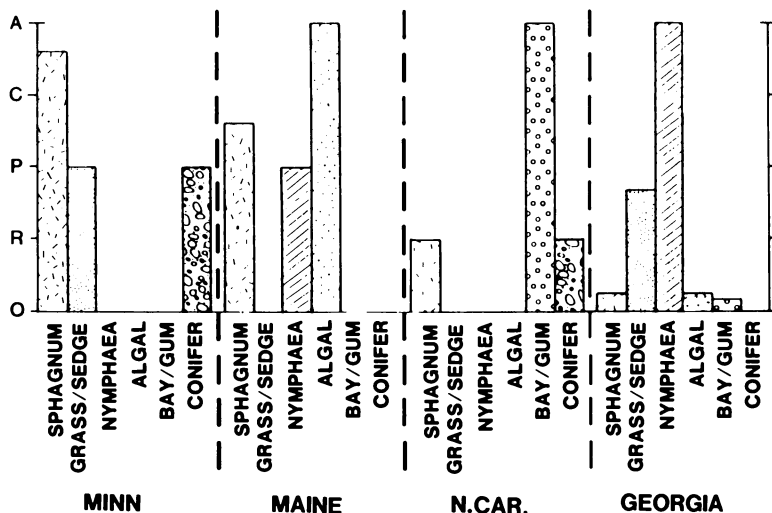


Figure 1a. Relative proportions of plant types identified from microtome sections of peats from Minnesota, Maine, North Carolina, and Georgia (A = abundant, C = common, P = present, R = rare, and O = absent).

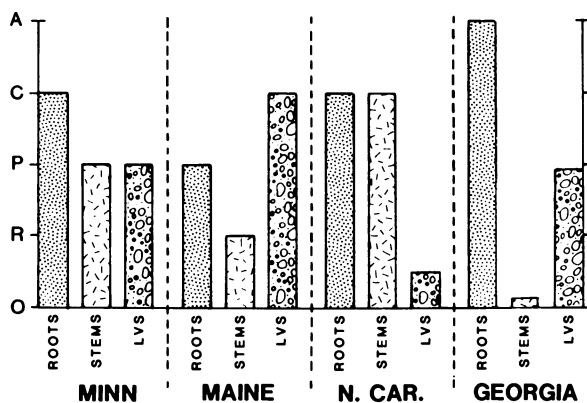


Figure 1b. Relative abundances of plant organs identified from microtome sections of peats from the same samples as in Figure 1a.

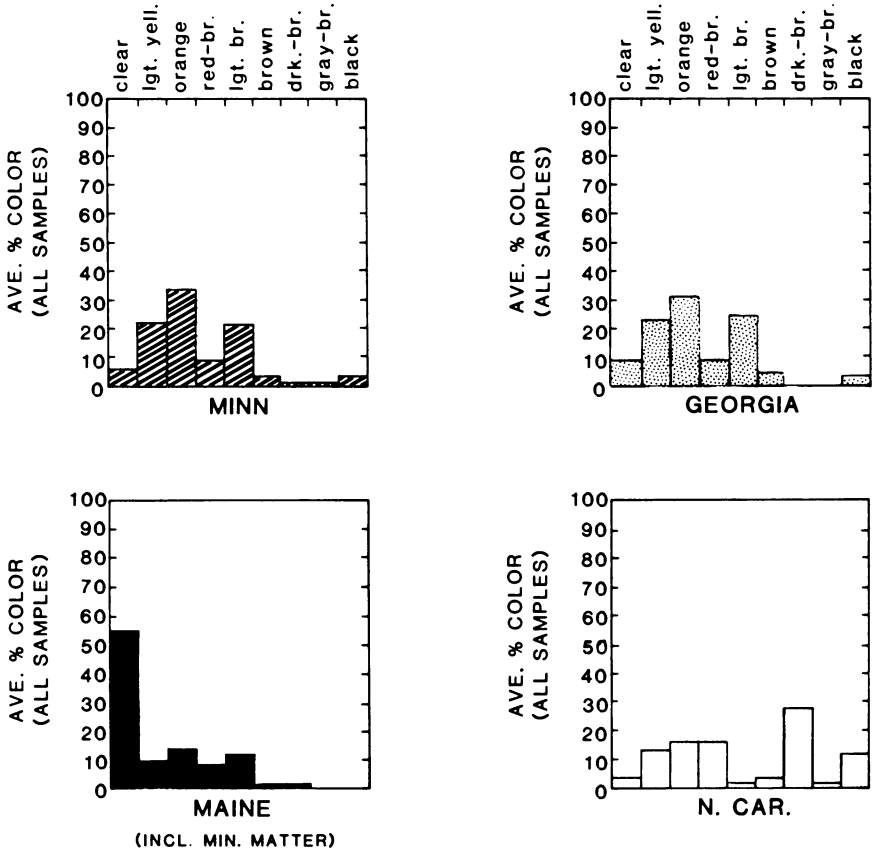


Figure 2. Color of all ingredients in the four peat types as determined by area point counts of microtome sections. (Average of three samples from each area)

Minnie's Lake Transect

Chesser Prairie Transect

STATION 41

STATION 6

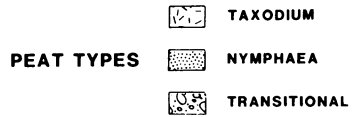
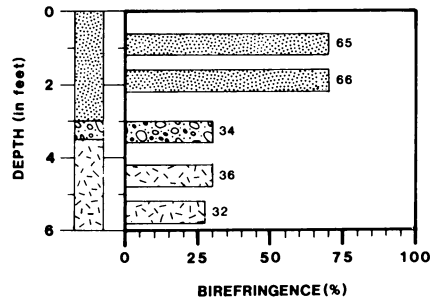
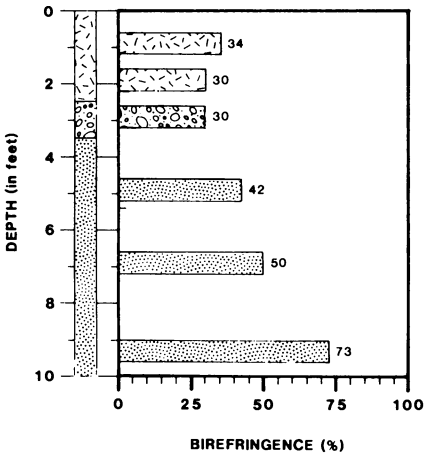


Figure 3. Percentage of birefringent organics compared with peat types in two cores from the Okefenokee Swamp.

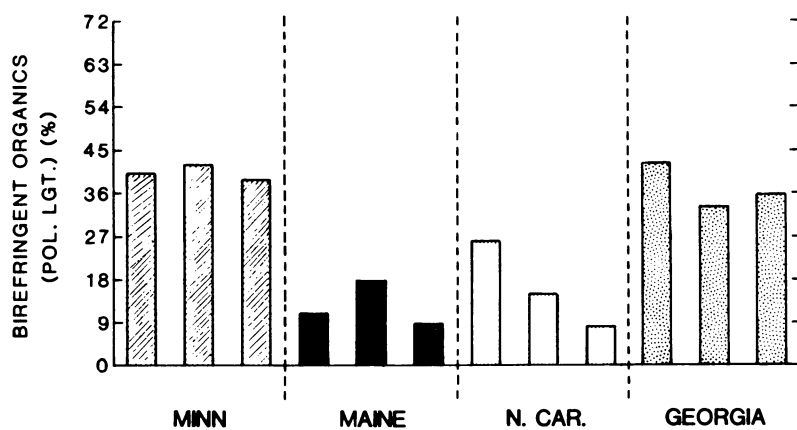


Figure 4. Percentage of birefringent organics in each of 3 samples of peat from Minnesota, Maine, North Carolina, and Georgia.

However, different plant types were found to produce different fluorescent colors and intensities. Furthermore, natural "staining" (i.e., darkening or coloring by natural impregnation or chemical alteration) of cell walls tended to effect birefringence and fluorescence in very different ways (Figures 5 and 6). Natural staining tended to correlate strongly with birefringence (i.e., the darker the staining the less the birefringence), but did not correlate well with overall fluorescence properties. For example, some tissues that were highly stained tended to have higher fluorescence intensities than those that were unstained (Figure 6).

Proximate and Ultimate Analyses and BTU. Figure 7 shows the results of proximate and ultimate analyses and BTU measurement. Note that the peat from North Carolina (a lower-coastal-plain, woody, dark, more inertinite-rich sample) had the highest fixed carbon, elemental carbon and sulfur content. Woody Taxodium peats from Georgia (not shown) and South Carolina (not shown) were similar in character to the North Carolina samples. The Georgia Nymphaea peats, which had the highest previtrinites, can be seen to have the highest oxygen, hydrogen, and volatile matter contents. Note that BTU values tended to correlate more strongly with ash contents than with maceral contents.

Summary and Conclusions

Preliminary correlations of petrographic characteristics of peats (i.e., peat types, premaceral proportions, and premaceral types) with proximate and ultimate analyses suggest the following trends:

1. Peats with the highest proportions of birefringent macerals tend to have the highest volatile matter (and H and O contents).
2. Fluorescence of macerals, on the other hand, seems to correlate only slightly with proximate and ultimate analyses.
3. Higher previtrinite contents (determined by color) tend to correlate with higher volatile matter contents.
4. Peats with higher preinertinites, prephlobaphenites (and pre-corpocollinites), and presclerotinites have the highest fixed carbon.
5. BTU correlates strongly with ash content and only slightly with maceral content.

Acknowledgments

This work was funded in part by Grant #EAR-79-26382 from the National Science Foundation and in part by funding from the Office of Basic Energy Sciences of the Department of Energy.

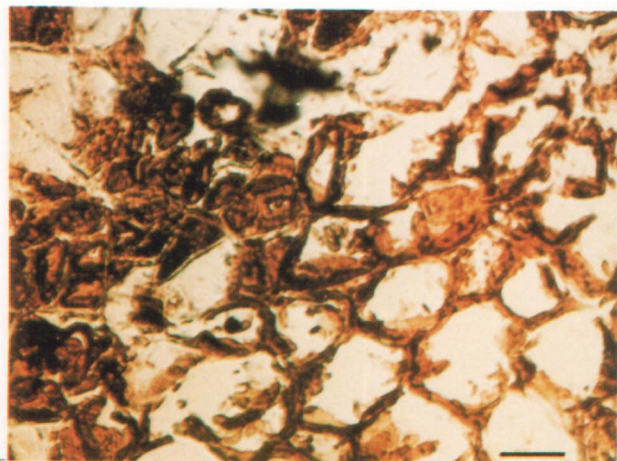


Figure 5a. Photomicrograph of a microtome section of peat in transmitted light. Note that the cell walls in the upper left half of the figure (even though filled with reddish-brown tanniferous material) are not as darkly stained as the cells in the lower right half of the figure. Scale bar equals 100 microns.



Figure 5b. Same view as 5a except under cross-polarized light to show birefringent ingredients. The less stained walls are the most birefringent.

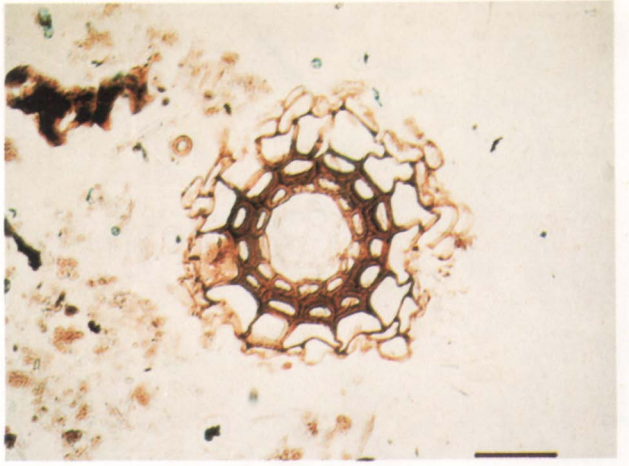


Figure 6a. Photomicrograph of a microtome section of peat showing a cross section of a naturally stained Woodwardia virginica (chain fern) rootlet (transmitted light). Scale bar equals 250 microns.

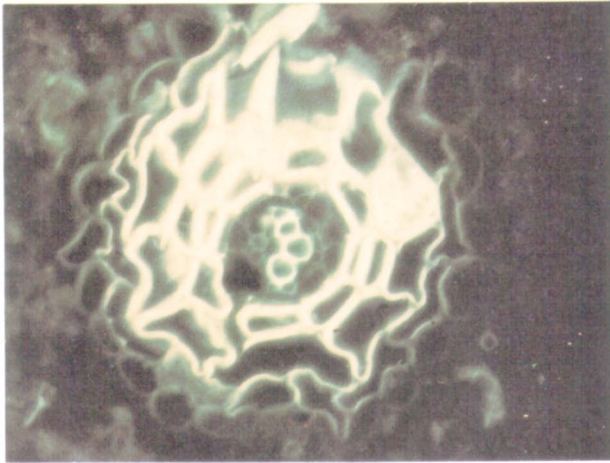
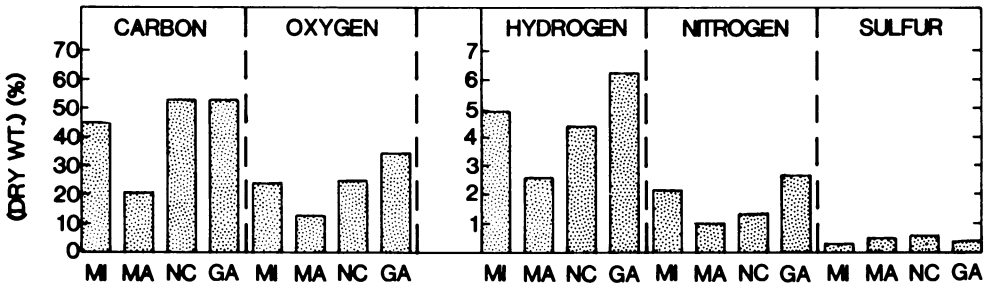
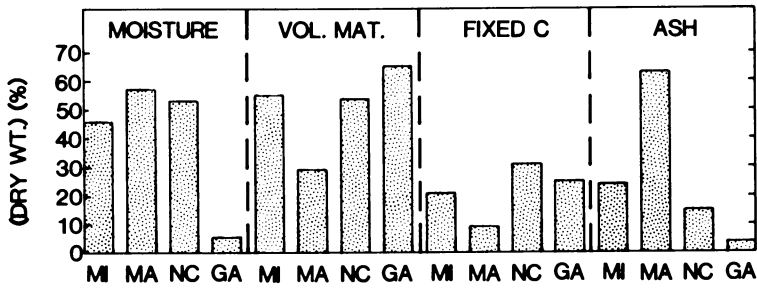


Figure 6b. A similar view as in Fig. 6a of a slightly larger root of Woodwardia but observed under blue light fluorescence. Note that (in contrast to birefringence) the more darkly stained tissues tend here to be more highly fluorescent.

Ultimate Analyses



Proximate Analyses



Heating Value

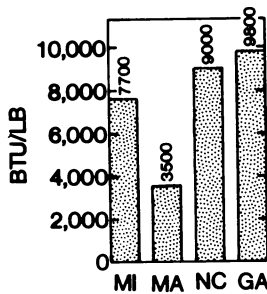


Figure 7. Proximate and ultimate analyses of samples from Minnesota (MI), Maine (MA), North Carolina (NC), and Georgia (GA).

Literature Cited

1. Cohen, A. D. Ph.D. Thesis, Pennsylvania State University, 1968.
2. Cohen, A. D.; Spackman, W. Geol. Soc. Am. Bull. 1972, 83, 129-142.
3. Cohen, A. D. Testing of Peats and Organic Soils, STP 820, Am. Soc. for Testing and Materials, Philadelphia, PA, 21-36, 1982.
4. Corvinus, D. A.; Cohen, A. D. Compt. Rendu. IX Inter. Carb. Congress, In Press.

RECEIVED January 6, 1984

Characterization of Coal Macerals by Fluorescence Microscopy

JOHN C. CRELLING

Department of Geology, Southern Illinois University at Carbondale, Carbondale, IL 62901

DAVID F. BENSLEY

Coal Research Section, The Pennsylvania State University, University Park, PA 16802

The use of fluorescence microscopy to characterize coal macerals is a successful recent innovation. Compared to conventional white-light analysis, fluorescence microscopy reveals a greater number and variety of macerals, as well as, characteristic textures and structures. Although the spectra of fluorescent macerals are broad-peaked and, at this time, not suitable for chemical structure analysis, they are characteristic of maceral types and rank. Spectral analysis of the liptinite macerals in single coals of the Illinois Basin shows that the macerals can be grouped or discriminated both petrographically and statistically using various spectral parameters, specifically the wavelength of maximum intensity (λ_{\max}) and the red/green quotient ($Q = \text{intensity } 650\text{nm}/500\text{nm}$). In a number of cases the spectral data reveal the presence of more than one variety of a given maceral type in some samples. Maceral groupings on the basis of increasing λ_{\max} and Q consistently show the same order: fluorinite, resinite, sporinite, cutinite. For example, in the Brazil Block Seam (Indiana) the following maceral groups can be distinguished: fluorinite ($\lambda_{\max} = 520 \text{ nm}$, $Q = 0.58$), sporinite type I ($\lambda_{\max} = 550 \text{ nm}$, $Q = 0.85$), sporinite type II ($\lambda_{\max} = 590 \text{ nm}$, $Q = 1.00$), cutinite ($\lambda_{\max} = 610 \text{ nm}$, $Q = 1.47$). In addition, altered (weathered) forms of sporinite ($\lambda_{\max} = 690 \text{ nm}$, $Q = 1.22$) and cutinite ($\lambda_{\max} = 650 \text{ nm}$, $Q = 2.27$) were also observed. Studies on other coal samples of different ranks indicate that the fluorescence properties are very sensitive to changes in rank.

One of the major problems of coal science is that very little is known about the basic properties of the various macerals that make

up coal. Two of the main reasons for this lack of knowledge are that they are extremely difficult to separate from coal and that they are non-crystalline organic compounds and, therefore, not good subjects to analyze with such standard methods as x-ray diffraction or electron-microprobe analysis. Some of the most successful characterization of coal macerals to date has been done by petrographic methods, in which the individual macerals do not have to be separated. In the steel industry, for example, petrographic techniques have proven so successful in allowing the prediction of the coking properties of coal that most major steel companies have now established petrographic laboratories. Another petrographic technique that has only recently been applied to coal analysis is quantitative fluorescence microscopy. With this technique, the visible fluorescent light excited from the macerals reveals shapes, textures, and colors not visible in normal white-light viewing. The technique also yields quantitative spectra that are characteristic of both the individual maceral type and the rank of the coal. It is now also well established that all of the liptinite macerals (coal components derived from the resinous and waxy plant material) and many of the vitrinite macerals (coal components derived from woody tissue of plants) will fluoresce, and that some recently discovered liptinite macerals can only be identified by their fluorescence properties.

Some of the first measurements of the absolute intensity of fluorescence of coal macerals at specific wavelengths were made by Jacob (1,2). Relative intensity measurements of fluorescent spectra of modern plant materials, peats and coals have been reported by van Gijzel (3,4,5). Teichmuller (6,7,8) described three previously unidentified members of the liptinite group of macerals in part by demonstrating their distinctive spectral properties. Ottenjann et al (9), Teichmuller (10), and Teichmuller and Durand (11), illustrated the correlation of changes in fluorescence spectra of sporinite with rank, and Crelling and others (12) and Crelling (13) have demonstrated the use of fluorescence spectra to discriminate macerals. In addition, Ottenjann et al, Fisher (14), Teichmuller (10), and Teichmuller and Durand (11) have been able to relate the fluorescence spectra of vitrinite macerals to the technological properties of coal. These studies have shown the potential of using fluorescence measurements in the study of liptinite and vitrinite macerals.

The overall objective of current fluorescence studies at Southern Illinois University at Carbondale is to determine the kinds and relative amounts of fluorescent macerals in various coals and to classify and discriminate them on the basis of their fluorescence spectra. Additional objectives are to define the manner in which the fluorescent macerals vary with coal rank, and to determine which of the macerals are of primary and secondary origin.

Equipment and Methods

The fluorescence microscopy system used for this study in the SIUC Coal Characterization Laboratory is a Leitz MPV II reflectance microscope which is fitted with a 100 watt mercury arc lamp, a Pleom illuminator and a Leitz oil immersion 40X objective with a 1.3 numerical aperture. For spectral measurements the light from the mercury arc passes through a UG1 ultra-violet filter to a TK400 dichroic mirror which reflects light with wavelengths less than 400 nm to the sample. The fluorescent light excited from the sample is passed through a 430 nm barrier filter to a motorized interference wedge in front of the photometer. The interference wedge controls the wavelength of the fluorescent light hitting the photometer so that the intensity variations from 430 to 700 nm can be scanned and recorded in about 20 seconds. The spectral data are then fed from the microscope system into a computer and digitized, corrected, and analyzed. Each spectrum is corrected for the effects of background fluorescence and for the effects of the microscope system, especially the sensitivity of the photomultiplier tube, following correction procedures described by van Gijzel (13). For comparison, the various spectra are normalized and reduced to a number of parameters such as: 1) the wavelength of maximum intensity peak (λ max); 2) the red/green quotient (Q) where $Q = \text{relative intensity at 650 nm} / \text{relative intensity at 500 nm}$; 3) the area less than λ max; 4) the area greater than λ max; 5) area blue (430 to 500 nm); 6) area green (500 to 570 nm); 7) area yellow (570 to 630 nm); and 8) area red (630 to 700 nm).

Results and Discussion

In coals of the Illinois Basin, standard white-light petrographic methods generally reveal three types of liptinite macerals; resinite, sporinite and cutinite. These macerals are identified on the basis of their petrographic properties such as reflectance, size, shape and texture. When fluorescence microscopy is used, the fluorescence colors and intensities reveal the presence of larger amounts of these macerals plus the presence of the new maceral, fluorinite. The combined results of maceral analyses in both white-light and fluorescent light as well as the reflectance value for the Herrin (No. 6) Brazil Block and Hiawatha coals are given in Table 1.

Fluorinite was first defined by Teichmüller (6) and is characterized by a very high fluorescence intensity. It commonly occurs in most coals of the Illinois Basin and is shown in Figures 1 and 2 along with photomicrographs of sporinite and cutinite. When fluorescence spectral analysis is used on these samples, the resulting spectral data distinguish these four types of liptinite macerals plus additional varieties of resinite, sporinite and cutinite. For example, spectral analysis of the various liptinite macerals in samples of Herrin (No. 6) coal seam with a

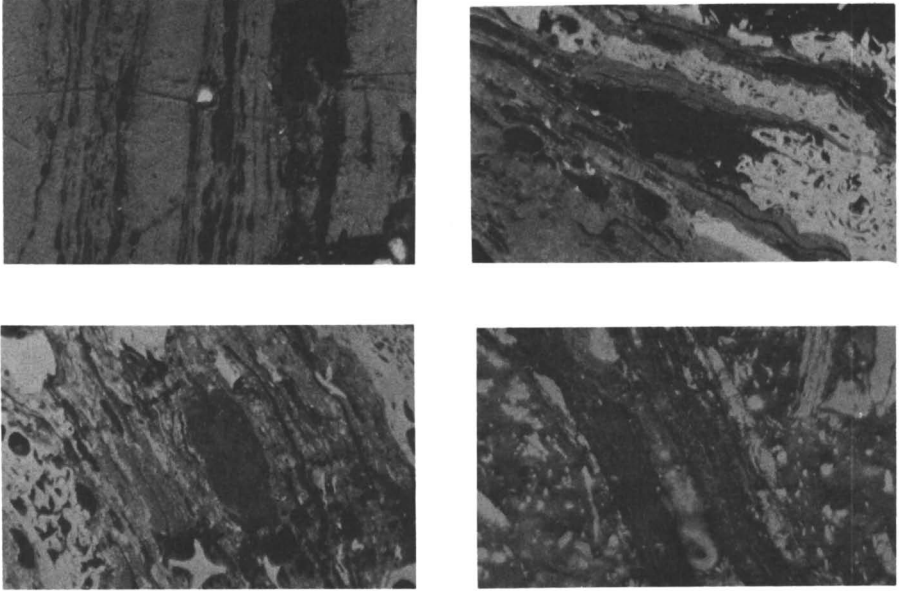


Figure 1. White-light (reflected) photomicrographs of liptinite macerals. Diameter of frames is 300 μm . 1a (upper left) - vertical zones of liptinite (dark gray) at left and center. Bright spot in center is a pyrite crystal. 1b (upper right) - some sporinite lenses (dark gray) in center of frame, 1c (lower left) - large liptinite mass at center and some scattered spores (dark gray), 1d (lower right) - some liptinite stringers running from top left to bottom right.

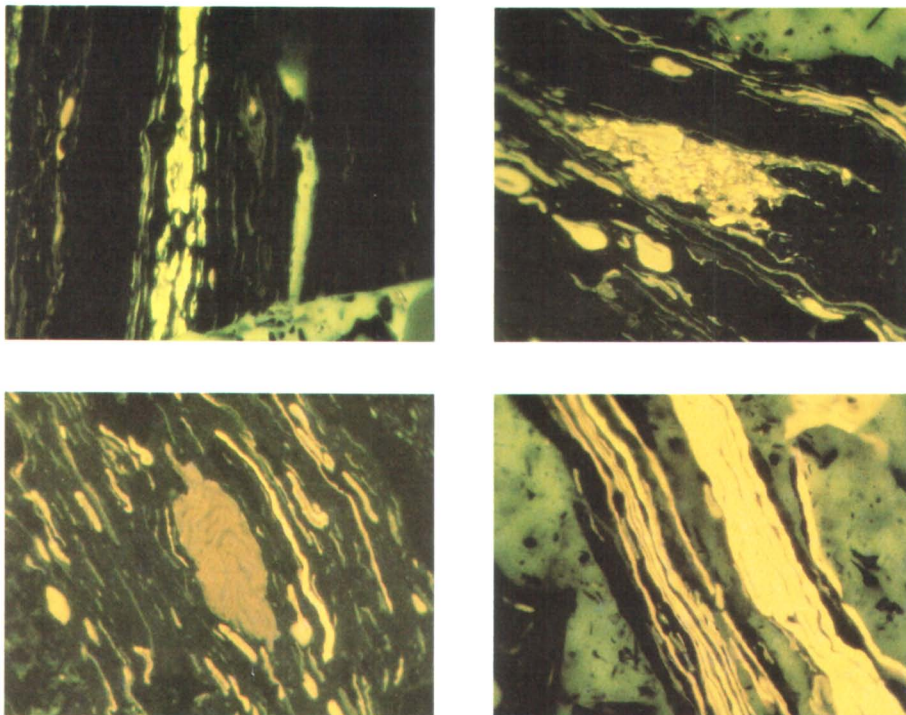


Figure 2. Blue-light photomicrographs of liptinite macerals. Diameter of frames is 300 μm . 2a (upper left) same frame as 1a, center zone of fluorinite showing intense yellow fluorescence, sporinite with less intense range fluorescence is seen at left, green at lower right is the fluorescence from the mounting medium, 2b (upper right) same frame as 1b - fluorescence reveals spore (yellow ovoids) and a mass of granulated liptinite in center of frame, 2c (lower left) same frame as 1c - fluorescence reveals large mass at center as a spore sac (sporangium), yellow ovoids are sporinite and yellow stringers are cutinite. 2d (lower right) same frame as 1d - fluorescence reveals two different types of cutinite - a brighter thicker variety on the left and a darker thinner variety on the right.

Table 1. Results of Combined White-Light and Fluorescent Light Petrographic Analyses

Coal Seam	Herrin (No. 6) Saline Co., IL	Brazil Block Parke Co., IN	Hiawatha Carbon Co., UT
Reflectance (in oil at 546 nm)	0.65%	0.58%	0.52%
Vitrinite	65.1	56.3	73.7
Pseudovitrinite	19.8	8.7	7.8
Fluorinite	0.3	0.2	0
Resinite	0.1	0.7	6.9
Sporinite	3.0	14.1	0.5
Cutinite	0.4	2.0	0.8
Amorphous			
Liptinite	1.8	4.2	1.0
Semi-fusinite	5.7	4.9	4.2
Fusinite	2.1	3.4	1.3
Micrinite	1.7	5.5	3.8

reflectance of 0.65% (in oil at 546 nm) showed distinctive spectra for the macerals fluorinite, resinite, sporinite and cutinite. In this case (Herrin No. 6), the spectra were assigned to maceral groups on the basis of the petrographic identification of macerals from which the spectra were obtained. When the groups of spectral data for each maceral type were subjected to discriminant function analysis of the eight different parameters for each spectrum, the maceral types were well separated. From this analysis it was easily seen that there are two different groups of resinite macerals. Thus, the statistical analysis of the spectral parameters of the macerals revealed two varieties of the resinite maceral group that could not be readily distinguished by normal petrographic means. The average spectra of the various maceral types distinguished by the discriminate function analysis are plotted in Figures 3-6. Additional study of these samples indicates that there are also two varieties of fluorinite present. The average spectral data for all of the varieties of the fluorescent macerals in these samples are given in Table II.

In a study of the fluorescence properties of the Brazil Block seam (Parke Co., IN), a somewhat different approach was used. In this case, about a hundred individual spectra were taken on a variety of fluorescing liptinite macerals. Although the macerals from which the spectra were taken were not identified at the time of measurement, photomicrographs in both normal white-light and fluorescent light were taken for documentation. The spectral parameters for each spectrum were calculated and these data were subjected to cluster analysis to test the degree to which the

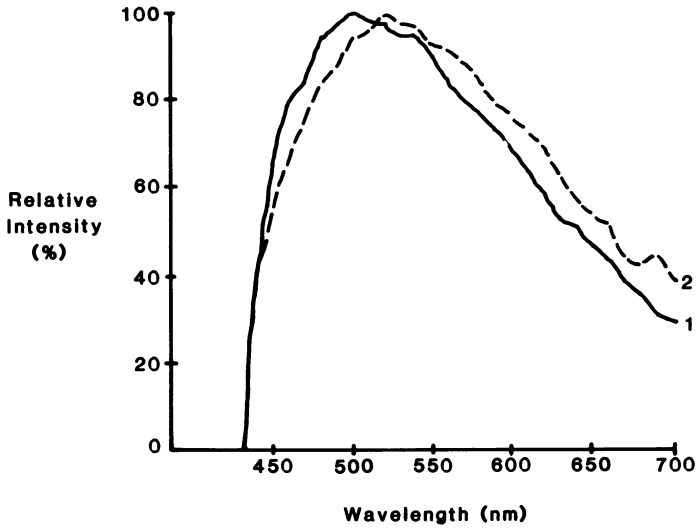


Figure 3. Average fluorescence spectra for two varieties of fluorinite in the Herrin (No. 6) seam. The reflectance of the seam is 0.65%.

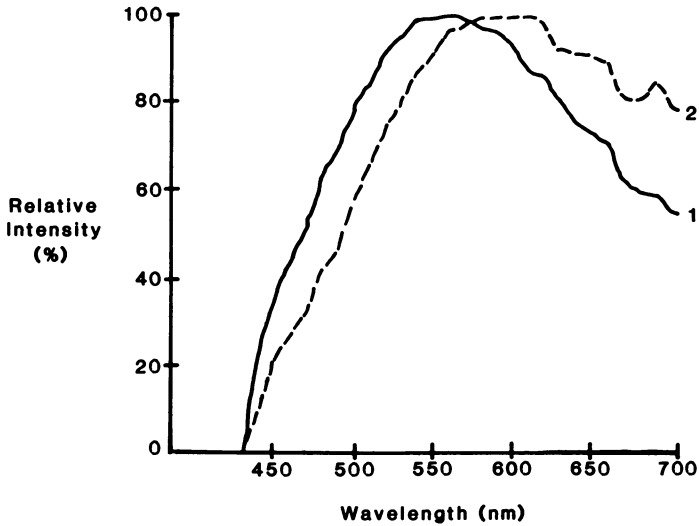


Figure 4. Average fluorescence spectra for two varieties of resinite in the Herrin (No. 6) coal seam. The reflectance of the seam is 0.65%.

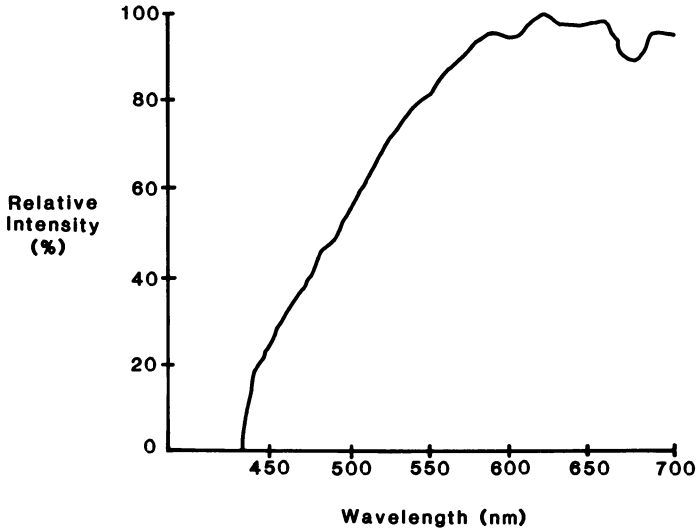


Figure 5. Average fluorescence spectrum for sporinite in the Herrin (No. 6) coal seam. The reflectance of the seams is 0.65%.

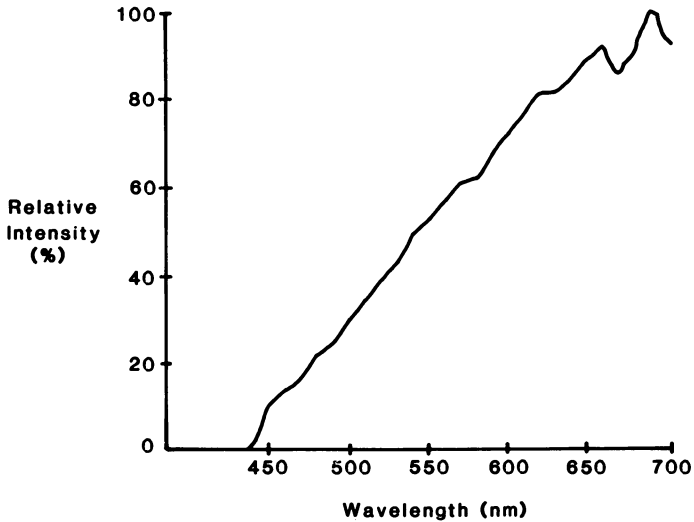


Figure 6. Average fluorescence spectrum for cutinite in the Herrin (No. 6) coal seam. The reflectance of the seam is 0.65%.

Table II. Spectral Parameter of the Average Spectral of Maceral Varieties in the Herrin No. 6 Coal Seam (Saline Co. - $R_0 = 0.65\%$)

Parameter	Fluorinite		Resinite		Sporinite	Cutinite
	I	II	I	II		
Peak (nm)	500	524	553	604	657	682
Red/Green Quotient	0.47	0.57	0.94	1.67	1.63	2.99

groups could be separated on the basis of their spectral parameters. It was found that seven groups could be distinguished. The basic petrographic data for the Brazil Block coal seam are given in Table I and the average spectral parameters for each maceral group are given in Table III. When the macerals from which the spectra were taken were identified from the photomicrographs, it was found that each group corresponded to a separate maceral type or a variety of a maceral type. There was type of fluorinite, one type of resinite, three types of sporinite and two types of cutinite. While this correspondence of maceral types and varieties to statistical groupings of spectral data was not unexpected, it is further confirmation that the spectral parameters of macerals are unique to maceral type and variety.

Table III. Spectral Parameters of Average Spectra of the Brazil Block Coal Seam

Parameter	Fluorinite	Resinite	Sporinite			Cutinite	
			I	II	III	I	II
Peak (nm)	480	520	550	590	690	610	650
Red/Green Quotient	0.32	0.58	0.85	1.00	1.22	1.47	2.27
Area Blue (%)	37	19	16	14	13	12	7
Area Green (%)	38	43	36	34	31	32	29
Area Yellow (%)	15	23	25	28	26	28	29
Area Red (%)	10	15	23	24	30	28	35
Area Left of Peak (%)	21	33	40	53	93	59	60
Area Right of Peak (%)	79	67	60	47	7	41	40

An interesting result of this analysis is that one of the

sporinite varieties (II) and one of the cutinite varieties (II) distinguished by statistical means showed petrographic evidence of alteration (weathering). Because the coal sample itself was collected from a fresh exposure at an active mine, it appears that the weathered maceral varieties were weathered before they were incorporated into the peat that was later coalified.

The results of these two studies show that fluorescence spectral analysis can distinguish, on a quantitative basis, the various types of liptinite macerals and, indeed, even varieties of each type. That the various spectra are unique to the individual macerals is further indicated by the recurrent order of the spectral parameters, especially the wavelength of maximum intensity (λ max) and the red/green quotient in any given coal. For example as shown in Figures 3-6 for the Herrin (No. 6) seam and as seen in Table III for the Brazil Block seam, the order of the maceral types on the basis of increasing λ max and Q is fluorinite, resinite, sporinite and cutinite. It should be noted, however, that as the rank of coal increases, all of the spectral peaks shift toward longer wavelengths and diminish in intensity and are, thus, eventually difficult or impossible to distinguish from each other. Weathering of the macerals has a similar effect.

The preliminary results of studies now underway suggest that the spectral peak (λ max) of some macerals, is more sensitive to variation in coal rank than previously believed. In the high volatile bituminous coals studied, an increase of 3 V-types (0.45 - 0.75% reflectance) resulted in about a 50 nm increase of λ max.

Even when macerals have been altered by large increases in rank, or weathering, or other processes, fluorescence microscopy can still be quite useful in characterizing coal macerals. For example, some coal seams in the western U.S. have an abundance of resinite which in some cases is being extracted and commercially exploited as a chemical raw material. The resinite in these seams most often occurs as a secondary material, filling fissures and voids in the coal. Numerous flow textures, inclusions of coal in resinite veinlets, and intrusive relationships throughout coal seams indicate that the resinite was mobilized at some point in its history. These secondary resinites are often difficult to detect in normal white-light viewing; however, they all tend to fluoresce strongly displaying a variety of colors and are therefore, quite amenable to fluorescence analysis. When samples of the Hiawatha seam from Utah were examined by Crelling et al (12) four types of secondary resinites, each with a different fluorescence color - green, yellow, orange, red-brown - were seen. Each resinite type has a spectrum that is distinctive and the various types can be statistically separated on the basis of their spectral parameters. The average spectra of the four resinite types are shown in Figure 7 and the basic petrographic analysis of the sample from the Hiawatha seam is given in Table I. It should be noted that, at this time, the only way to distinguish the various types of secondary resinite is with fluorescence microscopy.

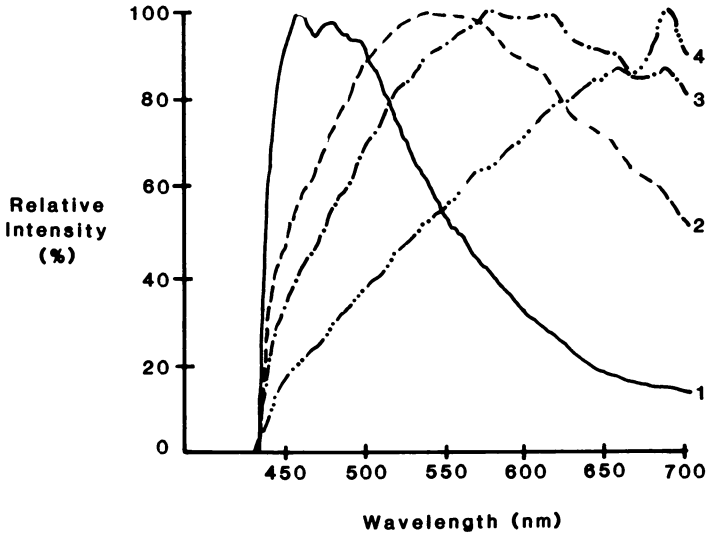


Figure 7. Average fluorescence spectra for four varieties of resinite from the Hiawatha Seam, Utah. Varieties 1, 2, and 3 have a definite shape and a brittle fracture while variety 4 occurs only as a void filling. The reflectance of the seam is 0.65%.

Work is now underway to separate these various resinite types using density gradient techniques and to chemically characterize the separated resinite fractions.

Summary

Although the characterization of coal macerals on the basis of their fluorescence spectra is a recent innovation, it has already proven to be an excellent fingerprinting tool for the various macerals. In some cases, it is even more sensitive than normal petrographic analysis. The initial results of fluorescence spectral studies show that the various fluorescent macerals in single coals can be statistically discriminated on the basis of their spectral parameters and that even varieties of a single maceral type can be distinguished. Although the spectra obtained at this time are rather broad and not suitable for chemical structure analysis, the potential for structural analysis exists and may be realized with improvements in instrumentation.

Acknowledgments

Much of this work has been supported by the Gas Research Institute under Grant No. 5082-260-0618 and also by the Coal Research Center at SIUC. This support is gratefully acknowledged.

Literature Cited

1. Jacob, H., Neue Erkenntnisse auf dem Gebiet der Lumineszenz-Mikroskopie fossiler Brennstoffe. -Fortschr. Geol. Rheinld. u. Westf. 1964, 12, 569-588.
2. Jacob, H., Mikroskop-Photometrie der organischen Stoffe von Boden I. Organopetrographische Nomenklatur und mikroskop-photometrische Methodik. -Die Bodenkultur, 1972, 23, 217-226.
3. van Gijzel, P., Autofluorescence of fossil pollen and spores with special reference to age determination and coalification. Leidse Geol. Meded., 1967, 50, 263-317.
4. van Gijzel, P., Review of the UV-fluorescence microphotometry of fresh and fossil exines and exosporia. "Sporopollenin"; Brooks, J., Grant, P. R., Muir, M. D., van Gijzel, P., and Shaw, G., Eds.; Academic Press: New York, 1971, pp. 659-685.
5. van Gijzel, P., Polychromatic UV-fluorescence microphotometry of fresh and fossil plant substances with special reference to the location and identification of dispersed organic material in rocks, in "Petrographic Organique et Potential Petrolier"; Alpern, B., Ed.; CNRS: Paris, 1975, pp. 67-91.
6. Teichmuller, M., Uber neue Macerale der Liptinit-Gruppe und die Entstehung von Micrinit. Fortschr. Geol. Rheinld. u. Westf., 1974a, 24, 37-64.
7. Teichmuller, M., Entstehung and Veranderung bituminoser Sub-

- stanzen in Kohlen in Beziehung zur Entstehung and Umwandlung des Erdols. Fortschr., Geol. Rheinld. u. Westf., 1974b, 24, 65-112.
8. Teichmuller, M., Generation of petroleum-like substances in coal seams as seen under the microscope. Advances in Organic Geochemistry-1973.
 9. Ottenjann, K., Teichmuller, M., and Wolf, M., Spectral fluorescence measurements in sporinites in reflected light and their applicability for coalification studies, in "Petrographic Organique et Potentiel Petrolier"; Alpern, B., Ed.; CNRS: Paris, 1974c, pp. 379-407.
 10. Teichmuller, Marlies, Fluoreszenzmikroskopische Anderungen von Liptiniten und Vitriniten mit zunehmendem Inkohlungsgrad und ihre Beziehungen zu Bitumenbildung und Verkokungsverhalten. Geologischer Landesamt Nordrhein-Westfalen, Krefeld, 1982, pp. 1-119.
 11. Teichmuller, M., and B. Durand, Fluorescence microscopical rank studies on liptinites and vitrinites in peat and coals and comparison with results of the rock-eval pyrolysis. Int. Jour. of Coal Geology, 1983, 2, pp. 197-230.
 12. Crelling, John C., Dutcher, Russell R., and Lange, Rolf V., Petrographic and fluorescence properties of resinite macerals from western U.S. coals. Proceedings of the Fifth Symposium on the Geology of Rocky Mountain Coal., 1982, pp. 187-191.
 13. Crelling, John C., Current uses of fluorescence microscopy in coal petrology. Journal of Microscopy, 1983, 132, pt. 3, 132-147.
 14. Ottenjann, K., Wolf, M. and Wolf-Fischer, E., Beziehungen zwischen der Fluoreszenz von Vitriniten und den technologischen Eigenschaften von Kohlen. Proc. International Conf. of Coal Science, 1981, pp. 86-89.
 15. van Gijzel, P., Manual of the techniques and some geological applications of fluorescent microscopy. Workshop sponsored by Am. Assoc. of Strat. Palynologist, Core Laboratories, Inc., Dallas.

RECEIVED January 1, 1984

Microscopic IR Spectroscopy of Coals

DOUGLAS BRENNER

Exxon Research and Engineering Company, Linden, NJ 07036

A new microscopic IR (infrared) spectroscopy technique now makes possible chemical functional group analysis of individual macerals in coals. Regions as small as 20 micrometers across can be analyzed. The technique utilizes a computer-controlled IR microspectrophotometer in conjunction with newly-developed procedures for preparing uncontaminated thin sections of coals. During preparation, the coal is held by a completely soluble adhesive. The adhesive is removed from the ground thin section using a solvent chosen to have minimal effect on the coal. This new IR technique differs from most analyses of chemical functionalities in coals which use ground-up particulate samples. These samples generally contain a great variety of organic maceral types which are intermixed on a microscopic level, as well as various minerals. Analyses of such samples give only averaged information, rather than being characteristic of any individual component. In contrast, with the microscopic IR spectroscopy technique described here, individual subcomponents of the coal are IR analyzed and in addition they can be observed visually in the microspectrometer in the context of their surroundings. Using this technique, variations from specimen to specimen within a given maceral type, or even heterogeneities within a single maceral, can be studied. In this chapter, details of this new technique are discussed and representative spectra of single macerals of vitrinite, and individual megaspores in Illinois No. 6 coal are described.

0097-6156/84/0252-0047\$06.00/0
© 1984 American Chemical Society

**American Chemical
Society Library
1155 16th St., N.W.
Washington, D.C. 20036**

Coals are heterogeneous on a microscopic scale. Because of this it is desirable to characterize the coal at as fine a spatial level as possible. IR (infrared) spectroscopy is widely used in coal science and technology to identify both organic and inorganic functional groupings in coals; however, it has only been able to analyze macroscopic samples. The conventional preparation of coals for infrared analysis uses finely ground samples. This is because of the opacity of the coal in some spectral ranges. For this reason, the particles should generally be less than about 20 micrometers thick. Techniques in common use include incorporating the particles in potassium bromide disks (1), or slurring them in a hydrocarbon oil such as Nujol (2). Such particulate samples generally include a wide range of types of vitrinite and other macerals which are derived from different plants (such as trees, bushes, and grasses) and from various parts of each plant (such as trunks, stems, roots, leaves, etc.). In addition, inorganic substances of various types and degrees of dispersion are generally mixed in. Because of their different derivations, the various organic plant remnants are likely to have different physicochemical characteristics; however, because of the intimate mixing of these subcomponents, which usually occurs on a microscopic scale, it is difficult to separately characterize the different maceral components. Therefore, IR spectra obtained on pulverized coal samples give averaged information rather than being characteristic of any individual component in the coal. A few techniques have been utilized in the past to overcome this problem. These include the hand separation of macerals (3,4), sink-float techniques, and the recently developed method of centrifugal separation of very finely pulverized coal (5). These preparation techniques provide a mixture of material which is highly enriched in a selected maceral type. These maceral concentrates can then be analyzed by a variety of chemical procedures. The averaged properties of a maceral type can be characterized using these procedures, but they do not enable the IR analysis of individual microscopic macerals.

The particulate samples of coal used for infrared analysis must be finely ground because of the high absorbance of the coal. The particles must be less than roughly 20 micrometers thick (depending on the rank) for substantial transmission of the IR radiation in the more absorbing regions of the spectrum. The small particles of coal cause considerable scattering to appear in the IR spectrum. Other complications are the differences in the thicknesses of the various particles of the sample, and the variations in thickness along each particle. For example, the thinner edges (with respect to the illuminating beam) of the particles will be more transparent than the central regions, so the volume of the particles may

not be sampled uniformly. This can be a problem for a heterogeneous material such as coal. Thin section samples of coal having a relatively uniform thickness of 20 micrometers or less have been used occasionally in the past (6). However, the difficulties in preparing these thin section samples and problems of contamination with the adhesives used in the preparation of the sections (7) has limited their usage. Also, because the cross sectional area of the samples must be several square millimeters or more for analysis with most IR spectrometers, microscopic components of the thin sections could not be individually analyzed.

In this chapter a new technique for the IR spectroscopic analysis of individual microscopic components in coals is described. This method combines new procedures for preparing uncontaminated thin section specimens of coal with a sensitive IR microspectrophotometer which has recently become commercially available. Details of this new technique are discussed and some representative spectra are described.

Experimental

The technique used to prepare uncontaminated thin section samples of coals was as follows. A chunk of coal about 1.5 cm across was cut perpendicular to the bedding plane to produce a roughly flat surface. This surface was ground smooth on a 20 cm diameter wheel using 600 grit and then 8 micrometer silicon carbide on disks. To avoid surface relief in the sample, only hard surface abrasive disks were used; polishing cloths were not employed. The flat surface was cemented to a glass slide with a thermoplastic hydrocarbon-based adhesive (Paraplast, manufactured by the Lancer Company) which is soluble in hexane. Hexane is a good choice for the solvent since it has relatively little effect on the coal. A temperature of about 70°C was used in melting and applying the adhesive. The coal was exposed to this temperature for only about a minute before cooling was started. The coal on the slide was ground to a thickness of 15 micrometers using the abrasives described above. The grinding of petrographic samples using standard techniques on a conventional horizontal grinding wheel having a hard abrasive surface is well known to produce highly flat, low relief surfaces. For the thin section, the upper and lower surfaces may not be precisely parallel. However, this causes only very slight differences in thickness across the observed or analyzed area because one sees only a very small, highly magnified region of the surface. In any case, it is possible to detect differences in thickness of less than a micron across a sample by using a high numerical aperture objective having a very shallow depth of field.

The completed sample was soaked in hexane at room temperature until the thin specimen floated off of the slide. The sample came off as a number of small pieces of various sizes from less than a millimeter across to several millimeters long. Although no residual adhesive could be observed on the pieces of coal, to insure complete removal of the adhesive the samples were immersed in a large excess of fresh solvent for several days. Then the hexane was decanted off and the specimens were stored in nitrogen at room temperature until they were used.

If desired, the preparation process can be carried out in an inert atmosphere by enclosing the equipment in a dry box, a plastic glove bag or simply in a plastic bag with slits for the hands. An inert atmosphere may be desirable for cementing the coal to the slide -- especially if temperatures above about 100°C are used for melting the thermoplastic. For other parts of the preparation an inert atmosphere is not as important since oxidation at room temperature is much slower.

The choice of the thermoplastic adhesive and the solvent used to remove it from the coal are important for obtaining thin sections of coal which are only minimally affected by the preparation process. Some considerations in choosing the adhesive are listed below. (1) The adhesive should have reasonably good adhesion to the coal and to the glass slide. (2) The adhesive should be readily soluble in the solvent and should leave no residue. (3) The solvent used should have minimal effect on the coal with respect to chemical and physical interactions, extraction, and swellability. (4) The solvent should be completely removed from the coal on drying. (5) The temperature required for cementing the coal should be as low as possible to avoid thermal changes in the coal, but not so low that the adhesive will be softened during subsequent grinding. (6) The adhesive should be relatively inert to avoid reaction with, or attachment to, the coal. (7) The viscosity of the adhesive during cementing of the coal should be no lower than necessary in order to minimize penetration of the adhesive into the microstructure of the coal. (8) The molecular weight of the adhesive should preferably be high to minimize diffusion of the adhesive molecules into the coal structure. (9) It is desirable that the adhesive not have absorption peaks in regions where the coal has important spectral peaks. Also, it is desirable that the adhesive have one of its strongest absorptions in a region where the coal has no strong peaks so that any residual adhesive could be easily detected and compensated for. (10) The adhesive should preferably be a reasonably pure material so that the possibility of minor constituents being selectively absorbed or reacting with the coal is avoided. It is difficult to simultaneously optimize all of these criteria, so the adhesive employed is generally a compromise.

The microscopic infrared spectrophotometer used in this work (NanoSpec/20IR manufactured by Nanometrics Inc.) operates in transmission and contains reflecting lenses. The visual as well as the IR image is normally observed in the transmitted radiation mode. Though, if desired, the sample can also be illuminated with a light source from above and viewed visually in reflected light. A schematic diagram of the apparatus is shown in Figure 1. Because of the reflecting optics, the visual and IR images of the sample correspond and the region of the sample being analyzed can readily be identified visually while it is in place in the IR microscope. This enables unambiguous correlation of visual microscopic characterization and IR analysis for the same area of the sample. The condenser and the objective of the microscope are both 15 power, 0.28 numerical aperture reflecting lenses. The part of the sample to be IR analyzed is optically delineated by an adjustable aperture at the image plane of the objective, so no masking is needed at the sample itself to define the analyzed area. The useful IR range of the instrument is from about 4000 to 700 cm^{-1} (2.5 to 14 micrometers). The IR monochromator is a variable interference filter. The resolution is only about 1% of the wave number value over the IR range; however, this should be adequate for many applications with coal because of the breadth of most of the absorbances. The IR source is a Nernst Glower and the detector is a liquid nitrogen cooled mercury cadmium telluride photodetector having high sensitivity. The operation of the spectrometer is computer-controlled and the data, which is stored digitally, can be automatically averaged and difference spectra can be obtained.

Results

In this preliminary study, spectral characteristics of vitrinite and liptinite macerals in Illinois No. 6 coal (high volatile C bituminous rank) were examined to evaluate the utility of this new technique for microscopic IR analysis of coals. In Figure 2, a photomicrograph of a thin section specimen consisting of a megaspore (a form of liptinite) surrounded by relatively homogeneous vitrinite is shown. The thin section was placed on a barium fluoride disk on the stage of the IR microscope. The megaspore and a region of the vitrinite lying close to the megaspore on the same specimen were analyzed with the IR microscope. The analyzed regions are indicated by rectangles drawn on the photograph of the sample; they are each about 55 micrometers wide by 180 micrometers long. Spectra of the two regions were taken in air at room temperature; they are compared in Figure 3. The spectra are displaced vertically to avoid overlapping. The displayed spectra actually involve a reference or background scan which

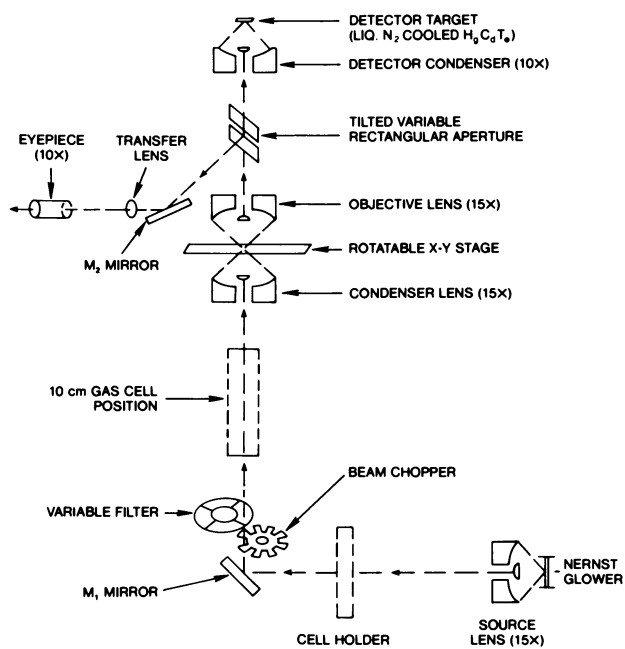


Figure 1. Optical diagram of microspectrophotometer.

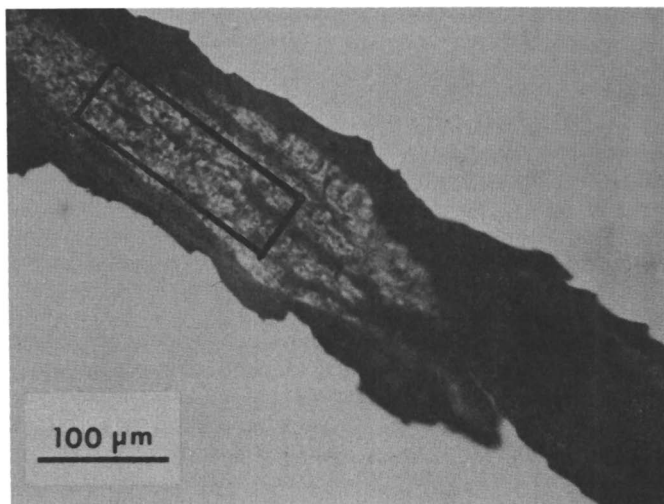


Figure 2. Thin section sample of Illinois No. 6 coal containing regions of vitrinite and liptinite.

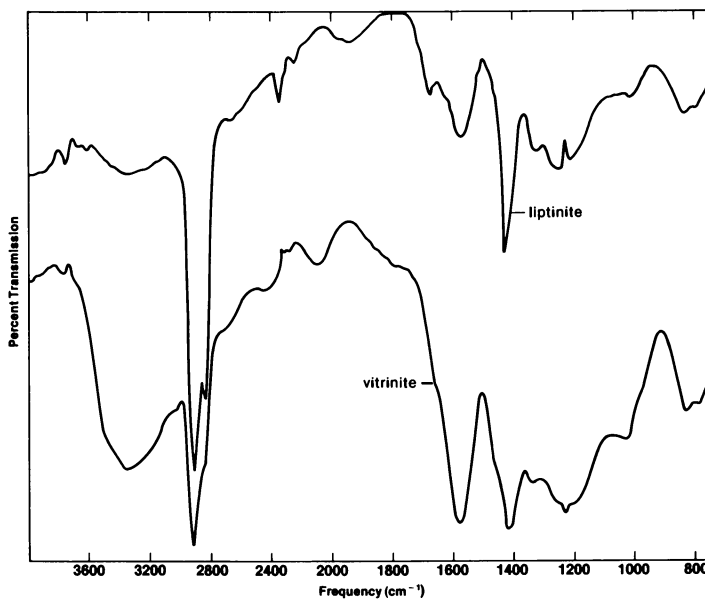


Figure 3. IR spectra of microscopic regions of vitrinite and liptinite in the same thin section sample of Illinois No. 6 coal.

was taken without the sample present but with all other conditions the same. The subsequent sample spectra are automatically normalized with respect to the background spectrum which is stored in the microcomputer. Each of the two sample spectra in Figure 3 are 2 minute scans.

There is a very high signal to noise ratio for the scans in Figure 3. Subsequently a 1 minute scan was made on a similar sample of vitrinite. This spectrum was taken on a smaller region which measured only 25 by 100 micrometers. For this scan there was no obvious noise on the trace from 4000 cm^{-1} down to 1400 cm^{-1} . Below about 1400 cm^{-1} noise was easily seen. After the first scan, a second 1 minute scan was taken. The repeat scan lay almost exactly on top of the first scan from 4000 cm^{-1} down to 1400 cm^{-1} indicating good reproducibility. Below about 1400 cm^{-1} the scans were less coincident because of the slight amount of noise.

A number of differences between the liptinite and vitrinite spectra are apparent in Figure 3. Note that since the thicknesses of the liptinite and vitrinite regions are very nearly the same and since scattering is minimal, these spectra can be directly compared quantitatively on a per unit volume basis. Some of the more prominent of the differences are as follows. The broad hydroxyl peak around 3350 cm^{-1} is much deeper for the vitrinite. This probably is caused chiefly by a much larger number of phenols in the vitrinite, but water absorbed in the vitrinite could also contribute to this peak. Between 2800 and 2975 cm^{-1} the liptinite shows a much stronger absorption than the vitrinite. This indicates much more aliphatic hydrogen in $-\text{CH}$, $-\text{CH}_2$, and $-\text{CH}_3$ groups in the liptinite. In this aliphatic absorbing region it is also evident that at about 2850 cm^{-1} the liptinite shows a substantially larger peak than the vitrinite on the side of the larger absorption. At about 1600 cm^{-1} the vitrinite peak is much larger than the liptinite peak probably indicating much more aromatic character in the vitrinite. (Note, however, that oxygen-containing functional groups can also contribute to this region.) Conversely, the carboxylic acid peak near 1700 cm^{-1} and the CH_2 , CH_3 peak around 1440 cm^{-1} are much more pronounced for the liptinite. The spectra clearly contrast the more aromatic and hydroxyl (or possibly water) containing structure of the vitrinite to the more aliphatic structure of the liptinite.

Mention should be made of some artifacts which appear in the spectra of Figure 3. At about 2350 cm^{-1} there is a peak caused by changes in the CO_2 concentration of the air. The major contributor to the changes is probably the operator's breathing. Smoking in the vicinity can cause particularly large changes. (This peak could be eliminated, if desired, by sealing the region of the beam path and maintaining a nitrogen

atmosphere). At about 2250 cm^{-1} and 1230 cm^{-1} are peaks caused by changes in the IR filters. Three filters are used to obtain the full spectrum, and small peaks occur where the second and third filters are brought into use. These peaks are probably a consequence of the abrupt changes in transmittance which occur when the filters are changed. Another artifact is broad peaks seen around 2100 cm^{-1} in the liptinite spectrum, 1950 cm^{-1} in the vitrinite spectrum and in some other areas. These peaks are caused by interference fringes which arise from the IR radiation being internally reflected from the top and bottom surfaces of the sample. The fringes can be misleading if they are not correctly identified. One other effect which could potentially lead to spurious peaks is small deviations in the positioning of the filters by the stepping motor. These positional deviations are far below the resolution of the instrument, but if sharp peaks are present in the background spectrum, these deviations could cause small peaks to appear at the positions of the steepest slopes of the nulled-out background peaks.

The applicability of this technique for "in situ" IR analyses during chemical treatments and the ability to perform kinetic measurements was tested by observing the effect of applying deuterated pyridine to a thin section of vitrinite and then allowing it to dry. An area 40×180 micrometers was analyzed. (Although the thin sample had been stored at room temperature in dry nitrogen gas, it quickly equilibrates with the room air.) First a spectrum was taken of the untreated sample. Then the solvent was placed on the sample and repetitive scans were made to monitor changes in the IR spectrum as the deuterated pyridine evaporated. Figure 4 shows spectra of the untreated sample, the sample wet with pyridine, and the sample after drying for about 20 minutes. For this last spectrum, peaks characteristic of deuterated pyridine are still prominent, such as those at about 950 and 820 cm^{-1} . Scans at later times showed no appreciable lessening of the peaks. The retention of some of the pyridine is consistent with the results of Collins *et. al.* (8).

Tests were made to determine the minimum area of analysis which could be conveniently used with thin sections of coal by this technique. Figure 5 shows spectra of regions of a tiny, roughly 30×30 micrometer, piece of vitrinite. One spectrum was taken using a 21×21 micrometer analyzing area, and the other spectrum was taken using a 20×30 micrometer analyzing area. Four minutes were used for each scan. For this scan time, the smaller area gives quite a noisy spectrum, but the 20×30 micrometer spectrum is much better. By using a longer scanning time, or by accumulating repetitive scans this spectrum could probably be made quite respectable. The spectral region having the greatest problem in the analysis of

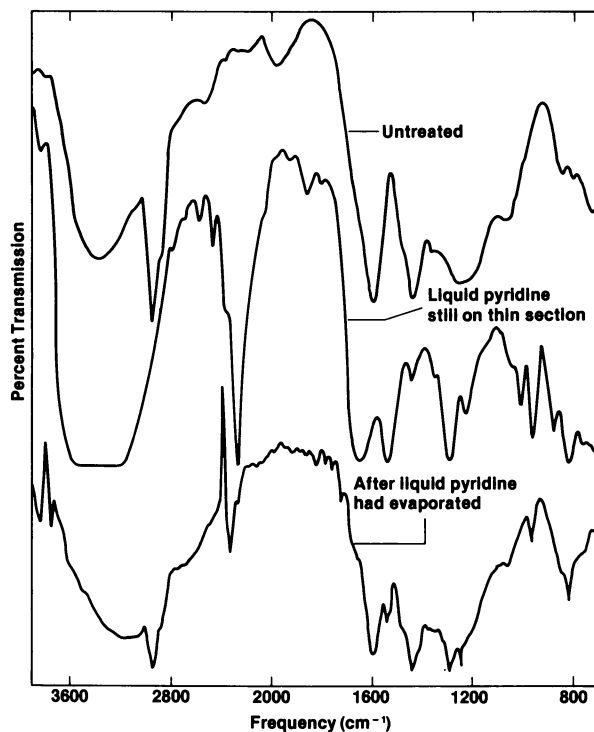


Figure 4. IR spectra of a microscopic region of vitrinite in a thin section of Illinois No. 6 coal. Top: untreated sample; middle: liquid deuterated pyridine on the sample; bottom: after pyridine has evaporated.

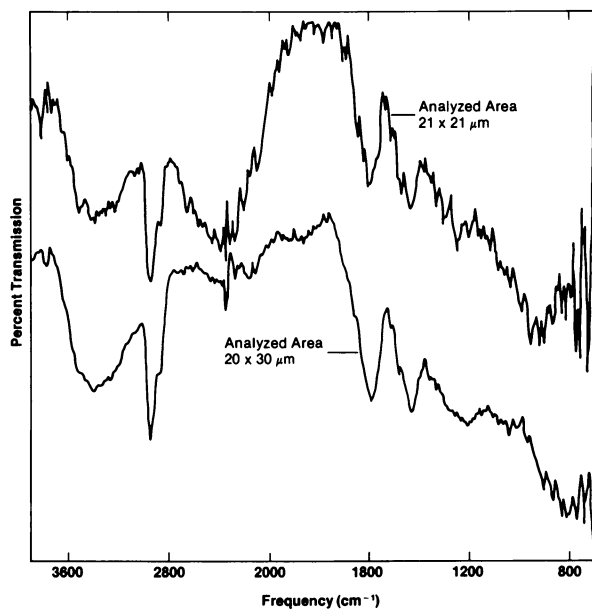


Figure 5. IR spectra of a thin section sample of Illinois No. 6 coal having an area of 30 μm x 30 μm . Top: delineated area is 21 μm x 21 μm ; bottom: delineated area is 20 μm x 30 μm .

such very small areas is below 1000 cm^{-1} where the sensitivity of the spectrometer falls off. Subcomponents or macerals in the coal which are somewhat less than 25 micrometers across can probably be IR analyzed by using long data accumulation times. Preferably such small subcomponents should be physically separated from the surrounding material. Alternatively, the spectrum of a region including the subcomponent as well as some of the surrounding material could be subtracted (using an appropriate normalization factor) from a spectrum only of the surrounding material in order to isolate the contribution of the subcomponent. Note, however, that for subcomponent sizes near the wavelength of the IR radiation the possibility of interference effects from the edges of the sample must be considered. Such effects ought to be made apparent by comparing spectra from subcomponents having different sizes or shapes.

Discussion

Infrared spectra of good quality have been obtained on uncontaminated individual microscopic macerals and microscopic subregions in coals. This development enables the IR characterization of microscopic individual subcomponents of coals and other solid fossil fuels as opposed to obtaining statistically averaged data on complex mixtures. In addition to characterizing the chemical functionalities of the major classifications of macerals in bituminous and brown coals, variations of chemical functionalities within each maceral classification can be studied. Substantial differences are to be expected, especially in the younger coals in view of the range of biological derivations within each maceral classification. Variations in functionalities over microscopic distances within a single maceral can also be studied. Effects of chemical and thermal treatments on the various maceral types can be examined either by treating the coal on the stage of the IR microscope or by spectroscopically analyzing the same microscopic region of a sample before and after treatment. This technique should also be applicable for the analysis of virtually any chemical process or chemical treatment of coal which causes changes in the IR spectrum and in which the area of interest is identifiable after the treatment.

In Figure 3 the IR spectrum of a subregion of vitrinite about 0.010 mm^2 in area is compared with the IR spectrum from an equal area which is within a single megaspore. The two regions of analysis are on the same piece of thin section and they are separated by only about 160 micrometers. The two minute scans of the 15 micrometer thick samples give excellent signal to noise ratios. As described in the results section, these spectra clearly contrast the more aromatic and hydroxyl-

containing structure of the vitrinite to the more aliphatic structure of the megaspore. The ability to analyze closely lying regions having identical preparation, equal areas being analyzed, and the same thickness, facilitates quantitative comparisons of the regions. Thus, while these data are generally consistent with the results of Bent and Brown (9) taken on maceral concentrates, the present technique enables a more direct quantitative comparison of the spectra.

The spectra in Figure 4 demonstrate the "in situ" treatment of an uncontaminated thin section of coal. One operational difficulty is the possibility of movement of the sample during treatment which would make analysis of the same microscopic region before and after treatment difficult. For example, application of a drop of solution to the coal is likely to cause movement. Movement can be avoided by securing the sample, but this may be difficult for small samples or it may affect the sample. Alternatively, if the region under analysis is carefully recorded, such as on a photograph, then during or after treatment the sample can be accurately repositioned on the stage.

Figure 5 demonstrates that isolated samples of coal less than 30 micrometers across can be satisfactorily IR analyzed and that delineated regions of a sample less than 25 micrometers across can be characterized by IR. Signal to noise levels which are improved over those shown in Figure 5 can be obtained by using longer data accumulation times. Alternatively, if better quality data is required only for some small regions of the spectrum, then those regions alone can be scanned to shorten the time needed to obtain an acceptable signal to noise level. The ability to analyze small regions of a coal sample is important even for a single maceral type such as vitrinite. For example, substantial variations occur in the structure (10,11) and swellability (12) of different microscopic areas of vitrinite from the same coal.

In the IR microscope the region of the sample being analyzed is delineated by a variable aperture at the image plane of the objective. Therefore, no spacial restrictions are placed around or near the sample itself. Since the image of the sample has been substantially magnified at this image plane, it is relatively easy to accurately define even very small subregions of the sample for analysis with the aperture. However, the geometrical region delineated by the variable aperture which is observed visually is not nearly so well defined for the infrared radiation because of diffraction effects. The spatial uncertainty is proportional to the wavelength, so the resolution is considerably poorer near the long wavelength end of the IR range. The divergence or angular spread of the IR beam passing through the sample, which is determined by the numerical aperture, will further diminish

the spatial specificity of the delineated area. Of course, the thicker the sample, the more of a problem this becomes. For analysis of a very small subregion in the coal, the most unambiguous way to avoid contributions from contiguous material is to physically remove the subcomponent from the surrounding material.

The 15 micrometer thickness of the Illinois No. 6 coal used for these spectra is quite satisfactory since the percent transmissions of a number of the larger peaks are below 40 percent, but without saturation. Also, at this thickness the thin sections can be conveniently manipulated without fracturing. Using the described grinding technique for preparation, samples containing any maceral types and even substantial amounts of mineral matter can be prepared. There appears to be no reason why the technique can not be applied to peat on up in rank through the bituminous coal range -- perhaps even to anthracites if samples can be made thin enough. The only requirement is the preparation of samples sufficiently thin for the IR radiation to penetrate and which are more than about 20 micrometers across. So far we have successfully examined coals of ranks from subbituminous to high volatile A bituminous.

The interference peaks which occur in the spectra of Figure 3 can be misleading when trying to interpret the spectra. These fringes occur when some of the IR radiation reflects from the top and bottom surfaces of the sample and then interferes with the unreflected beam. The fringes are particularly a problem where the top and bottom surfaces are nearly parallel and where the thickness of the sample is comparable to the wavelengths of the radiation, such as for the thin section specimens used in the technique described here. However, the intensity of the interfering beam is not large since it is reflected twice and it passes through the sample three times instead of once. Thus, as seen in Figure 3, the fringes are most prominent in the spectral regions having low absorbance. The fringes can be partially compensated for by determining their position and intensity in a low absorbance region and then calculating and subtracting out their contribution to other parts of the spectrum where their presence is less obvious. Alternatively, tilting the sample, or using samples of different thicknesses and of higher adsorbance can be used to identify the effects of the fringes on a spectrum so that they can be compensated for.

In conventional transmission IR of coal where crushed particulate samples are used, the variation of thickness along each particle may cause a problem in their quantitative analysis. This problem occurs because the amount of radiation passing through an object decreases exponentially with thickness rather than linearly. So, for peaks which absorb a

substantial fraction of the radiation, the thicker regions of the particle are "sampled" by the IR beam differently from the thinner (e.g. edges) regions. Among the consequences of such nonuniform sampling would be effects on the peak heights and peak shapes. Similarly, if the radiation passes through a number of particles in traversing the sample, then appreciable variations in the cumulative amount of material passed through at different points in the cross section would cause problems. The problem is illustrated in Figure 6. On the left in the figure is a uniform distribution of material. On the right is the same quantity of material but it has a thickness of one unit over one-half of the area and a thickness of seven units over the other half. If the absorptivity of the material is such that it transmits 37 percent of the incident radiation for the uniform thickness shown in the figure, then the same quantity of material with the nonuniform thickness shown on the right of the figure will transmit 48 percent of the incident radiation. Only for samples which at their thickest part absorb only a small fraction of the incident radiation (for the selected wavelengths) will the intensity of radiation passing through a sample of nonuniform thickness closely approximate the intensity transmitted by the same quantity of material of uniform thickness. (For high volatile C bituminous coal having a thickness of 15 micrometers, the stronger bands absorb over 50 percent of the incident radiation.) Grinding coal much below 15 micrometers is difficult with many conventional mechanical grinders. In addition, nonuniform distribution of the particles sometimes occurs. It should be noted that even when nonuniform sampling of the coal particles by the IR beam occurs, linear increases in absorbance with increased sample concentration (e.g. satisfying Beer's law) can occur. In particular, Beer's law holds approximately for a sample in which the particles cover only a small fraction of the cross sectional area of the radiation beam, even though within the individual particles, regions of different thickness are averaged differently. For this reason, in quantitative IR work with particulate samples of coal, it is desirable to examine the sample with an optical microscope to estimate the transparency or thickness of the individual particles and the uniformity of distribution of the particles. For example, if particles five micrometers or more across cover an appreciable fraction of the cross sectional area of the sample, or if the sample appears mottled or grainy in color under, say, 20 power magnification in transmitted light, then problems with quantitative analysis are a possibility. Unless considerable care in sample preparation is taken, nonuniform particle distributions and/or substantial quantities of particles or particle agglomerates over five micrometers thick may occur. The difficulties from nonuniform thickness described above for

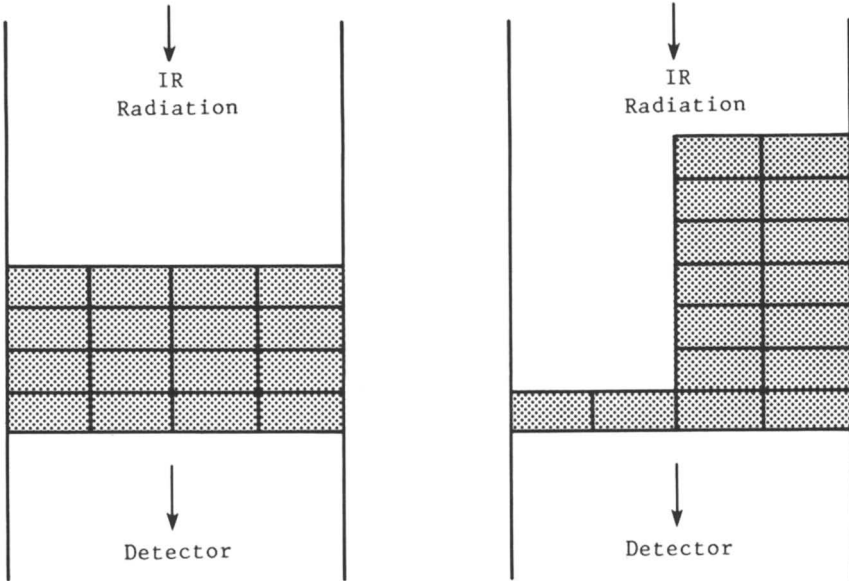


Figure 6. The intensity of radiation transmitted through the same amount of material is different for uniform versus nonuniform thickness.

IR analysis of particulate coal do not occur with the thin section samples used in this work which have highly uniform thicknesses. However, a related problem resulting from the convergent beam of the IR microscope can occur and is described below.

High N.A.'s (numerical apertures) for the condenser and the objective are desirable in microscopes in order to achieve good resolution and have good light gathering qualities. However, high N. A.'s mean that the radiation strikes the sample over a wide range of angles. For radiation passing through a sample of uniform thickness, the greater the angle from the normal, the greater will be the distance through the sample which the radiation travels and the greater will be the absorption. Therefore, the average thickness of material through which the beam travels will be greater than the true thickness of the sample. Furthermore, the radiation is attenuated exponentially with distance travelled in the sample rather than linearly. This means that for IR bands which have substantial absorption, radiation passing through the sample at the different angles will not average together linearly with respect to distance travelled in the sample. If necessary, these effects can be compensated for either by experimental calibration or by calculation if the intensity of radiation at the various angles is known. For bands with high absorbances the effects of the different angles will depend on the amount of radiation absorbed and therefore calibration must be done over a range of absorbances.

Summary and Conclusions

Microscopic macerals and subregions in coal have been characterized by infrared spectroscopy using a new technique. Individual macerals or subcomponents of the coal as small as about 20 micrometers across can be analyzed. The technique utilizes new procedures for preparing uncontaminated thin sections of coal in combination with a recently available microscopic IR spectrometer.

Because the thin section specimens are not contaminated with adhesives or embedding materials, and because the samples are readily accessible on the stage of the IR microscope, this technique is well suited for "in situ" treatments of the coal. Alternatively, since the 15 micrometer thick specimens of coal can ordinarily be handled and transported without damage (if proper care is taken), an untreated sample can be initially analyzed, then it can be removed from the instrument for chemical or thermal treatment, and finally, the same specimen can be returned to the microspectrometer for determination of the changes in the IR spectrum. The analysis of the same specimen before and after treatment is highly desirable for micro-heterogeneous substances such as coals.

The microscopic IR spectroscopy technique described here differs from and complements prior IR work on maceral concentrates in being able to spatially delineate an individual subcomponent being IR analyzed and to characterize it visually in the context of its surroundings.

Preliminary IR measurements on microscopic subregions of individual macerals of homogeneous-appearing vitrinite and of megaspores in Illinois No. 6 coal clearly demonstrate quantitative as well as qualitative chemical differences between these macerals. This work demonstrates that good quality IR spectra of microscopic subregions of coal can be obtained.

Acknowledgments

The author wishes to acknowledge the excellent technical assistance of Mark S. Beam in the preparation of the samples for these studies.

Literature Cited

1. Gordon, R. R.; Adams, W. N.; Pitt, G. J.; Watson, G. H. Nature 1954, 174, 1098.
2. Brooks, J. D.; Durie, R. A.; Sternhell, S. J. Appl. Sci. 1958, 9, 63.
3. Fenton, G. W.; Smith, A. H. V. Gas World 1959, 149.
4. van Krevelen, D. W.; Schuyer, J. "Coal Science;" Elsevier: Amsterdam, 1957; p. 240.
5. Dyrkacz, G. R.; Horwitz, E. P. Fuel 1982, 61, 3.
6. Cannon, C. G.; Sutherland, G. B. B. M. Trans. Faraday Soc. 1945, 41, 279.
7. Mackowsky, M.-Th. in "Stach's Textbook of Coal Petrology" Gebruder Bontraeger: Berlin 1975, p. 243.
8. Collins, C. J.; Hagaman, E. W.; Jones, R. M.; Raen, V. F. Fuel 1981, 60, 359.
9. Bent, R.; Brown, J. K. Fuel 1961, 40, 47.
10. Taylor, G. H. in "Coal Science;" Given, P. H. Ed.; ADVANCES IN CHEMISTRY SERIES No. 55, American Chemical Society: Washington D.C., 1966; p. 274.
11. Brenner, D. Proceedings of the International Conference on Coal Science, 1981, Verlag Gluckauf GmbH: Essen, p. 163.
12. Brenner, D. in "Preprints of the Division of Fuel Chemistry;" American Chemical Society, National Meeting, 1982, Vol. 27, No. 3-4, p. 244.

RECEIVED October 13, 1983

Variations in Properties of Coal Macerals Elucidated by Density Gradient Separation

GARY R. DYRKACZ, C. A. A. BLOOMQUIST, L. RUSCIC, and E. PHILIP HORWITZ

Chemistry Division, Argonne National Laboratory, Argonne, IL 60439

Based on a recently developed separation procedure for coal macerals, closely spaced narrow density fractions of macerals have been examined for petrographic content and ultimate analysis. Each maceral group or maceral type clearly exhibits a range of densities (a density band) and corresponding range of atomic ratios. In general, the H/C and S/C ratios decrease monotonically with density, reflecting changes in the macerals since as density increases the macerals separate in the order: exinite, vitrinite, inertinite. The overall range of H/C values for typical high volatile bituminous coals can vary from as much as 1.2 to 0.4 within the same coal if all three maceral groups are represented. Within each maceral group, less variation is observed. In most bituminous coals, there is 15 to 20% total variation in H/C ratio across the individual maceral bands. The O/C and N/C ratios show different behavior. Relative to the vitrinite O/C and N/C ratios the exinite ratios are very low, but rise steadily as density increases. Within the vitrinite band there is some additional increase before finally leveling off. The inertinite ratios have intermediate values between those of vitrinite and exinite and vary only slightly with density.

Our recent development of a new procedure for the density separation of macerals offers a method for obtaining high resolution separation of the three maceral groups: exinite, vitrinite, and inertinite, and can further resolve individual maceral types within these macerals groups, e.g., sporinite from alginite in the exinite group (1,2). The procedure

utilizes well-known techniques of density gradient centrifugation (DGC) to separate the coal into its components in an aqueous CsCl continuous density gradient. Density gradient centrifugation has been used for many years in the biosciences. We have taken that knowledge and technology and applied it to coal. The technique of density gradient centrifugation results in a series of bands representing the density variations in maceral groups and maceral types. The information obtained is similar to a chromatographic trace. At the simplest level this density profile represents a density "fingerprint" of a coal. When coupled with micropetrographic analyses, the density distribution of each maceral group can be obtained.

The observed changes in density are related in a complex way to the chemical structure of the coal or maceral (3). In order to better understand the chemical variations occurring in coal macerals we have examined the ultimate analysis of selected density fractions separated from the same coal.

EXPERIMENTAL

Separation

The basic procedures for DGC separation of macerals with advantages and disadvantages has been discussed previously (1,2).

Chemical Analysis

Because of the small samples often generated, ultimate analysis of selected density fractions was performed with a modified Perkin-Elmer 240, C, H, N, analyzer (modification XA by Control Equipment Corp.) using a modified burn procedure which includes increasing the time of burn and the amount of O₂ used in the burn. Good correlation for carbon and hydrogen ($r^2 = 0.98$) with ASTM methods was found for a range of coals from sub-bituminous to anthracites.

Maceral Analysis

The microscopic analyses of the coals follows standard practices. Details of the analysis of the fine maceral particles has been documented (1). We use the term maceral type and maceral group in a specific sense in this article. Maceral type refers to the individual maceral species which comprise the three maceral groups: exinite, vitrinite, and inertinite.

Separation Scheme

Since very detailed explanations for most of the procedures have been published, we will only provide a brief summary of the important aspects of the separation process (1,2). The methodology we have developed for the separation of the

macerals is shown in Figure 1. One of the most important aspects is the liberation of one maceral from another. Inadequate comminution will severely restrict the density resolution of the various macerals. However, there are practical limitations on the severity of comminution that can be tolerated. The most significant limit for general maceral separation and characterization is the ability to microscopically resolve the particles into the three maceral groups. This places a lower limit on particle size of two to three microns. In our case, grinding is carried out under nitrogen in two stages: First, to <200 microns with a planetary ball mill and then to the final size with a fluid energy mill.

The fine coal is then demineralized under nitrogen using HCl and HF. Normally, the demineralized coal is vacuum dried at 60° and stored for future use. However, we have noted that sub-bituminous coals show a significantly different density pattern compared to coal that was not dried. Time is also a complicating factor. When sub-bituminous coals stored either wet or dry after demineralization are periodically examined over several months by DGC the vitrinite peaks shift to progressively higher densities. At this time, we do not fully understand the reason for this behavior. Our present information suggests that the problem is related to the physical coal structure rather than to the chemical nature of the coal. Nevertheless, very reproducible density patterns can be achieved for sub-bituminous coals if they are stored as an aqueous slurry and separated within 24 hours after demineralization. This is our current procedure. This problem does not occur with sub-bituminous coals that have not been demineralized or any higher rank coals.

All density gradient separations are carried out in aqueous cesium chloride solutions to which a nonionic surfactant has been added (polyoxyethylene-23-lauryl ether, Brij-35). The surfactant is necessary to disperse the fine coal particles in the aqueous medium. Without complete particle dispersion the separation will most likely not be optimal.

Although bituminous coals do not appreciably retain surfactant in the separation procedure (<0.01%), the sub-bituminous coals apparently do. It's presence in the separated fractions has been inferred from nmr and pyrolysis/mass spectrometry, but the amount retained is uncertain (4).

We use several related modes for the DGC separation (Figure 1). The first, analytical DGC, is used primarily to obtain only a density "fingerprint" of a coal; it has the advantage of being a very rapid analysis (3-5 hours). Only small gradients are used (~45 ml) and small amounts of coal (1-10 mg) are applied. We use this type of DGC to preview coals or treated coals before doing larger scale

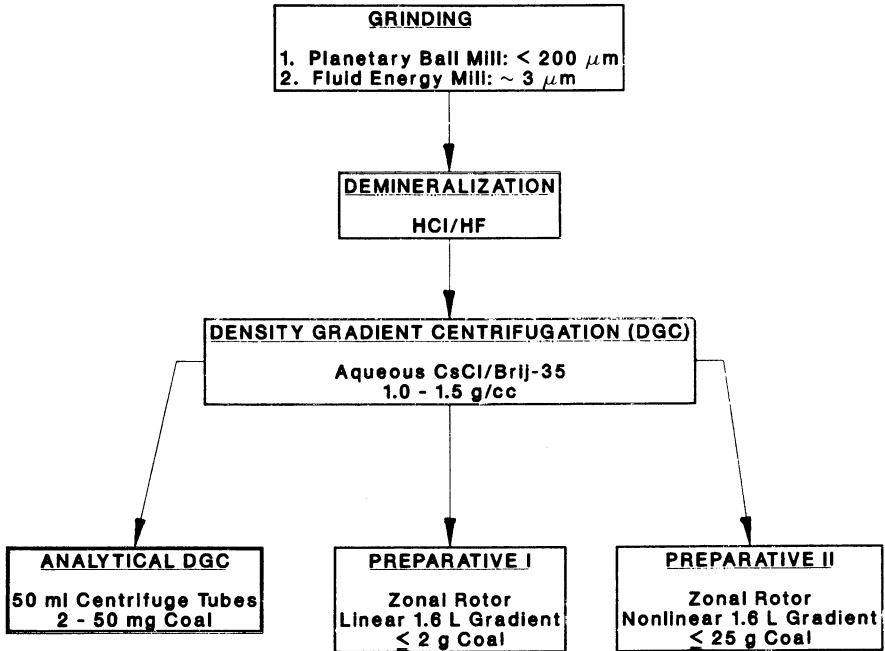


Figure 1. Procedure for density gradient centrifugation separation of coal macerals.

separations. The only disadvantage with this technique is that the small sample size usually precludes obtaining detailed information on the distribution of each maceral group.

For obtaining the maceral information as well as chemical information the DGC mode designated as Preparative I is used. A special, commercially available, zonal rotor is used for this type of DGC. Zonal rotors are available in a number of sizes and designs. Ours (Beckman Instruments Co.) holds 1.9 liters of which 1.6 liters is allocated for the gradient. With this system, up to two grams of coal can be separated on a 1.0 - 1.5 g/cc density gradient that is linear with volume. After separation in the gradient the contents of the rotor are pumped out through a density monitor (DMA 45, Mettler) and to a fraction collector. Normally, each fraction has a density range of ~ 0.01 g/cc and 40-60 fractions will be collected for each coal. The fractions are filtered, washed with water and ethanol, dried in a vacuum, weighed, and stored under argon. This entire procedure takes approximately two weeks per coal.

Preparative II DGC in Figure 1 is a scaled-up version of Preparative I which uses a combination of the sink-float separations followed by non-linear density gradient separation. With this technique 20-25 g of a maceral concentrate can be separated. In effect, for a three-fold increase in time for separation, isolation, and characterization, we obtain at least a ten-fold increase in the yield of maceral materials.

Selected fractions from a Preparative DGC are then mounted in epoxy for incident light microscopic analyses. Because of the small particle size we usually cannot identify individual maceral types within a maceral group. Only the major maceral groups can be identified. Figure 2 shows the density distribution data for the high volatile coal, PSOC-106, and the microscopic images observed at several fractions along this density distribution curve. The first two photographs at the low end of the density gradient are taken in the fluorescence mode. The bright particles are the exinite macerals. Black areas represent non-fluorescing vitrinite or inertinite. The intermediate grey background is the epoxy matrix. Note in the second photograph the small nature of the particles. This is commonly observed and makes analysis extremely difficult in the region between exinites and vitrinites. At the same time the difference in color between exinites and vitrinites is becoming obscured. The remaining photographs are taken in incident white light and the exposure time was the same for each photograph. The grey particles are vitrinite, the white or lighter grey particles are inertinite and the black is epoxy. In some cases bright specks are due to unpolished particles just below the polished epoxy

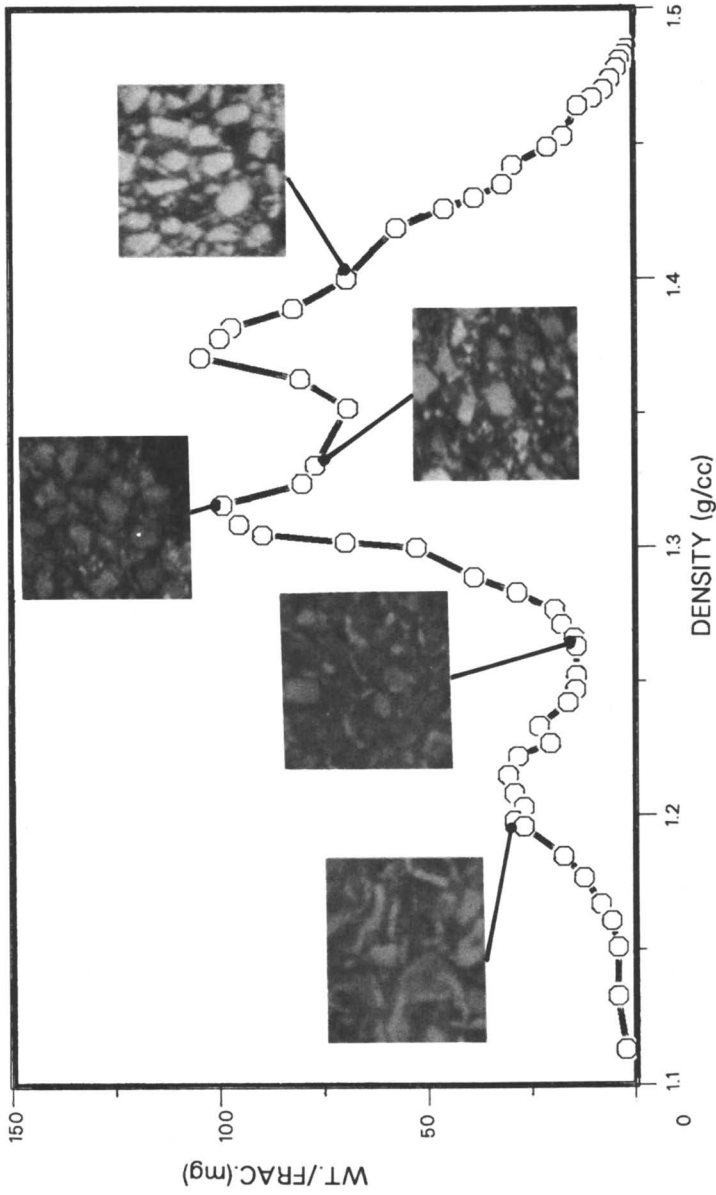


Figure 2. Maceral density distribution of a high volatile bituminous coal, PSOC-106. All densities are aqueous densities at 25 °C. Magnification of photographs is 1250x.

surface. These photographs were chosen to be representative of the whole sample. Since we are interested in finding the density of only pure macerals particles, when analyzing we also note whether or not a particle under scrutiny contains more than 10% of another maceral. Using this information, we can mathematically eliminate these mixed maceral particles. By combining the coal weight per density fraction data with the microscopic data we can derive the density distribution of each maceral group. This is shown in Figure 3a for the PSOC-106 coal.

RESULTS AND DISCUSSION

All the coals used here were obtained from the Pennsylvania State University Coal Data Base. The data for the coals are given in Table I. The separation of all these coals was performed in the same way and all coals were resolved to the same degree using Preparative I DGC. We have previously published detailed separation data on the high volatile B bituminous coal, PSOC-106, which gave good yields of all three maceral groups (1,2). The exinite in this coal is mainly sporinite, while the inertinite is mainly semi-fusinite. Figure 3a shows the distribution of the pure maceral particles as a function of density for PSOC-106. Pure maceral particles refer to those particles which by optical microscopy are composed of only one maceral species. Figure 3b shows the corresponding atomic ratios, H/C, S/C, N/C, and O/C.

Table I. Analytical and Maceral Analyses of Demineralized Coals

Coal	C	H	N	S % Wt.	O	Ash	E ^a % Vol.	V % Vol.	I
106	79.7	4.38	1.29	0.76	13.9	0.36	19.0	35.1	45.9
268	83.2	4.91	1.04	1.09	9.4	0.35	7.2	82.4	10.4
297	78.6	5.47	1.39	1.58	11.6	1.40	19.0	62.6	18.4
592	77.1	4.92	0.92	2.01	14.7	0.37	12.5	53.1	34.4

^aE = exinite; V = vitrinite; I = inertinite.

The selected fractions taken for elemental analysis represent density fractions consisting of at least 88% by volume of a single maceral species. The lines connecting sets of points between maceral groups must not be taken literally. The intermediate regions between the exinite group and vitrinite group consist of particles with two or more macerals composing a single particle or two distinct populations of

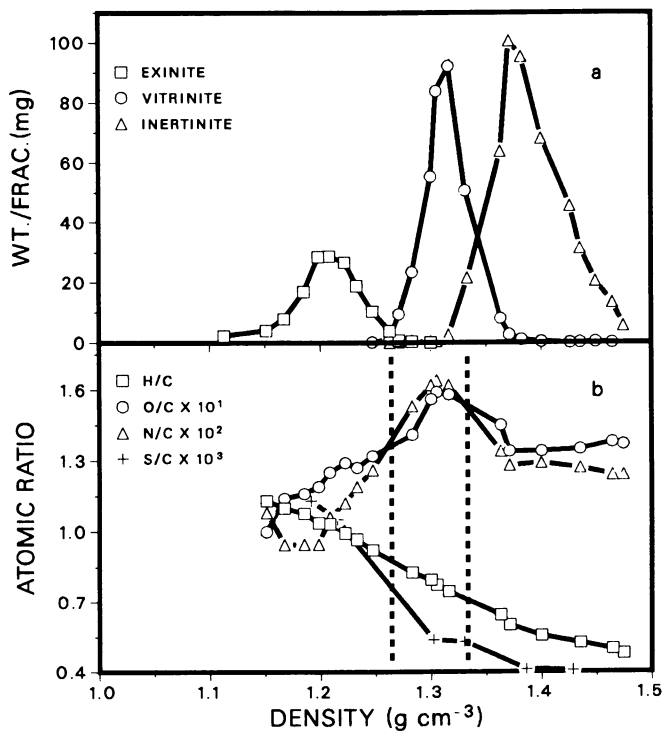


Figure 3. (a) Pure maceral distribution of PSOC-106.
(b) Variations of atomic parameters.

pure maceral particles. The region between the vitrinite group and inertinite group contains almost exclusively 2 separate pure particle populations rather than mixed maceral particles. Thus, whether or not the connecting lines between maceral groups represent the atomic value in that region, their only purpose for this discussion is to aid the eye in following trends between maceral groups.

The H/C ratio exhibits a very large range of values over the entire coal: From 1.13 at the lowest density monitored to 0.48 at the highest density. The S/C ratios follow a similar trend: The highest sulfur values in exinites and the lowest in inertinites. These sulfur values represent almost all organic sulfur since pyritic sulfur has been eliminated by the separation procedure. The S/C data is consistent with data found by an 'in situ' method of sulfur analysis in coal (5). Because of the nature of the separation method we can also see significant variations not only between maceral groups, but within each maceral group. Figure 4 is an attempt to provide some idea of the magnitude of variation that exists in the H/C ratio in the three maceral groups. The distributions are incomplete because of overlapping of maceral bands or composite maceral group densities which give unreliable data. Table II represents the range of H/C values for each band and combined with previous ^{13}C with solid probe nmr data for f_a , shows the ring index or number of rings per carbon atom (6). The data for 50% of the coal refers to the chemical composition of the coal centered around each peak value. It shows the bulk of each maceral group has wide variations in composition. The ring index includes all aromatic, aliphatic, and heterocyclic rings. The number of rings per carbon is roughly the same for all the maceral groups and indicates, as expected, that the maceral groups are all highly condensed species. However, the ratio of aromatic to aliphatic rings increases dramatically from exinites to inertinites. Exinite tends to exhibit wide variations in its composition, while vitrinite and inertinite are somewhat less variable. In all cases, though, the indications are that substantial variations in each maceral group are being observed by the density separation method. The oxygen and nitrogen data also show strong variations within the exinites and vitrinites, while inertinites do not.

In Figure 5 we have used the graphical densimetric method to show how the ring index and aromaticity varies with the density of the macerals (7). As can be seen, the data parallels the increase in aromaticity.

The change in atomic ratios is not unique to the particular coal, PSOC-106. Figures 6a and 6b show data on three more bituminous coals which contain substantial amounts of all three maceral groups. (The very high H/C value of 1.4 for PSOC-297 is due to alginite appearing at a very low

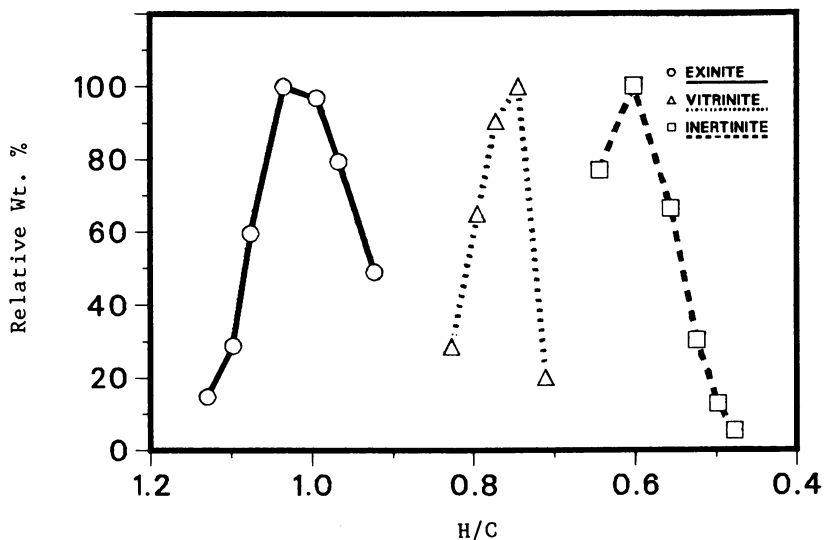


Figure 4. Distribution of coal macerals in PSOC-106 as a function of H/C ratio.

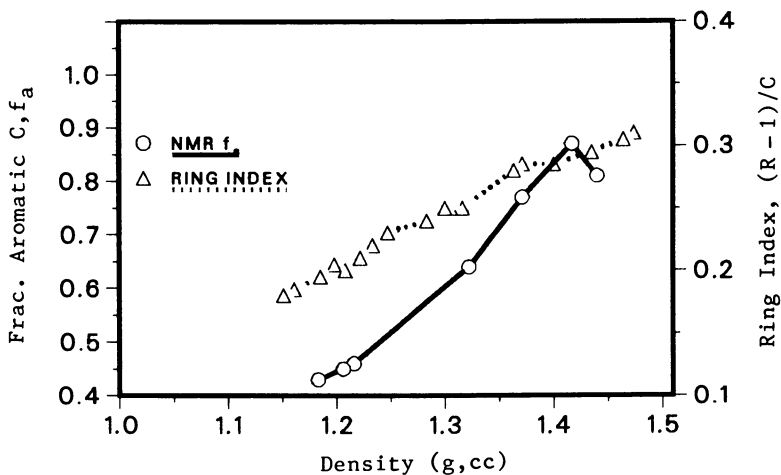


Figure 5. Variation of f_a and ring index with density in PSOC-106.

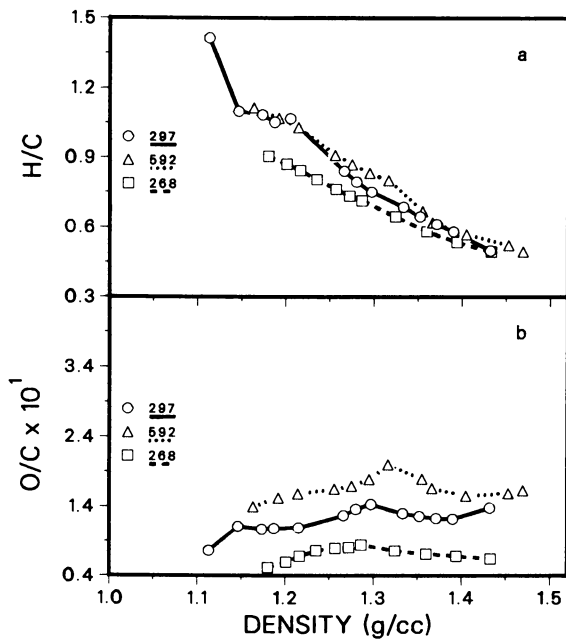


Figure 6. Variation of atomic ratios with density for several high volatile bituminous coals (a) H/C ratio; (b) O/C ratio.

density in this coal.) Although all the coals exhibit their own character with respect to the magnitude and range of the H/C values, they all show significant chemical changes across each maceral band in a similar manner to PSOC-106. Similar data also holds for coals that contain >95% vitrinite.

Table II. Range of H/C and Ring Index Values of Coal Macerals in PSOC-106

Maceral	Maximum Observed H/C Variation	H/C Range 50% of Coal ^a	Overall Ring Index Variation ^b
Exinite	1.13 - 0.92	1.08 - 0.96	0.21 - 0.32
Vitrinite	0.83 - 0.71	0.79 - 0.73	0.26 - 0.34
Inertinite	0.65 - 0.52	0.65 - 0.57	0.27 - 0.34

^aRefers to 50% (by weight) centered on peak; this is a crude measure of the chemical variation of each maceral group.

^bThe ring index $[(R-1)/C]$ is the total number of aromatic and aliphatic rings per carbon for a polymeric material it is equal to R/C and can be derived from the equation $2 R/C = 2 - f_a - H/C$.

What do these variations represent? There are a number of factors which can be invoked to explain the changes observed. Each of the three major maceral groups is composed of sub-macerals or maceral types. Exinite is composed of the maceral types sporinite, resinite, alginite, and cutinite. Since the source materials for each maceral type had different chemical structures, some artifact of these differences might be expected to remain. This is one source of variation. Moreover, within a single maceral type itself, significant petrographic changes can be observed. For example, different spore species show different fluorescence color; also vitrinite and semi-fusinite can have broad reflectance ranges within a coal. All these microscopically observable changes suggest differences in chemical structure. Qualitatively, we do see regular variations in fluorescence and reflectance across the maceral bands. It is apparent that density gradient centrifugation can, to some extent, isolate these physical and chemical variations and, in a sense, provide more homogeneous materials. However, the chemical variations we see by DGC have to be considered as lower limits of the chemical heterogeneity expected for coal. Since we are still dealing with discrete particles, the observed density may still be a weighted average of the maceral variants comprising the particle, even though these variants are below optical resolution. Further grinding may separate these variants, but

problems of mechanochemistry and surface problems may then become significant.

CONCLUSIONS

Substantial variation in the chemical composition of macerals has been shown for a number of coals. Density gradient techniques can provide better defined, more homogeneous materials as well as provide a lower limit on the heterogeneity of macerals.

The fact that not only heterogeneity due to maceral groups, but some heterogeneity due to variations within maceral groups can be reduced implies density gradient centrifugation is not merely a curiosity. The method is a tool for examining the fine structure of coal and allowing us to explore, through the separated density fractions, the chemical variation that coal contains.

ACKNOWLEDGMENT

This work was performed under the auspices of the Office of Basic Energy Sciences, Division of Chemical Sciences, U.S. Department of Energy under contract W-31-109-ENG-38.

LITERATURE CITED

1. Dyrkacz, Gary R. and Horwitz, E. Philip, Fuel, 1982 61, 3.
2. Dyrkacz, Gary R., Bloomquist, C.A.A., and Horwitz, E. Philip, Separation Science and Technology 1981 16, 1571.
3. Van Krevelen, D.W., 'Coal', Elsevier 1961, p. 315.
4. Dyrkacz, Gary R, Pugmire, R.J., Winans, R.E., unpublished results.
5. Raymond, R., International Conference on Coal Science, Proceedings, Dusseldorf, 1981, p. 857.
6. Pugmire, R.J., Zilm, K.W., Woolfenden, W.R., Grant, D.M., Dyrkacz, G.R., Bloomquist, C.A.A., and Horwitz, E.P., Jour. Org. Geochem., 1982, 4, 79.
7. Van Krevelen, D.W. and Chermin, H.H.G., Fuel 1954 33, 338.

RECEIVED January 10, 1984

Structural Variations in Coal Macerals

Application of Two-Dimensional and Dipolar Dephasing ^{13}C -NMR Techniques

RONALD J. PUGMIRE, WARNER R. WOOLFENDEN, CHARLES L. MAYNE,
JIRINA KARAS, and DAVID M. GRANT

University of Utah, Salt Lake City, UT 84112

Coal has been described as an organic rock. In order to better utilize coal supplies, however, the chemical structure of coal needs to be known in much greater detail so that methods can be developed to convert coal to a clean burning liquid or gaseous fuel.

Coal is known to be a physically heterogeneous substance with inorganic mineral matter mixed randomly in the organic material. The organic matter is further subdivided into maceral groups which reflect the floristic assemblages available at the time of the formation of the coal deposits. The chemical structural detail of the organic components of these materials is not well known, even though researchers have been working for decades on structure analysis. Of interest is the nature of the carbon skeleton including the aromatic and aliphatic groups; the level, type and role of oxygen, nitrogen, and sulfur; the type and extent of cross-linking; and the molecular weight distribution of the macromolecules.

Useful reviews and monographs published on coal structural analysis include works by Van Krevelen (1), Ignasiak (2), Tingey and Morrey (3), Davidson (4), Larsen (5), and Karr (6). These reports indicate the following: Coal is a highly aromatic substance (65-90% aromatic carbon, variable with rank but with few coals having aromaticities lower than 50%), with clusters of condensed rings (up to approximately four rings); the aliphatic part of the coal appears to be mostly hydroaromatic rings and short aliphatic chains connecting the aromatic clusters; the oxygen has been found in the form of phenols, quinones, ethers, and carboxylic acids, but less detail is known about the nature of the organic sulfur or nitrogen.

The study of the aromaticity of coal has included infrared spectroscopy (7) and various chemical methods (8,9), but the most

promising analytical tool appears to be cross-polarization/magic angle sample spinning nuclear magnetic resonance spectroscopy (CP/MAS C-13 NMR). This technique, initially developed by Pines, et al (10), has been successfully applied to coals by several workers in order to obtain aromatic-to-aliphatic ratios (11-14) (f_a). There is evidence that further structural information on coals and coal macerals can be gained from the CP/MAS C-13 NMR experiments (15-19). The aliphatic part of coal has also been characterized by a novel chemical method involving a trifluoroacetic acid/aqueous hydrogen peroxide oxidation of the aromatic rings to yield aliphatic acids and diacids (20). Chemical test results may be spurious, however, due to the severity of the reaction conditions and the insoluble and heterogeneous nature of coals.

CP/MAS ^{13}C NMR offers a powerful non-destructive tool for the analysis of carbonaceous solids. Depending on the nature of the carbonaceous material and the concomitant resolution obtainable, a wide range of structural information can be obtained. In complex organic sediments, the diversity of structural components leads to broad bands that frequently lack detail. However, employing multiple pulse techniques, it is possible to obtain additional structural information. The dipolar dephasing (DD) technique reported by Opella (21,22) discriminates protonated from nonprotonated carbons in a CP/MAS spectrum on the basis of the ^1H - ^{13}C dipolar interaction. Gerstein and co-workers (23-25) have demonstrated the utility of DD spectroscopy in studying coal structure.

We wish to report data on a series of whole coals and coal macerals using conventional CP/MAS, dipolar dephasing, and 2-D dipolar dephasing techniques. These data provide a wealth of new structural information and demonstrate that multiple pulse and 2-D spectroscopic techniques can be utilized on complex carbonaceous materials. We also report data obtained on maceral samples separated by the density gradient centrifugation method which separates coal maceral groups according to density.

Experimental

All ^{13}C NMR CP/MAS spectra were obtained on a Bruker CXP-100 instrument equipped with a Z32DR ^{13}C -MASS superconducting magnet probehead for proton enhanced magic angle spinning experiments (CP/MAS). Samples were packed in carefully prepared rotors machined from boron nitride (body material) and Kel-F (spinner head material) in Andrew-Beams type rotors (26). Boron nitride is used as the body material because of its good tensile strength and its resistance to deformation at high spinning speeds, whereas the Kel-F material is used for the rotor head material because of its better resistance to wearing as it comes into contact with the stator assembly during start ups and stops. Neither material

contributes any extraneous carbon resonance signals. The spinning speed was approximately 4.2 KHz to avoid complications due to overlapping of spinning side bands with other spectral components.

The carbon-proton cross polarization time was 1.5 msec and the cycle time was 0.3 seconds. Experiments performed at this laboratory have shown that such short cycle times are indeed feasible with coals because of the inherent free radical induced short relaxations times (27). Each spectrum resulted from averaging 10,000 repetitions on samples of approximately 100 mg size. The dipolar dephasing experiments involved a 40 μsec delay inserted between the contact time and the acquisition period during which no irradiation was applied. It is well known that this delay period will decrease the signal intensities of all carbon peaks compared to their intensities in the normal CP/MAS spectrum due to T_2 relaxation effects. However, no effort has been made to correct for this decrease in intensity to effect a material balance between compared spectra since the decrease in intensity of the nonprotonated carbon-13 peak is small under these experimental conditions (28). Thus, care must be taken to compare relative rather than absolute spectral parameters associated with DD experiments. Chemical shifts are reported referenced to TMS. Hexamethylbenzene was used as an external referencing material. A rotor of the reference solid is used to adjust the magic angle and the carbon/proton power levels for the Hartman Hahn condition such that the aromatic and aliphatic carbon peaks are of essentially equal intensities. The coal samples were then substituted using the same rotor without changing any resolution or referencing parameters. The upfield peak of hexamethylbenzene is presumed to be at 18 ppm from TMS.

The 2D data on the Aldwarke Silkstone exinite sample was obtained using the DD pulse sequence described above varying the dephasing time from 2-256 μsec in 2 μsec steps. This produced a 128 by 1024 data matrix which was Fourier transformed to yield the 2D spectrum.

Coal Macerals and Maceral Separation

The coals designated as PSOC-2 and PSOC-858 were obtained from the Coal Data Bank at the Pennsylvania State University. The maceral groups from these coals were separated by the density gradient centrifugation (DGC) technique described by Dyrkacz (29,30). The SGC profiles are presented in Fig. 1 and Table I. The samples designated by PSMC-67, -19, -34, -43, -47, and -53 were vitrinite concentrates obtained from Professor Alan Davis at Penn State and the analytical and CP/MAS data have been previously reported (16). The British maceral concentrates designated as Aldwarke Silkstone, Teversal Dunsil, Woolley Wheatley Lime, Markham Main, and North Celynen were obtained from

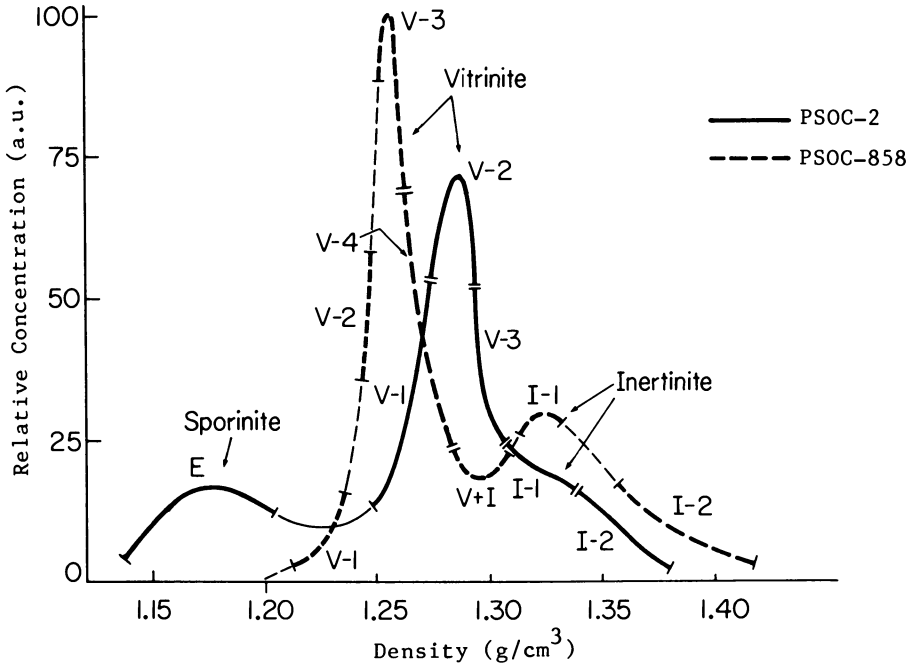


Figure 1. Fractograms for preparative DGC separation runs on PSOC-2 and PSOC-858. The heavy lines indicate density ranges of the samples used for NMR analysis. Letter designations: E, V, and I refer to exinite, vitrinite, and inertinite. The relative concentration has been normalized to absolute units for each coal.

Table I. Elemental Analysis and Maceral Composition of Coal PSOC-2 and PSOC-858 Separated by Density Gradient Centrifugation Techniques

Petrographic analysis (DMMF Volume %)	COAL	
	<u>PSOC-2</u>	<u>PSOC-858</u>
<u>Liptinites</u>		
Alginites	0.0	0.0
Resinite	1.2	0.3
Cutinite	1.4	-
Sporinite	33.6	-
Exinite (Anal.)		2.2
<u>Vitrinite</u>	29.6	53.9
<u>Inertinites</u>		
Micrinite	8.7	1.2
Semifusinite	8.3	39.7
Fusinite	7.0	2.1
Macrinite	7.7	0.5
Total Liptinites	36.2	2.5
Total Vitrinite	32.1	53.9
Total Inertinites	31.7	43.6
Elemental Analysis (DMMF %)*		
C	85.49	85.13
H	5.56	5.35
N	1.46	1.18
S	0.62	0.56
O (by difference)	6.79	7.76
Mineral Matter Content of Coal* (before Demineralization)	3.82	22.06
Vitrinite Reflectance* (mean maximum)	0.89	0.74
Class*	HVAB	HVBB
Coal Type	Channel Lithotype	

* Values reported by Penn State on different samples of the same coal.

Professor Peter Given at Penn State and the analytical data on these coals are given in Table II. The samples were provided to Professor Given by the British National Coal Board and were stored under nitrogen since their preparation.

Results and Discussion

We have recently established in our laboratory the capability to separate coal macerals by the density gradient centrifugation technique (DGC) described by Dyrkacz (29,30). The DGC fractograms of PSOC-2 and PSOC-858 presented in Figure 1 are examples of this separation technique and exhibit the density delineation of the maceral groups. It is noted that PSOC-858 exhibits a profile due only to vitrinite and inertinite. PSOC-2 exhibits peaks due to sporinite and vitrinite plus a shoulder which is due to the inertinites. While the reflectance data on the high density samples ($\rho > 1.30 \text{ g/cm}^3$) of PSOC-2 indicates a significant increase over that measured on samples attributed to the vitrinite peak ($\rho = 1.25 - 1.30 \text{ g/cm}^3$), it is not possible to quantify the relative purity of the "inertinite" shoulder ($\rho > 1.30 \text{ g/cm}^3$). The minimum between the vitrinite and inertinite peaks ($\rho = 1.28-1.31$) in PSOC-858 is also assumed to be a mixture of vitrinite and inertinite. The two inertinite samples ($\rho = 1.33$ and $\rho = 1.38$), however, display significantly higher white light reflectance than the three vitrinite peaks and this observation is evidence that the inertinite samples are relatively free from vitrinite. The stacked CP/MAS spectra of PSOC-2 and PSOC-858 whole coals and fractions separated by the DGC technique are given in Figure 2. Note the variation in the band shapes in the aliphatic regions of the vitrinite and inertinite maceral groups for both coals. These data clearly indicate that additional structural information is obtainable from studies of coal maceral groups which have been separated from a given coal as previously reported (17,18). Within the vitrinite samples of each coal, large variations in spectral characteristics indicate structural differences as a function of small density variance. Similar structural variations are observed in the inertinite samples.

Carbon resonances arising from both nonprotonated and protonated aromatic carbons may appear at the same frequency under proton decoupling. Yet these two resonances could possess very different relaxation behavior and in a solid could evolve very differently due to local proton dipolar fields which attenuate with the carbon-proton distances as $1/r_{\text{CH}}^3$. When the spin locking pulse for proton nuclei is turned off, carbons with directly bound protons such as methines and methylenes rapidly dephase in the local proton fields and their spectral response is rapidly diminished. The rapid internal motion of CH_3 groups greatly decreases the effectiveness of methyl protons. Nonprotonated carbons are only dephased by remote and therefore

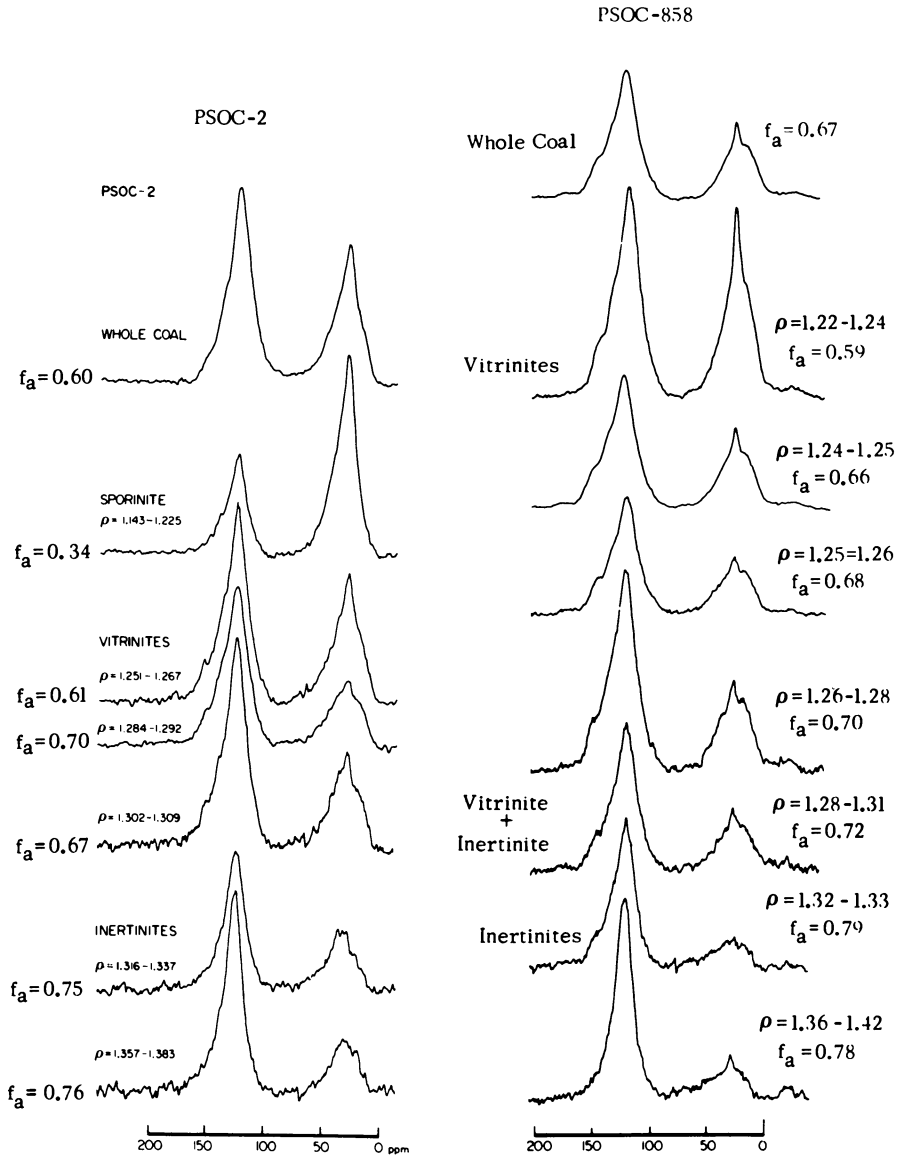


Figure 2. CP/MAS spectra of PSOC-2 and PSOC-858 whole coals and the maceral groups separated from the coal by density gradient centrifugation. The density ranges represent the range of densities employed as indicated in Figure 1. The corresponding f_a values are given for each sample.

much weaker magnetic fields. Gerstein and co-workers have reported DD experiments on an anthracite (23-25) and asphaltene (23,24). In model compounds, Alemany (28) has observed that a 40-45 μsec interruption in the proton decoupling will cause all of the CH and CH_2 resonances to essentially vanish, while the intensity of the nonprotonated carbons experience only minor attenuation. The dephasing of a methyl group is more complex but approximately 50% of the methyl carbon signal is still observed after a 40 μsec dephasing delay (31). Hence, by appropriately varying the interruption of the decoupler one can differentiate among methine/methylene, methyl and nonprotonated carbons. This type of response is given in Figure 3 using the pulse sequences first proposed by Rybaczewski et al (32) and popularized by Opella (21,22) for powders. These two spectral traces demonstrate how carbon atoms with protons are significantly attenuated following a 40 μsec dephasing time. The fraction of the carbon in the sample which is aromatic and nonprotonated, f_a^N , is obtained by comparing the relative intensities of the aromatic region of the spectra with decoupler pulse delays of 0 and 40 μsec before data acquisition. The fraction of total carbon that is aromatic and protonated is f_a^H ; thus $f_a^H + f_a^N = f_a$. The upfield portion of the aromatic peak due to protonated carbons and essentially all of the aliphatic region are attenuated leaving primarily the nonprotonated aromatic carbons and methyl carbons (the two high field peaks in the lower trace which have chemical shift values for aliphatic and perhaps aromatic CH_3 carbons). The small vestigial remnant of the once very strong methine/methylene/quaternary peak appears as the lowest field of the three distinct aliphatic peaks. Thus, this spectral response is limited to a subportion of the total spectrum contained in the upper trace.

Dipolar dephasing data have been acquired on a large number of samples and the data on 36 coal and maceral samples are given in Table III. The data are indicative again of the highly variable structure found in coal samples. The values designated as f_a^S and f_a^B are the fraction of aromatic carbon atoms which are substituted and those which are bridgehead carbons respectively. This separation is based strictly on the chemical shift range of the nonprotonated aromatic carbons; i.e., in the dipolar dephasing spectrum, it is assumed that nonprotonated carbon resonance shifts greater than 133 ppm are substituted while those with chemical shifts less than 133 ppm are bridgehead carbons. This arbitrarily chosen chemical shift value has, of course, been assigned from previous experience using the spectral assignments of known compounds. The values found in the last column of Table II reflect the fraction of the aliphatic region which is both nonprotonated carbons and methyl carbons and has been designated as f_s^* .

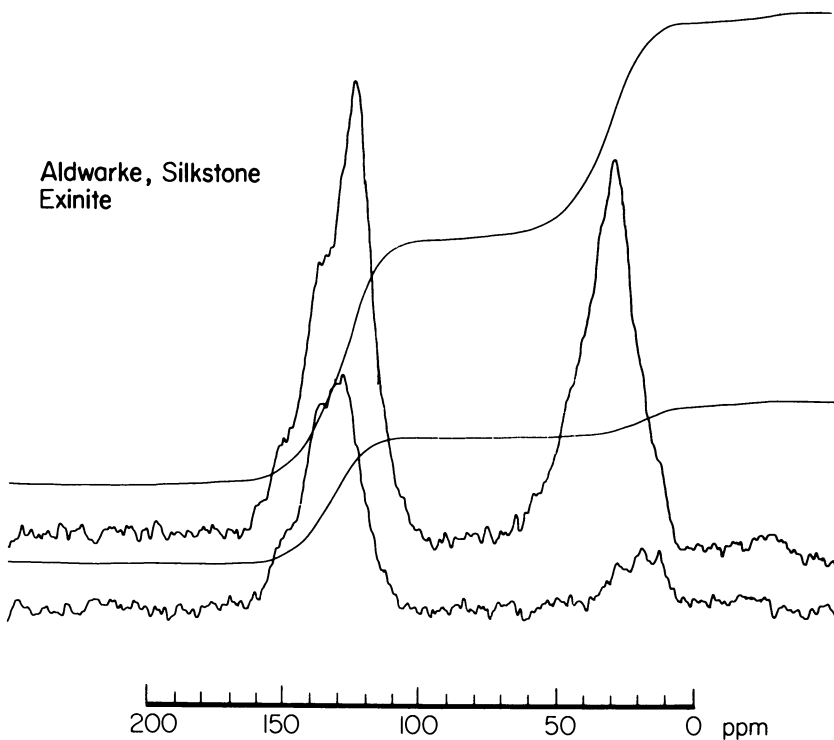


Figure 3. CP/MAS (top) and dipolar dephasing data with lower trace acquired following 40 μ sec pulse delay. Note three separate peaks in the aliphatic region due to methyls and CH_2 's.

Part of this data in Table II is a series of British maceral concentrates. The Woolley Wheatly Lime sample is 93% fusinite while the Teversal Dunsil concentrate is 80% semifusinite with 13% fusinite. The Aldwarke Silkstone sample contains 43% semifusinite and 43% fusinite. The petrographic analysis of PSOC-2 reveals nearly equivalent amounts of fusinite, semifusinite, micrinite, and macrinite (6.8, 8.1, 7.5 and 8.5% respectively in the whole coal) while PSOC-858 contains primarily semifusinite as the inertinite. The differences in f_a^H values for these inertinite samples are greater than the experimental error and these differences suggest that NMR techniques may be useful in characterizing the chemical structural differences between inertinite macerals.

The f_a values previously reported (33,34) for coal macerals have been consistent with the order fusinite > micrinite > vitrinite > exinite given by Dormans et al (35) for macerals of a specific rank. The f_a values found in this study are in the order inertinite > vitrinite > exinite as expected. An interesting observation is that f_a^H , the fraction of the total carbon in the coal that is aromatic and protonated, decreases in that same order for the samples studied. These data imply that there is a significant diversity in the amount of ring substitution and/or cross linking among the aromatic carbons in the various macerals as seen in the estimated values for the fraction of aromatic substituted and bridgehead carbons, f_a^S and f_a^B . An examination of the pure vitrinite series PSMC-67, -19, -34, -43, -47, and -53, which is a suite of samples from a common depositional environment but of varying rank, reveals a similar trend in samples of increasing rank. The CP/MAS data reported earlier (16) exhibited a decrease in functionality with progressing rank (i.e., loss of alkyl and aromatic oxygen groups). The dipolar dephasing data of this report indicate that this loss of functionality leads to a net increase in the fraction of protonated aromatic carbons. Ring condensation reactions alone cannot explain these results as ring condensation would produce an opposite effect. It appears that reactions associated with vitrinite maturation in these samples must also include some ring protonation reactions accompanying ring defunctionalization and the data suggests that these protonation reactions are preferred to ring condensation reactions.

We have included data on Beluga River (Alaska) lignite to illustrate a rather common observation in low rank coals. The value of f_a is in the range of many bituminous coals. On the other hand the ring protonation index (f_a^H) is only 0.17, a value approximately one-half of that observed in vitrinites. The value of the bridgehead carbon index (f_a^B) is 0.07 while the relative value of the substituted aromatic carbons (f_a^S) is 0.40. Both values are extreme among the data given in Table II. The aliphatic CH_2/CH index (f_s^H) and the methyl index (f_s^*) are also rather high.

Thus, otherwise overlapping spectral information has been obtained by employing in a subtle way the differing dipolar properties of the different types of carbons. If this spectral feature is made the basis of a two dimensional (2-D) FT spectrum, one may simultaneously obtain spectral information on both nonprotonated and protonated carbons directly. Figures 4 and 5 contain such a 2-D spectrum for the Aldwarke Silkstone exinite. In Figure 4 a contour plot of the spectral intensities is given for the rate of dipolar dephasing along the F_1 -axis vs. chemical shift along the F_2 -axis. Thus, the nonprotonated and methyl carbons show steep fall off in the intensity contours while protonated carbons are represented by much broader (along F_1 -axis) spectral responses. Several cuts through the 2-D surface parallel to the chemical shift axis are given in Figure 5. Hence, we observe in a more typical format the spectral response as a function of a dipolar dephasing frequency. For a solid powder the C-H dipole-dipole vectors span all possible orientations and thus zero frequency responses are found for all resonances, albeit the spread in aliphatic response is distributed over such a much greater range of dephasing frequencies as to reduce this part nearly to the noise level. The successive slices in Figure 5 show most clearly the CH_2 peak persisting to higher dephasing frequencies. The three dimensional plot (Figure 6) of the aromatic portion of Figures 4 and 5 helps one to appreciate the power of the technique to discriminate between protonated and nonprotonated aromatic carbons. Note in the plot sharp peaks corresponding to nonprotonated carbons resting on broader features corresponding to protonated carbons as illustrated in the inset. Curve fitting techniques could be used to quantitate this observation.

Thus, using very sophisticated spectral resolving techniques, one can obtain important structural information on coal. Hence, multiple pulse/multidimensional spectroscopy offers an exciting new analytical tool for the study of complex materials such as coal and coal macerals.

Acknowledgments

This work was supported by the Department of Energy Office of Fossil Energy Research under Contract No. DE-FG-22-80PC30226 and the Office of Basic Energy Sciences, Division of Chemical Sciences, U. S. Department of Energy under Contract No. DE-AC02-78ER-05006. We are indebted to Professor Peter Given for supplying the British maceral concentrates which were obtained from the British National Coal Board.

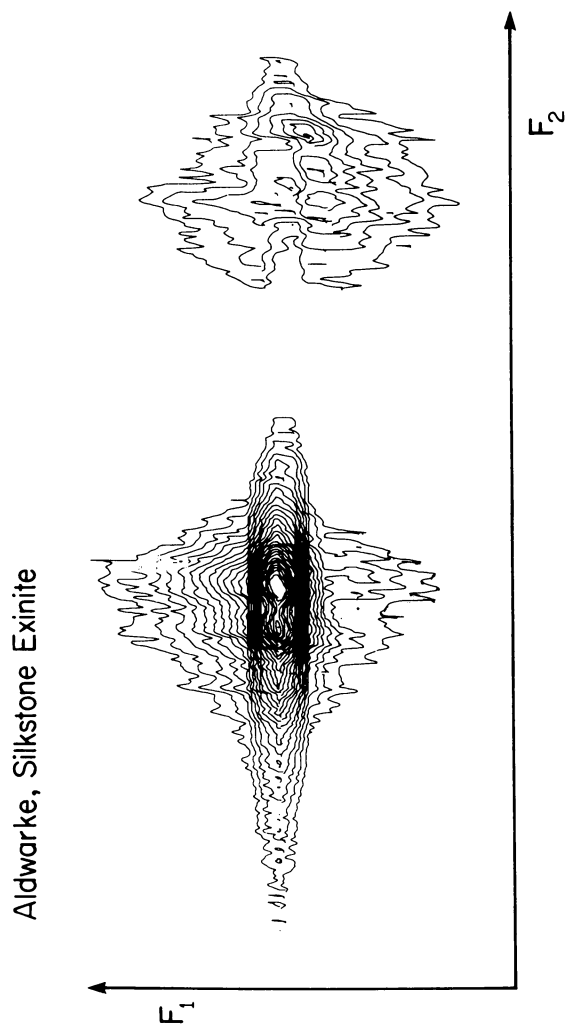


Figure 4. Contour plot for 2-D dipolar dephasing experiment.

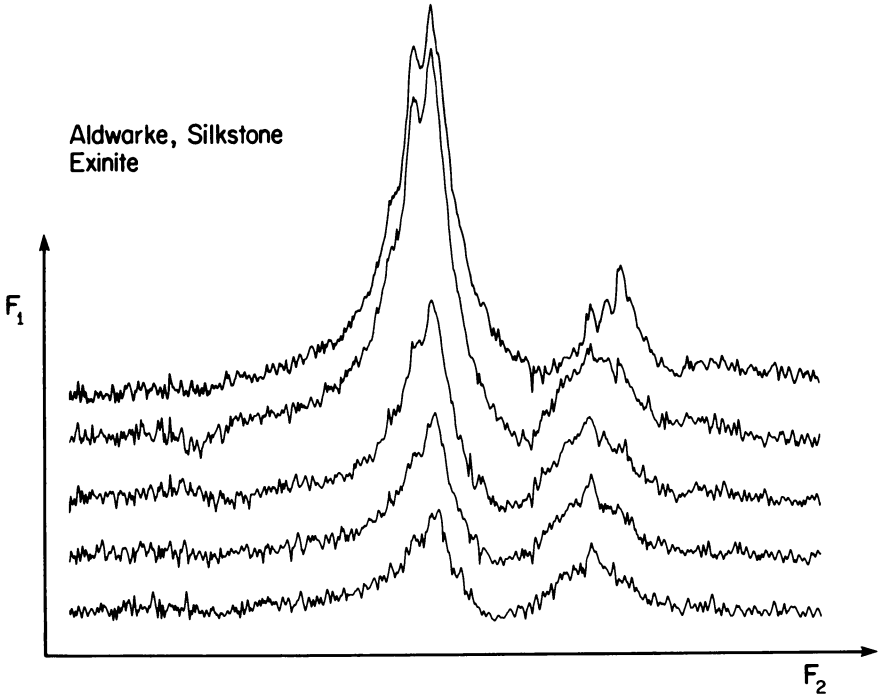


Figure 5. Spectral slices at 977 Hz intervals taken from Figure 4.

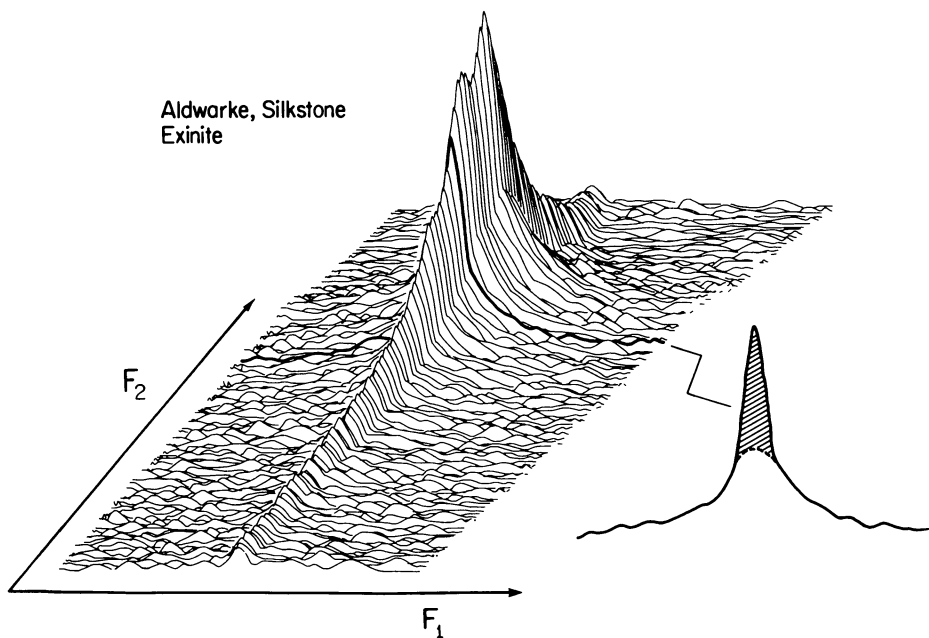


Figure 6. Three dimensional plot of aromatic region. Shaded portion is nonprotonated carbon on top of resonance from protonated aromatic carbon.

Literature Cited

1. P. W. Van Krevelen, "Coal" Elsevier Publishing Company, New York, 1961.
2. B. S. Ignasiak, T. M. Ignasiak, and N. Berkowitz, *Reviews in Analytical Chemistry*, 1975, 2, 278.
3. G. L. Tingey, and J. R. Morrey, "Coal Structure and Reactivity", TID-16627 Batelle Pacific Northwest Labs, Richland Washington, 1973.
4. R. M. Davidson, "Molecular Structure of Coal" IEA Coal Research, London, 1980.
5. J. W. Larsen, "Organic Chemistry of Coal" ACS Symposium Series 71, Washington, D. C. 1978.
6. C. Karr, "Analytical Methods for Coal and Coal Products", Vol. I-III, Academic Press, New York, 1978.
7. H. L. Retcofsky, *Applied Spectroscopy*, 1977, 31, 166.
8. S. K. Chakrabarty, and H. O. Kretschmer, *Fuel*, 1974, 53, 132.
9. J. L. Huston, et al, *Fuel*, 1976, 55, 281.
10. A. Pines, H. G. Gibby, and J. S. Waugh, *J. Chem. Physics*, 1973, 59, 569.
11. D. L. VanderHart, and H. L. Retcofsky, *Fuel*, 1976, 55, 202.
12. V. J. Bartuska, G. E. Maciel, J. Schaefer, and E. O. Stejskal, *Fuel*, 1977, 56, 354.
13. V. J. Bartuska, G. E. Maciel, and F. P. Miknis, "C-13 NMR Studies of Coals and Oil Shales," American Chemical Society, Division of Fuel Chemistry, Preprints, 1978, 23.
14. K. W. Zilm, R. J. Pugmire, D. M. Grant, W. A. Wiser, and R. E. Wood, *Fuel*, 1979, 58, 11.
15. K. W. Zilm, R. J. Pugmire, S. R. Larter, J. Allen, and D. M. Grant, *Fuel*, 1981, 60, 717.
16. R. J. Pugmire, D. M. Grant, S. R. Larter, J. Allen, A. Davis, W. Spackman, and J. Sentfle, *New Approaches in Coal Chemistry*, ACS Symposium Series No. 169, 1981, p 23.
17. R. J. Pugmire, K. W. Zilm, W. R. Woolfenden, D. M. Grant, G. R. Dyrkacz, C. A. A. Bloomquist, and E. P. Horwitz, *Proceedings of the International Conference on Coal Science*, Dusseldorf, Germany, September 7-9, 1981, p. 798-806.
18. R. J. Pugmire, K. W. Zilm, W. R. Woolfenden, D. M. Grant, G. R. Dyrkacz, C. A. A. Bloomquist, and E. P. Horwitz, *Carbon-13 NMR Spectra of Macerals Separated from Individual Coals*, *Org. Geochem.*, 1982, 4, 79.
19. A. Pines and D. E. Wemmer, "Developments in Solid State NMR and Potential Applications to Fuel Research", ACS Division of Fuel Chemistry, Preprints, 1978, 23, 15.
20. N. C. Deno, B. A. Greigger, and S. G. Stroud, *Fuel*, 1978, 57, 455.
21. S. J. Opella, and M. H. Fry, *J. Amer. Chem. Soc.*, 1979, 101, 5854.
22. S. J. Opella, M. H. Fry, and T. A. Cross, *J. Amer. Chem. Soc.*, 1979, 101, 5856.

23. B. C. Gerstein, P. D. Murphy, and L. M. Ryan, "Aromaticity in Coal" in *Coal Structure*, Ed., R. A. Meyers, Academic Press, New York, 1982, pp. 87-129.
24. P. D. Murphy, B. C. Gerstein, V. L. Weinberg, and T. F. Yen, *Anal. Chem.*, 1982, **54**, 522.
25. P. D. Murphy, T. J. Cassidy, and B. C. Gerstein, *Fuel*, 1982, **61**, 1233.
26. K. W. Zilm, D. W. Alderman, and D. M. Grant, *J. Mag. Res.*, 1978, **30**, 563.
27. See also M. J. Sullivan and G. E. Maciel, *Anal. Chem.* 1982, **54**, 1615.
28. The quantitative nature of this assumption has been studied in our laboratory on a set of six different coals ranging in rank from lignite to anthracite. The average correction factor for nonprotonated aromatic carbons is 6%. See M. A. Wilson, L. B. Alemany, W. R. Woolfenden, R. J. Pugmire, P. H. Given, D. M. Grant, and J. Karas, "Carbon Distribution in Coals and Coal Macerals as Determined by CP/MAS ¹³C NMR Studies", submitted for publication.
29. G. R. Dyrkacz and E. P. Horwitz, *Fuel*, 1982, **61**, 3.
30. G. R. Dyrkacz, C. A. A. Bloomquist and E. P. Horwitz, *Sep. Sci. and Tech.*, 1981, **15**, 1571.
31. L. B. Alemany, R. J. Pugmire, D. M. Grant, T. D. Alger, and K. W. Zilm, Cross Polarization and Magic Angle Spinning NMR Spectra of Model Organic Compounds III. The Effect of Dipolar Interaction on Cross Polarization and Carbon-Proton Dephasing, *J. Am. Chem. Soc.*, in press. The dipolar dephasing data on an Illinois No. 6 coal has allowed the semi-quantitative separation of methyl, CH₂ plus aliphatic methine, and protonated and nonprotonated aromatic carbons, L. B. Alemany, D. M. Grant, R. J. Pugmire, and L. M. Stock, Solid State Magnetic Resonance Spectra of Illinois No. 6 Coal and Some Reductive Alkylation Products, *Fuel*, (in press).
32. E. F. Rybaczewski, B. L. Beff, J. S. Waugh, and J. S. Sherfinski, *J. Chem. Phys.*, 1977, **67**, 1231.
33. R. E. Richards and R. W. York, *J. Chem. Soc.*, (London), 1960, 2489.
34. H. Tschamler and E. deRuiter, *Coal Science*, R. F. Gould, Ed., *Advances in Chemistry Series 55*, American Chemical Society, Washington, D.C., 1966, p 332.
35. H. N. M. Dormans, F. J. Hutjens, and D. W. Van Krevelen, *Fuel*, 1957, **36**, 321.

RECEIVED January 6, 1984

Relationships Between the Organic Structure of Vitrinite and Selected Parameters of Coalification as Indicated by Fourier Transform IR Spectra

DEBORAH W. KUEHN¹, ALAN DAVIS, and PAUL C. PAINTER

College of Earth and Mineral Sciences, The Pennsylvania State University, University Park, PA 16802

Quantitative data for the organic functional groups in 24 vitrinite concentrates were obtained by FTIR analysis of samples collected from the Lower Kittanning coal seam in western Pennsylvania and eastern Ohio. Absorption areas for aliphatic and aromatic CH groups were determined and compared to selected parameters of coalification in bivariate and principal components analyses. Aliphatic CH₃ and CH groups displayed a slight positive increase with increasing coalification and varied dependently with calorific value and moisture content. Aliphatic CH₂ groups decreased with an increase in coalification and components analysis revealed partial dependent relationships with volatile matter, carbon content, and reflectance. Aromatic bands at 884, 815, 801, and 750 cm⁻¹ representing 1, 2, 3, and 4 adjacent hydrogens, respectively, and total aromatic content all showed strong positive correlations with increasing coalification. Principal components analysis revealed interdependent relationships and similar patterns of variation among these bands. The aromatic bands at 864, 834, and 785 cm⁻¹ exhibited differing patterns of variation and it is suggested that they, in fact, may not be aromatic in nature.

Variations in organic structure of vitrinite concentrates were determined with Fourier transform infrared spectroscopy (FTIR). FTIR is a relatively new method for obtaining quantitative data from the organic constituents of coal and provides spectra of greater quality than conventional infrared spectrometers. The system employs an on-line minicomputer which enables the user to analyze data and perform a variety of mathematical manipulations.

¹Current address: Department of Geosciences, University of Tennessee at Chattanooga, Chattanooga, TN 37402

The objectives of this study were (1) to reveal trends between selected regions of the infrared spectrum and accepted indicators of coalification; (2) to determine the nature and degree of interdependency among these data using statistical analyses; and (3) to evaluate the usefulness of FTIR data in measuring degree of coalification.

Twenty-four vitrinite concentrates were obtained from samples of the Lower Kittanning coal seam in western Pennsylvania and eastern Ohio by hand picking the bright bands in the coal. A location map of sample sites with their designated identification numbers is given in Figure 1. The Lower Kittanning seam is well suited for this study because it is known to display a broad range of coalification (high volatile B to low volatile bituminous). Some chemical and optical parameters of coalification are reported in Table I for the vitrinite concentrates. Total vitrinite content is included as an indication of sample purity.

Equipment

FTIR analyses were performed on a Digilab FTS 15/B spectrophotometer having a spectral range of 10,000 - 10 cm^{-1} . The system is calibrated automatically with a helium-neon laser and is accurate to 0.2 cm^{-1} . The on-line computer system is a 16 bit/word mini-computer containing 32 K words of memory. Disk storage of 256 K words contains the system programs, user programs, and infrared data, among others.

Sample Preparation

Pressed disks were prepared from a mixture containing 300.0 mg of potassium bromide and 1.2 mg of coal. This mixture was ground in a vibrating mill for 30 sec and placed in a desiccator for 24 h. After drying, the mixture was pressed under vacuum for 1 min using 9000 kg of load.

Potassium bromide was selected as the binder because it does not have specific absorption bands in the mid-infrared region although it does absorb water readily. Water masks the OH absorption at 3400 cm^{-1} , making interpretation of this region difficult.

Utilizing such small weights of coal (1.2 mg) in each disk can permit relatively large sampling errors. Previous experiments on the reproducibility of such small samples have revealed nonsignificant errors over the spectral regions under investigation. The average standard error was found to be $\pm 3\%$.

Procedure

Vitrinite concentrates were analyzed in the mid-infrared region between 3800 and 450 cm^{-1} using a spectral resolution of 2 cm^{-1} . Four hundred scans were co-added for each sample and a ratio was

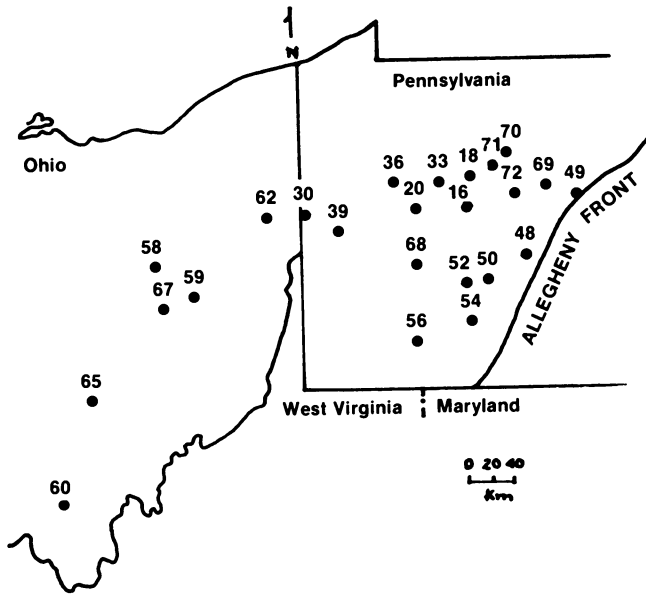


Figure 1. Sample sites of vitrinite concentrates from the Lower Kittanning seam.

Table I. Chemical and Petrographic Data for Vitrinite Concentrates

ID #	Total Vitrinite (mmf) Vol %	C (dmmf)	H (dmmf)	Moisture (mmf)	Volatile Matter (dmmf)	Calorific Value (mmmf)	Reflectance in Oil, %
16	98.4	86.6	5.6	2.1	33.3	15085	1.03
18	98.1	85.8	5.6	2.1	37.6	14883	0.87
20	99.0	85.4	6.0	2.2	40.7	15194	0.83
30	98.4	84.6	5.2	3.1	35.5	14407	0.89
33	99.0	83.0	5.3	2.1	39.4	14674	0.87
36	98.8	84.3	5.3	2.6	34.9	14405	0.96
39	98.8	85.1	5.7	1.8	40.7	15127	0.83
48	97.8	88.8	5.4	1.0	29.8	15628	1.19
49	98.0	88.3	5.3	0.9	26.4	15643	1.34
50	94.2	90.1	5.2	0.8	24.2	15846	1.43
52	97.6	91.3	4.8	1.0	21.8	15854	1.50
54	89.3	89.8	4.7	1.8	18.5	15378	1.71
56	98.4	89.4	5.3	1.2	30.7	15738	1.14
58	98.8	83.7	5.3	7.4	40.7	13675	0.55
59	95.5	83.3	5.6	4.1	42.0	14208	0.60
60	98.6	80.2	5.3	7.1	37.7	12932	0.60
62	98.8	84.7	5.5	3.7	36.4	14357	0.80
65	96.5	82.2	5.3	6.7	37.8	13407	0.64
67	97.8	83.2	5.6	5.4	41.4	13891	0.57
68	99.2	87.0	5.5	1.6	38.0	15441	0.92
69	96.1	85.2	5.2	1.1	28.9	15595	1.26
70	96.8	87.3	5.6	2.2	36.8	15278	0.89
71	96.2	85.5	5.6	2.4	33.6	14780	1.03
72	97.4	88.7	5.6	1.3	25.9	15703	1.31

taken to 400 scans of the atmosphere within the sample chamber. This step removed the effects of any water vapor which was not eliminated by the normal purge of the sample chamber with dry air.

Several computer programs were employed on the Digilab system for the adjustment of spectra. In order to eliminate effects due to variation in sample weights, all spectra were normalized to 1 mg using appropriate scaling factors. Also, a program for spectral subtraction was used to remove mineral calcite which appears as a small shoulder on the 864 cm^{-1} band in the aromatic out-of-plane bending region (1). Other techniques used to obtain quantitative data were derivative spectroscopy, integration, and least-squares curve fitting.

A typical infrared spectrum of a vitrinite concentrate is presented in Figure 2. Three regions of this spectrum are of interest here: aromatic stretching between 3100 and 3000 cm^{-1} , aliphatic stretching between 3000 and 2750 cm^{-1} , and aromatic out-of-plane bending between 900 and 700 cm^{-1} . Quantitative data were obtained for these regions both by integration and least-squares curve fitting. Integration is a method for determining the area under a selected region of the spectrum. It can provide data very quickly; however, it cannot provide data from the individual absorption bands found within a region. Least-squares curve fitting is a method which resolves a region into component bands. In a least-squares analysis, parameters are selected so that the differences between observed data and data calculated from a model are minimized (2). First, the number of major component bands is ascertained by taking the second derivative of the spectrum. Derivative spectroscopy enhances very weak shoulders in spectra so long as the peaks are separated by more than half their halfwidth. Details of this technique, as applied to these spectral regions, are reported elsewhere (1, 3, 4). Weak absorption in the aromatic stretching region does not permit the use of derivative spectroscopy, so individual component bands were not obtained. Second, a suitable mathematical function for characterizing the observed band shapes is chosen. Maddams (5) recently has reviewed methods for curve fitting and suggested employing a Lorentzian band shape. Other workers have used products or sums of Gaussian and Lorentzian curves (6, 7). Solomon, *et al.* (8) used Gaussian band shapes, exclusively. Our method was adopted from Jones, *et al.* (9) who obtained their best results using a sum of Gaussian and Lorentzian functions. In this study, curve fitting was performed on the aliphatic stretching region (using five component bands) and the aromatic out-of-plane bending region (using seven component bands). Table II lists the peak locations and assigned functional groups for both of these regions. The peak locations were not held constant for all samples so that the wavenumbers reported in Table II represent average values. When curve fitting was completed, areas for the component bands were calculated by integration.

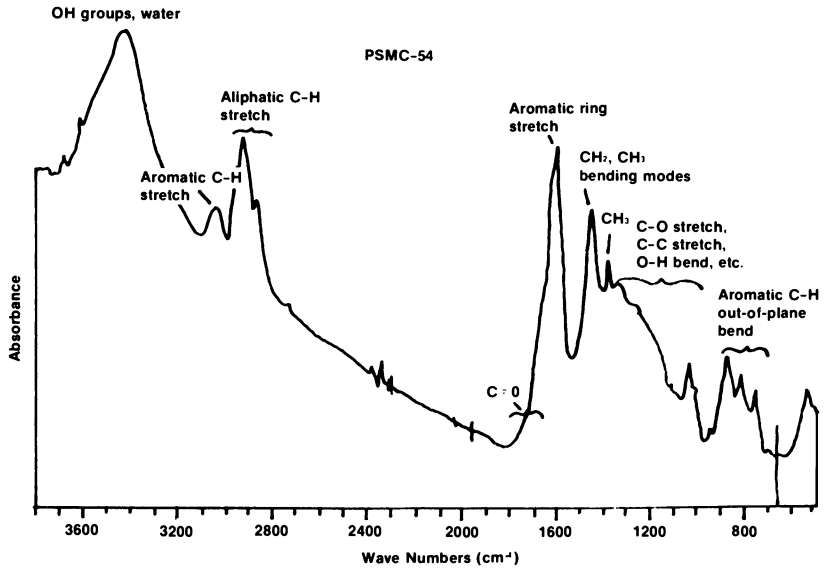


Figure 2. FTIR spectrum of a vitrinite concentrate.

Table II. Band Assignments for the Aliphatic Stretching and Aromatic Out-of-plane Bending Regions

Region	Peak Position (cm^{-1})	Assignment
Aliphatic Stretching	2956	CH ₃ groups (asymmetric stretch)
	2923	Composite of CH ₃ & CH ₂ (asymmetric stretch)
	2891	CH groups
	2864	CH ₃ groups (symmetric stretch)
	2853	CH ₂ groups (symmetric stretch)
Aromatic Out-of-plane Bending	884	1 Adjacent Hydrogen
	864	1 Adjacent Hydrogen
	834	Possible aliphatic rocking & secondary aromatic out-of- plane bending modes
	815	2 Adjacent Hydrogens
	801	3 Adjacent Hydrogens
	785	Possible isolated and 2 adjacent CH ₂ units
	750	4 Adjacent Hydrogens

Results and Discussion

Quantitative FTIR data were combined with chemical and petrographic data for the 24 vitrinite concentrates and subjected to bivariate and multivariate statistical analyses in order to identify the effects of coalification on the aliphatic and aromatic functional groups.

Bivariate Analysis. Correlation coefficients were calculated for every possible pair of variables in order to determine the nature and degree of linear interdependence between them. The correlation coefficient (r) ranges from +1 to -1, with the end members indicating a complete linear dependence and a zero indicating complete independence. A positive value for r indicates a direct relationship exists between a given pair of variables and a negative value signifies an inverse relationship. The significance of each r value was determined by comparison to tabled values (10). At the 95% confidence level, a correlation coefficient must exceed 0.404 to be significant based on a sample set of twenty-four. Anything less than 0.404 is nonsignificant, meaning it can be explained by random error.

Data obtained both by integration and least-squares curve fitting are compared in order to reveal possible differences in the quality of data produced. Integration over a spectral region takes only the time needed to input the information, whereas curve fitting may take 30 min to resolve the component bands be-

fore integration can be performed. Therefore, curve fitting should improve the results to justify its use. Table III lists correlation coefficients for both methods with selected parameters of coalification. Total area by curve fitting is obtained by adding the integrated areas of the component bands. There is little difference in correlation coefficients for total aliphatic CH; some correlations are higher for area by curve fitting, some are lower. All but the correlations with moisture and calorific value are nonsignificant. Therefore, curve fitting does not appear to improve the data for total area of aliphatic CH groups. The remaining significant correlations are low and suggest only a slight increase in aliphatic content as coalification increases.

Areas determined by integration both before and after curve fitting produce significant correlations with parameters of coalification for the aromatic out-of-plane bending region. However, correlation coefficients for the area obtained after curve fitting are consistently higher. Only five of the seven bands reported in Table II for this region are included in the total area by curve fitting because two bands do not appear to be aromatic in nature. Bands representing both isolated and two adjacent CH₂ units were reported at 834 and 785 cm⁻¹ by Drushel, *et al.* (11) and supported by Painter, *et al.* (12). These must be included, however, in the total area obtained by integration and probably account for the lower correlations using this method alone.

Also included in Table III is the integrated area for the aromatic stretching region. This region exhibits some of the highest correlations with parameters of coalification and appears to be a slightly better indicator of degree of coalification than the aromatic out-of-plane bending region.

A comparison of the two methods for obtaining data for total aromatic CH reveals that least-squares curve fitting is justified for the aromatic out-of-plane bending region, producing higher correlation coefficients than integration alone. However, the highest correlations are obtained for the aromatic stretching region by integration, which suggests that this region should be used for determining aromatic CH content.

Although least-squares curve fitting may not be a useful method in determining total area of a given spectral region, it does supply information on component bands not obtainable by integration alone. Areas for the component bands in the aliphatic stretching and aromatic out-of-plane bending regions are compared to the same parameters of coalification and presented as a correlation matrix in Table IV. No one parameter shows the best overall correlations with all bands. Calorific value gives the best correlations for five cases, vitrinite reflectance and elemental carbon each for three, and volatile matter for one.

The correlation coefficients for the aliphatic bands at 2956 and 2864 cm⁻¹, both of which belong to CH₃ groups, are inexplicably different. The asymmetric CH₃ stretch at 2956 cm⁻¹ produces

Table III. Correlations Between Methods of Determining Total Areas of Aliphatic and Aromatic Regions and Parameters of Coalification

	Carbon (dmmf)	Moisture (mmf)	Volatile Matter (dmmf)	Calorific Value (btu/lb, mmmf)	Reflectance in Oil, %
Aliphatic Stretching Region					
Integration	0.203	-0.489	0.266	0.475	-0.056
Least-squares Curve Fitting	0.274	-0.501	0.185	0.528	0.019
Aromatic Out-of-plane Bending Region					
Integration	0.867	-0.675	-0.683	0.783	0.743
Least-squares Curve Fitting	0.903	-0.749	-0.800	0.830	0.868
Aromatic Stretching Region					
Integration	0.888	-0.728	-0.932	0.821	0.965

Table IV. Correlation Matrix for Areas of FTIR Absorption Bands and Parameters of Coalification

Areas (dmmf) (Band Location, cm ⁻¹)	Carbon (dmmf)	Moisture (mmf)	Volatile Matter	Calorific Value (btu/lb, mmmf)	Reflectance in Oil, %
2956	0.659	-0.817	-0.421	0.849	0.585
2923	0.549	-0.748	-0.176	0.782	0.374
2891	0.560	-0.733	-0.123	0.768	0.321
2864	0.146	-0.346	0.323	0.377	-0.149
2853	-0.555	0.436	0.837	-0.445	-0.771
Total Aliphatic Area	0.274	-0.501	0.185	0.528	0.019
884	0.846	-0.620	-0.877	0.709	0.904
864	0.732	-0.697	-0.516	0.734	0.604
834	0.244	-0.218	0.124	0.225	-0.024
815	0.847	-0.716	-0.738	0.790	0.797
801	0.877	-0.691	-0.862	0.769	0.914
785	0.667	-0.574	-0.502	0.639	0.589
750	0.909	-0.765	-0.837	0.849	0.911
Total Aromatic Area	0.903	-0.749	-0.800	0.830	0.868

significant and higher correlations compared to the symmetric CH_3 stretch at 2864 cm^{-1} whose correlations are nonsignificant. This suggests that the assignment for the band at 2864 cm^{-1} should be re-examined. As shown in Figure 3, area of the 2956 cm^{-1} band increases as coalification (calorific value) increases. A calculated r^2 value of 72% means that coalification expressed by calorific value explains 72% of the variability observed in aliphatic CH_3 groups. A similar direct relationship is found between the area at 2891 cm^{-1} (assigned to lone CH groups) and calorific value. Finally, the symmetric CH_2 stretch at 2853 cm^{-1} shows the only indirect relationship with increasing coalification (Figure 4) with an r^2 of 70% (volatile matter is highest for low levels of coalification).

Correlation coefficients for the composite of CH_2 and CH_3 stretch at 2923 cm^{-1} suggest that the contribution of CH_2 is only minor. Not only are the values closer to those for asymmetric CH_3 stretch but, more important, they are positive. If the contributions of CH_2 and CH_3 to the 2923 cm^{-1} band were nearly equal, it would seem likely that their opposing trends would cancel and no significant correlations would be observed for this band.

Total aliphatic area has a positive correlation with coalification for moisture and calorific value; however, the correlations are weak. The highest r^2 value obtained is only 28%. The reason for the low correlations is the inverse relationship with increasing coalification shown by CH_2 groups at 2853 cm^{-1} . If the trend had been positive, the correlations for total area probably would have been higher.

The aromatic out-of-plane bending region has consistently higher correlations with parameters of coalification than the aliphatic region and all of them vary directly with increasing coalification. Figures 5 and 6 show examples of trends for the bands at 884 and 750 cm^{-1} having r^2 values of 82% and 83%, respectively. The data suggest that any one of the aromatic bands would appear to work equally well in expressing the degree of coalification of the coal. Since their trends show the same patterns with coalification, it is not surprising that the total aromatic area also shows high positive correlations with increasing coalification.

Some workers have reported that under increasing coalification the degree of substitution within aromatic units decreases, meaning that more hydrogens are attached to the aromatic nucleus (13-15). This finding also is suggested here. Although the band at 884 cm^{-1} assigned to one adjacent hydrogen shows the same positive correlation with coalification as the band at 750 cm^{-1} assigned to four adjacent hydrogens, the slopes of the lines in Figures 5 and 6 are different. The slope for area at 884 cm^{-1} versus reflectance is 145.4, whereas for 750 cm^{-1} it is 204.5. Therefore, the intensity of the 750 cm^{-1} band increases at a greater rate than the band at 884 cm^{-1} as coalification increases.

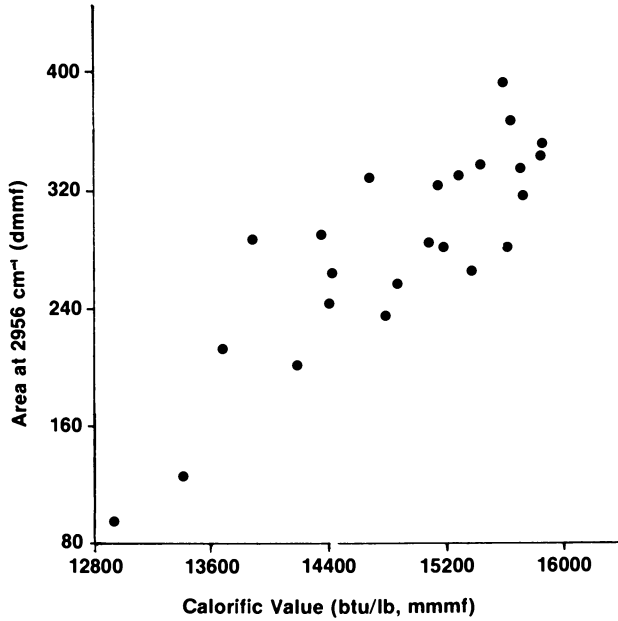


Figure 3. Spectral area for aliphatic CH₃ groups at 2956 cm⁻¹ (curve fitting) vs. calorific value.

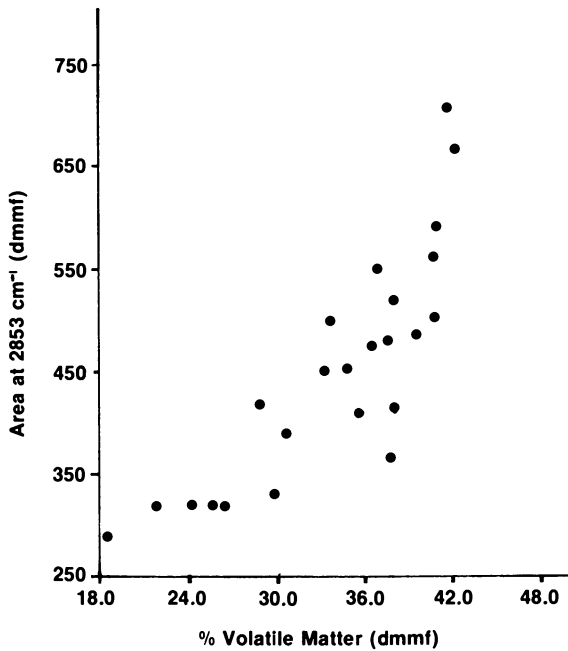


Figure 4. Spectral area for aliphatic CH₂ groups at 2853 cm⁻¹ (curve fitting) vs. volatile matter.

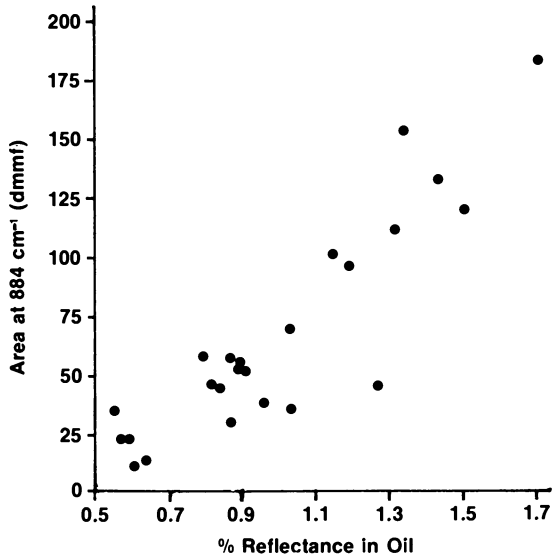


Figure 5. Spectral area for aromatic 1 adjacent hydrogen at 884 cm^{-1} (curve fitting) vs. reflectance.

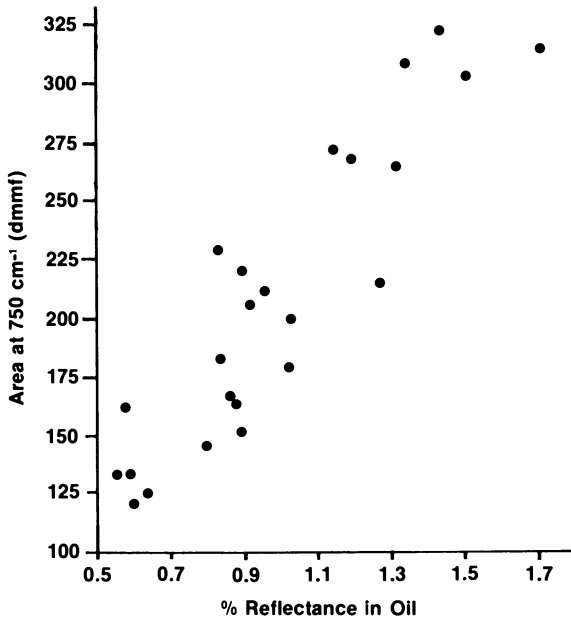


Figure 6. Spectral area for aromatic 4 adjacent hydrogens at 750 cm^{-1} (curve fitting) vs. reflectance.

Total area for the aromatic stretching region from 3100 - 3000 cm^{-1} (determined by integration alone) versus reflectance produced the highest correlation, and therefore, the highest r^2 value obtained in the correlation analysis ($r^2=93\%$); the plot is shown in Figure 7. This suggests that, if component bands could be extracted within this region, they also would have similar high correlations with parameters of coalification.

Principal Components Analysis. The purpose of a principal components analysis is to identify existing patterns of variation when all variables are analyzed simultaneously. The analysis uses the entire correlation matrix as input and groups the variables showing similar patterns of variation into separate components. Each component thus provides an independent source of information. When several variables load on a given component, they are considered to be redundant. The first component extracted explains the greatest percentage of the variation within the data set, the second component explains the next highest percentage of variation not explained by the first, and so on.

Principal components analysis was carried out on an IBM 370 computer using the program CORFAN (16). Two criteria were considered in choosing the best number of components to extract. First, the eigenvalues ($\text{Sum } \lambda_j$) were examined. In order to be considered significant, the eigenvalue of each component extracted should be greater than 1 (17). Each component, then, would explain at least as much variation as any one of the variables. The communality of a variable (the total amount of its variation retained in the extracted components) was the second consideration. A communality of 1.0 means that all the variance of a variable has been retained. In this study additional components were extracted until the communalities were greater than 0.8 (80% of the variation accounted for). After all the components were extracted, the matrix was rotated (18) and the component loadings were recalculated. If the rotated matrix yielded more information than the unrotated, it was used in the interpretation in place of the unrotated matrix.

Before the FTIR data were analyzed together with coalification parameters in a components analysis, it was first necessary to select which variables to use. In general, the number of variables should not exceed one-third of the number of samples (in this study the maximum number is 8). Components analyses were performed on data for the aliphatic stretching and aromatic out-of-plane bending regions of the infrared spectrum in order to eliminate those variables that did not provide new information. The results of a components analysis for the aliphatic stretching region are shown in Table V. The loadings of a variable to the components are similar in nature to correlation coefficients, therefore, the critical value used for significance at the 95% probability level is 0.404 (10). Only the significant loadings are given in Table V. Component 1 contains five variables and

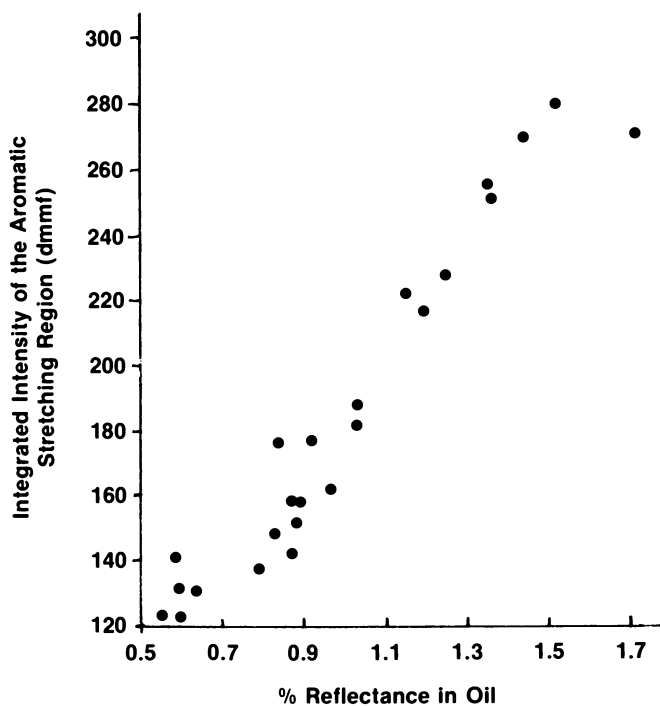


Figure 7. Spectral area for the aromatic stretching region from 3100-3000 cm^{-1} (integration only) vs. reflectance.

explains 69.0% of the total variation. Therefore, these five variables vary in the same manner and each variable provides the same information. Component 2 contains three variables, all varying in the same manner, and explains 26.6% of the variation. The band at 2853 cm^{-1} loads entirely on this component whereas the band at 2864 cm^{-1} shows partial loading. Consequently, the total area is split and loads partially on both components. This split loading may be a result of differing responses of these stretching modes to increasing coalification.

Table V. Rotated Matrix of Factor Loadings for Components
Analysis of FTIR Absorption Bands in the
Aliphatic Stretching Region

Band Location (cm^{-1})	C1	C2	Communalities
2923	0.988		0.979
2956	0.957		0.940
2891	0.956		0.918
Total Area	0.870	-0.485	0.993
2864	0.756	-0.593	0.924
2853		-0.987	0.979
$\sum \lambda_i^2$	4.138	1.593	
% Variation Explained	68.96	26.56	
Cumulative Variation Explained	68.96	95.52	

Some peculiarities were revealed when the band assignments for this region were considered. The band at 2923 cm^{-1} had the highest loading on component 1, yet it is a composite of asymmetric CH_2 and CH_3 stretch. It would be reasonable to assume that it should have been split, loading partially with the band at 2853 cm^{-1} assigned to symmetric CH_2 stretch. The band at 2864 cm^{-1} whose loading was split, is assigned to symmetric CH_3 stretch, but the asymmetric CH_3 stretch at 2956 cm^{-1} loaded entirely on component 1. This suggests that the band at 2864 cm^{-1} may in reality be a composite of bands. Two bands from this region were chosen for further components analysis: 2956 and 2853 cm^{-1} ; each providing an independent source of information.

Results of the components analysis for areas of the aromatic out-of-plane bending region are shown in Table VI. Three components were extracted with seven of the eight variables loading on component 1. The bands at 884, 815, 801 and 750 cm^{-1} and total area are completely interdependent. This suggests strongly that it is not necessary to resolve the individual bands in the aromatic region, because the total area contains the same information. The bands at 785 and 864 cm^{-1} were split among two and three components, respectively. The split was not surprising for

the band at 785 cm^{-1} because there is doubt about its validity as an aromatic band. The split loadings for the 864 cm^{-1} band, however, were surprising. The bands at 864 and 884 cm^{-1} both have been assigned to one adjacent hydrogen, yet they varied differently in the components analysis. These results suggest that the assignment for the 864 cm^{-1} band may be in error and should be re-examined. The loading of the 834 cm^{-1} band on component 3 indicates that this band is not aromatic in nature. It responds independently of all other aromatic bands. Three bands, 750 , 785 , and 834 cm^{-1} , were chosen from each of the three components for further analysis. In addition, the peak intensities for the bands at 864 and 785 cm^{-1} were included because it was observed that the change in their intensities did not appear to be consistent with their calculated areas. Both peak intensity and bandwidth at half height are used in the calculation of area. Solomon, *et al.* (8) has used a constant bandwidth for a given band in his curve-fitting routine; however a fixed bandwidth produced large standard deviations for our data. This suggested to us that the change in bandwidth is real.

Table VI. Rotated Matrix of Factor Loadings for Components Analysis of FTIR Absorption Bands in the Aromatic Out-of-Plane Bending Region

Band Location (cm^{-1})	C1	C2	C3	Communalities
750	0.935			0.939
884	0.922			0.930
801	0.886			0.930
Total	0.880			0.994
815	0.856			0.947
864	0.605	-0.483	-0.485	0.833
785	0.458	-0.848		0.979
834			-0.965	0.964
Sum λ_i^2	4.603	1.514	1.399	
% Variation Explained	57.54	18.92	17.49	
Cumulative Variation Explained	57.54	76.46	93.95	

Components analyses were performed next on variables selected from FTIR analyses together with some parameters of coalification. A preliminary components analysis on these parameters revealed that calorific value and moisture content were completely interdependent, so calorific value will be used here to represent both. In Table VII aliphatic CH_3 groups at 2956 cm^{-1} show complete dependency with calorific value on component 1. The aliphatic bands at 2923 and 2891 cm^{-1} also would show similar results because they were found to vary dependently with the band at 2956 cm^{-1} in

Table V. The band at 750 cm^{-1} is split evenly on three components so its presence is only partially related to calorific value. The bands at 884 , 815 , and 801 cm^{-1} and total aromatic content would show the same relationship.

Table VII. Rotated Matrix of Factor Loadings for Components Analysis of Selected FTIR Absorption Bands and Calorific Value

	C1	C2	C3	C4	Communalities
2956 cm^{-1}	0.959				0.957
Calorific Value	0.842				0.936
864 cm^{-1} *	0.698		-0.456		0.913
750 cm^{-1}	0.534	-0.563	-0.526		0.894
785 cm^{-1}	0.436	-0.731			0.840
785 cm^{-1} *		-0.921			0.932
2853 cm^{-1}			0.969		0.976
834 cm^{-1}				-0.981	0.989
Sum λ_j^2	2.654	1.988	1.589	1.219	
% Variation Explained	33.18	24.85	19.86	15.24	
Cumulative Variation Explained	33.18	58.03	77.89	93.13	
*Values for peak heights were used in place of areas					

Three variables are independent of coalification expressed by calorific value. The peak intensity of the band at 785 cm^{-1} loads entirely on component 2 although its area is split on two components. The symmetric CH_2 stretching mode at 2853 cm^{-1} in the aliphatic region loads on component 3 along with small amounts of three other bands. The 834 cm^{-1} band is once again independent of the other variables and also of coalification.

A components analysis containing volatile matter is shown in Table VIII. Volatile matter is split into two components, the largest loading being on component 1. Therefore, it contains two independent sources of information. No infrared bands show complete dependency with volatile matter. Bands at 2956 , 864 , 785 , and 750 cm^{-1} show partial loading, while the bands at 2956 and 834 cm^{-1} are completely independent.

The components analysis containing vitrinite reflectance is reported in Table IX. Reflectance is split into three components, loading most strongly on component 1. The aromatic bands represented by that at 750 cm^{-1} show complete dependency with reflect-

Table VIII. Rotated Matrix of Factor Loadings for Components Analysis of Selected FTIR Absorption Bands and Volatile Matter

	C1	C2	C3	C4	Communalities
2853 cm ⁻¹	-0.982				0.971
Volatile Matter	-0.825	0.432			0.952
750 cm ⁻¹	0.606	-0.554	-0.439		0.892
864 cm ⁻¹ *	0.513		-0.660		0.921
785 cm ⁻¹ *		-0.909			0.926
785 cm ⁻¹		-0.736	-0.416		0.842
2956 cm ⁻¹			-0.954		0.972
834 cm ⁻¹				-0.978	0.990
Sum λ_j^2	2.400	2.032	1.809	1.232	
% Variation Explained	30.00	25.40	22.61	15.40	
Cumulative Variation Explained	30.00	55.40	78.01	93.41	
*Values for peak heights were used in place of areas					

Table IX. Rotated Matrix of Factor Loadings for Components Analysis of Selected FTIR Absorption Bands and Reflectance

	C1	C2	C3	C4	Communalities
2853 cm ⁻¹	-0.982				0.972
Reflectance	0.747	-0.458	0.414		0.946
750 cm ⁻¹	0.613	0.566	0.427		0.901
864 cm ⁻¹ *	0.522		0.638		0.912
785 cm ⁻¹ *		-0.916			0.928
785 cm ⁻¹		-0.737	0.412		0.842
2956 cm ⁻¹			0.951		0.973
834 cm ⁻¹				-0.981	0.989
Sum λ_j^2	2.286	2.092	1.860	1.232	
% Variation Explained	28.58	26.15	23.26	15.40	
Cumulative Variation Explained	28.58	54.73	78.05	93.39	
*Values for peak heights were used in place of areas					

ance while aliphatic CH groups are only partially dependent. Again, the band at 834 cm^{-1} is independent of coalification expressed by reflectance.

The component loadings for elemental carbon were similar to those for reflectance, and therefore, the same interpretations as above can be made for carbon.

Summary and Conclusions

Statistical analyses were performed on FTIR data from the aliphatic and aromatic regions and selected parameters of coalification for 24 vitrinite concentrates from the Lower Kittanning seam. These analyses were performed for the purposes of revealing trends between infrared data and accepted indicators of coalification and for determining the nature and degree of their interdependency.

The following conclusions are drawn from statistical analysis of FTIR spectra:

1. Areas for the aliphatic and aromatic bands increase as coalification increases except for aliphatic CH_2 at 2853 cm^{-1} whose area decreases. However, trends for the aromatic bands are stronger than those for aliphatic bands.

2. Certain aliphatic and aromatic bands are interdependent, and therefore redundant, in principal components analyses. These are (a) aliphatic CH_3 at 2956 cm^{-1} and aliphatic CH at 2891 cm^{-1} , and (b) aromatic one, two, three, and four adjacent hydrogens at 884 , 815 , 801 , and 750 cm^{-1} , respectively, and total aromatic content. It is only necessary, then, to obtain data for one component from each of these two groups for study.

3. Some FTIR bands can be used to represent existing parameters of coalification because of their interdependent relationships. They are (a) aliphatic CH_3 at 2956 cm^{-1} (and CH at 2891 cm^{-1}) for calorific value and moisture content, and (b) aromatic CH at 750 cm^{-1} (also 884 , 815 , and 801 cm^{-1} bands and total aromatic content) for reflectance and carbon content.

4. Some FTIR bands are independent of certain parameters of coalification and cannot be used to represent them. These are: (a) aliphatic CH_2 at 2853 cm^{-1} for calorific value and moisture content, and (b) aliphatic CH_3 at 2956 cm^{-1} (and CH at 2891 cm^{-1}) for volatile matter.

5. The patterns of variation of some infrared bands suggest that their present functional group assignments should be re-examined. These are: (a) aliphatic asymmetric CH_3 stretch at 2864 cm^{-1} , and (b) aromatic band at 864 cm^{-1} representing one adjacent hydrogen.

6. Results from principal components analyses for the bands at 834 and 785 cm^{-1} support the findings of others that these bands are not aromatic in nature.

Acknowledgments

This work was funded by the United States Department of Energy under contract number DE-AC22-80PC30013.

Literature Cited

1. Kuehn, D. W.; Snyder, R. W.; Davis, A.; Painter, P. C. Fuel 1982, 61, 682-94.
2. Fraser, R. D. B.; Suzuki, E. in "Physical Principles and Techniques of Protein Chemistry"; Leach, S. J., Ed; Academic: New York, 1973; Part C, pp. 301-55.
3. Painter, P. C.; Snyder, R. W.; Starsinic, M.; Coleman, M. M.; Kuehn, D. W.; Davis, A. Appl. Spectrosc. 1981, 35, 475-85.
4. Painter, P. C.; Snyder, R. W.; Starsinic, M.; Coleman, M. M.; Kuehn, D. W.; Davis, A. in "Coal and Coal Products"; Fuller, E. L., Jr., Ed.; ACS Symposium Series No. 205, American Chemical Society: Washington, D. C., 1982, pp. 47-76.
5. Maddams, W. F. Appl. Spectrosc. 1980, 34, 245-67.
6. Pitha, J.; Jones, R. N. Can. J. Chem. 1966, 44, 3031-50.
7. Vandeginste, B. G. M.; DeGalan, L. Anal. Chem. 1975, 47, 2124-32.
8. Solomon, P. R.; Hamblen, D. G.; Carangelo, R. M. in "Coal and Coal Products"; Fuller, E. L., Jr., Ed.; ACS Symposium Series No. 205, American Chemical Society: Washington, D.C., 1982, pp. 77-131.
9. Jones, R. N.; Seshadri, K. S.; Jonathan, N. B. W.; Hopkins, J. W. Can. J. Chem. 1963, 41, 750-62.
10. Arkin, H.; Colton, R. R. "Tables for Statisticians"; Harper and Row: New York, 1963; p. 155.
11. Drushel, H. V.; Ellerbe, J. S.; Cos, R. C.; Lane, L. H. Anal. Chem. 1968, 40, 370-9.
12. Painter, P. C.; Yamada, Y.; Jenkins, R. G.; Coleman, M. M.; Walker, P. L., Jr. Fuel 1979, 58, 293-7.
13. Brown, J. K. J. Chem. Soc. 1955, Part I, 744-52.
14. Retcofsky, H. L. Appl. Spectrosc. 1977, 31, 116-21.
15. British Carbonization Research Association (BCRA), "An Infrared Spectroscopic Study of the Influence of Oxygen in Coal on the Plastic Stage of the Coking Process", Carbonization Research Report 64, 1979, 22 pp.
16. Ondrick, C. W.; Srivastava, G. S. "CORFAN - Fortran IV Computer Program for Correlation, Factor Analysis and Varimax Rotation; University of Kansas, 1970; Computer Contribution 42; 92 pp.
17. Davis, J. C. "Statistics and Data Analysis in Geology"; John Wiley and Sons: New York, 1973; Chap. 4.
18. Siegal, B. S.; Griffiths, J. C. The Moon 1974, 9, 397-413.

RECEIVED December 16, 1983

Electron Spin Resonance of Isolated Coal Macerals

Preliminary Survey

B. G. SILBERNAGEL and L. A. GEBHARD

Exxon Research and Engineering Company, Linden, NJ 07036

GARY R. DYRKACZ and C. A. A. BLOOMQUIST

Argonne National Laboratory, Argonne, IL 60439

Electron spin resonance determinations of g -values, linewidths, radical densities and saturation properties have been performed on carbon radicals in samples of coal macerals isolated by density gradient centrifugation techniques. These data are compared with elemental analyses and density measurements. Each maceral type exhibits a different ESR "signature" which can be understood in terms of the nature of the starting organic and the extent of coalification.

There have been a large number of electron spin resonance (ESR) studies of coal and coal products,⁽¹⁾ but a microscopic interpretation of the resulting data has been hampered by the chemical heterogeneity of the coal samples examined. While several surveys of specially selected macerals have appeared^(2,3), the recent evolution of maceral separation techniques⁽⁴⁾ now allows detailed ESR observations to be made on coals systematically fractionated in which coal rank, maceral type, and maceral density are simultaneously distinguished. The present report surveys the behavior of a variety of ESR properties of carbon radicals in exinite, vitrinite, and inertinite macerals in a variety of coals of different rank. These data are compared with other information on the macerals, including: petrographic examination, elemental analyses, physical density, and fractional aromaticity.⁽⁵⁾ The combination of microscopic ESR information with that from other techniques provides a new dimension in understanding these materials.

These ESR observations focus on carbon radicals, unpaired electrons in the carbonaceous matrix of the macerals associated with incomplete carbon bonds. In the macerals surveyed here, these radical densities span a substantial range of values: from $\sim 4 \times 10^{18}$ radical spins/g-carbon for some subbituminous

vitritinities to $\sim 3 \times 10^{20}$ spins/g-carbon for certain inertinites. This corresponds to one such unpaired electron per 13,000 carbon atoms for the subbituminous vitrinite, to one electron per 170 carbon atoms for the inertinite. Assuming that a typical structural element in the coal might have a molecular weight ~ 1000 (i.e., ~ 70 carbon atoms), this variation in radical number spans the range from nearly complete isolation of the resulting electrons (one electron per 200 structures in the subbituminous case) to close proximity (one electron for every two or three such structures for the inertinites). Since the intermediate radical concentrations are well represented, particularly for vitritinities of varying rank, the changes which occur as the number and type of radicals vary can be traced. The carbon radical ESR spectrum has a number of characteristic features which can be determined and related to the chemistry and history of the coal maceral.(6,7)

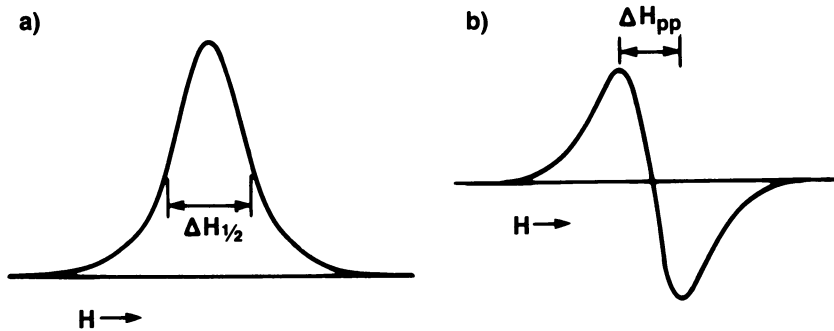


Figure 1. A schematic reproduction of the ESR absorption (a) and its derivative, with definitions of the quantities $\delta H_{1/2}$ and ΔH_{pp} .

A generalized form for the microwave absorption and its derivative is shown as function of magnetic field in Figure 1. The "position" of the resonance is commonly expressed in a frequency-independent form called the g-value:

$$g = 0.714492 \nu_0(\text{GHz})/H_0(\text{kG}) \quad (1)$$

where ν_0 is the microwave frequency expressed in GHz and H_0 is the magnetic field at the center of gravity of the ESR absorption spectrum, expressed in kG. For a "free electron", in the absence of any atomic or molecular influences, the g-value is 2.0023. If the electron is located on a molecule, these values shift slightly in ways which depend on the electronic state of

the host molecule occupied by the unpaired electron.(7) The presence of associated heteroatoms will lead to additional shifts of g-value, which can be predicted with considerable confidence.(8)

The width and shape of the ESR spectrum contain information about the environment of the radical. For isolated electrons located on a single structural element in the coal, the width often results from hyperfine interactions of the electron with protons on the molecular sub-units which comprise the element. For radicals isolated on a single type of molecule, a well-resolved spectrum consisting of a number of absorption lines is observed.(9) For the complex molecular forms encountered in coal, this articulation is lost and a single, unresolved line of width, $\Delta H_{pp} \sim 7$ G, is commonly seen (ΔH_{pp} is the splitting between the maxima of the derivative of the ESR absorption as indicated in Figure 1b). Other factors, like dipolar interactions between the magnetic spins of the electrons, can also contribute to increasing the linewidth. Conversely, electron motion, or strong exchange coupling between electrons, can produce a line considerably narrower than the 7 G width mentioned above. We shall discuss examples of both narrowing and broadening in the present study.

The intensity of the absorption signal is proportional to the number of carbon radicals in the sample. Computer-based techniques for integrating the absorption can determine intensity values with a typical accuracy of $\sim \pm 5-10\%$. A variety of factors influence the number of radicals in an organic system: the chemical form of the molecules, the chemical history of the sample, and the accessibility of reagents to the radicals that are generated. Molecular chemistry has a strong influence on the stability of radicals. Aliphatic radicals tend to be highly localized, very energetic, and extremely reactive. Conversely, an excess electron on a polynuclear aromatic molecule delocalizes and is not very energetic or reactive. Such aromatic radicals, if not exposed to a highly-reactive environment, tend to be kinetically, if not necessarily thermodynamically, stable. In addition to aromatic and cationic radicals, certain neutral odd electron molecules like the odd alternate perinaphthyl molecule, are also intrinsically paramagnetic. Issues of molecular chemistry, history, and accessibility will appear in the discussions which follow.

One last factor to consider is the saturation behavior of the carbon radical - its response to an applied microwave field. At low microwave powers the energy which a carbon radical absorbs from the microwave field is dissipated to its environment in a relatively short period of time in a process called spin-lattice relaxation. At sufficiently high microwave powers this relaxation process is no longer able to transfer the microwave energy absorbed by the spins to the environment rapidly enough for the spins to remain in thermodynamic equilibrium. This

deviation from equilibrium is called saturation.⁽¹⁰⁾ Saturation behavior can be quantitatively described, at least in simple cases, and its onset is detected experimentally by determining the integrated intensity of the ESR signal as a function of microwave power. At low powers, the signal varies linearly as a function of the microwave field strength, which corresponds to a variation proportional to the square root of the microwave power level. Thus, the quantity I/\sqrt{P} (I = integrated intensity, P = microwave power) is independent of P at low powers. This ratio decreases with the onset of saturation. Determining the power levels at which saturation occurs can provide valuable information about the coupling of a carbon radical to its environment.

The present sample set (37 samples) is relatively small. However, these data on g-value, linewidth, saturation, and intensity--when used in combination with information on the petrographic and chemical properties of the macerals--lead to the following preliminary conclusions about maceral groups:

- Exinite radicals are relatively few in number and remarkably uniform in g-value, width, and shape. The magnitude of the g-value and its variation with nitrogen content suggest nitrogen proximity to the radical.
- Inertinite radicals have very uniform g values, the magnitude of which suggests association with aromatic molecules. Radical densities can be extremely high (up to 25 x the levels seen in exinites). The linewidths are much narrower than in other maceral types (~1-2 Gauss vs ~7 G for exinites and vitrinites), and both widths and shapes depend sensitively on the maceral "history", as reflected in atomic H/C ratios and the density.
- Vitrinite radicals show a significant variability with coal rank, from subbituminous coals to anthracites. The radicals in subbituminous and high-volatile bituminous-C coals appear strongly oxygen-associated, while higher-rank coals have g values appropriate for aromatic radicals. Linewidths and intensities increase with coal rank. Saturation behavior also varies strongly with rank, suggesting strong radical-environment interactions in the high-rank coals.

Experimental Procedures

Some 37 samples from 16 coals of the Pennsylvania State University coal data base (PSOC) were examined. Separate density fractions were obtained by isopycnic density gradient centrifugation of small (~3 μ m) coal particles in an aqueous CsCl density gradient.⁽⁴⁾ The individual samples are listed by PSOC numbers, coal description, ASTM designation of coal-rank maceral type, and density in Table I. After separation, the samples

Table I. Maceral Resume

(Indicated numbers are maceral densities in g/cm³)

PSOC#	COUNTY, STATE, SEAM	RANK	VITRINITE	EXINITE	INERTINITE
U1*	---, Utah, Hiawatha	--	1.257		
81	Schuykill, PA, Buck Mtn.	an	-----whole coal-----		
106	Owen, IN, Block 1	hvBb	1.291	1.191	1.371
			1.330		1.413
			1.334		1.447
					1.475
151	McKinley, NM, Lower Splits of Blue	hvCb	1.335		
236	Pitkin, CO, Coal Basin B	mvb	1.278		
240	Lewis, WA, Big D	subB	1.407		
268	Wise, VA, Lyons	hvAb	1.272		
285	Williamson, IL, Davis	hvAb	1.276		
297	Mahoning, OH, Ohio #5 Kittaning	hvAb	1.264	1.165	1.340
			1.271	1.040	1.384
			1.305	1.149	1.436
				1.200	
				1.207	
317	Somerset, OH, Lower Freeport	lvb	1.317		
409	Le Flore, OK, Upper Hartshorne	nvb	1.302		
592	Fulton, IL, Illinois #5	hvCb	1.306		
594	Fulton, IL, Illinois #5	hvCb	1.332		
852	Delta, CO, D	hvBb	1.317		
975	Campbell, WY, Anderson	subC	1.408		
1005	Campbell, WY, Canyon A	subC	1.345		
			1.382		
			1.420		
			1.455		
			1.486		

*Not a PSOC coal. Supplied courtesy of Prof. L. Anderson, University of Utah.

were kept under dry nitrogen until they were transferred to ESR tubes and sealed under helium gas. Typical ESR sample weights were approximately 10 mg.

ESR observations were conducted at 9.5 GHz, using a Varian E-line ESR spectrometer with variable temperature capabilities from 90K-300K. The g value was determined using a Varian pitch standard with a g-value of 2.00302 ± 0.00005 . The integrated intensity was also calibrated to a Varian pitch standard. The parameters g, $\Delta H_{1/2}$, ΔH_{pp} and the radical density were determined for each sample. Saturation measurements were made on a selected subset of samples. Low temperature runs at 125 K were made for all inertinite samples, as well as for selected samples of the other maceral types. Little temperature variation in g value, linewidth, or lineshape, was seen in any sample. The integrated intensity varied approximately as 1/T, suggesting Boltzmann polarization of the spins at lower temperatures.

Petrographic analysis of the separated macerals, density determinations, and elemental analyses were performed at Argonne National Laboratories. The ash content of these samples is less than 1%. The oxygen levels reported here are obtained by difference. Computer correlations of the resulting parameters were done using the Statistical Analysis System on the VS/CMS system at the ER&E-Linden site. Linear-regression analyses are also performed with that system. In the correlation plots which follow, samples will be identified by coal rank and maceral group.

Experimental Results

ESR Systematics ($\Delta H_{1/2}$, ΔH_{pp} , Saturation). The ESR absorption for all macerals consists of a single component with no fine structure, as shown in Figure 2. The vitrinite and exinite macerals are generally similar, with widths on the order of 7 G. By contrast, most of the inertinite macerals show narrower lines -- between 0.9 and 2.0 Gauss. Figure 3 shows that the different maceral types are quite clearly distinguishable when examined as a function of ESR radical linewidth and physical density. The exinites are low density ($1.04 - 1.20 \text{ g/cm}^3$) forms, with a nearly constant linewidth of $\sim 6.5 \text{ G}$. Conversely, inertinites have high densities ($\rho > 1.35 \text{ g/cm}^3$), and most have narrow linewidths. Vitrinites are largely intermediate, and the data suggest that vitrinite density decreases--and linewidth increases--with increasing coal rank. Viewed in this figure, two of the samples petrographically identified as inertinites, appear to lie nearly in the vitrinite field.

These observations can be put on a more chemical basis by examining the variation of ΔH_{pp} with the atomic hydrogen-to-carbon ratio (Figure 4). Here, the clustering of exinite properties is even more prominent. The single deviant exinite point comes from a very different organic matter type--alginite, rath-

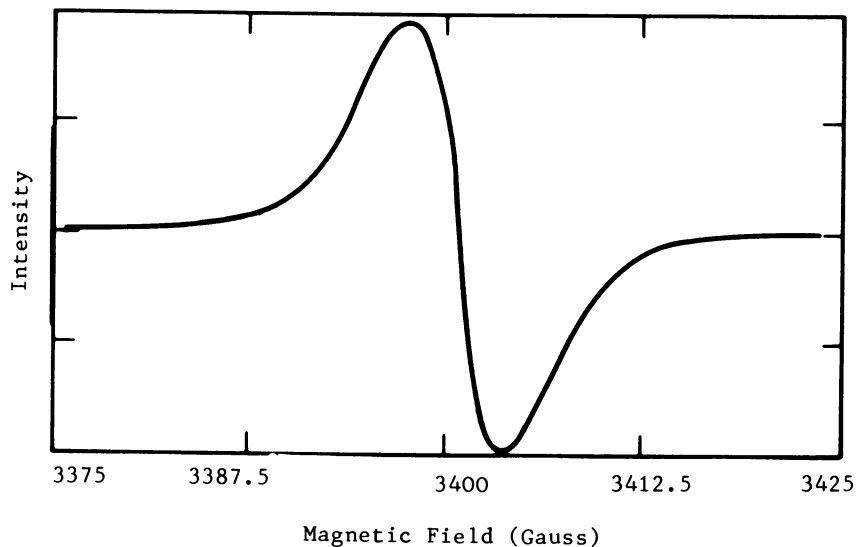


Figure 2. The ESR absorption of a vitrinite maceral sample from PSOC 297 illustrates the broad, fine structure free character of these spectra.

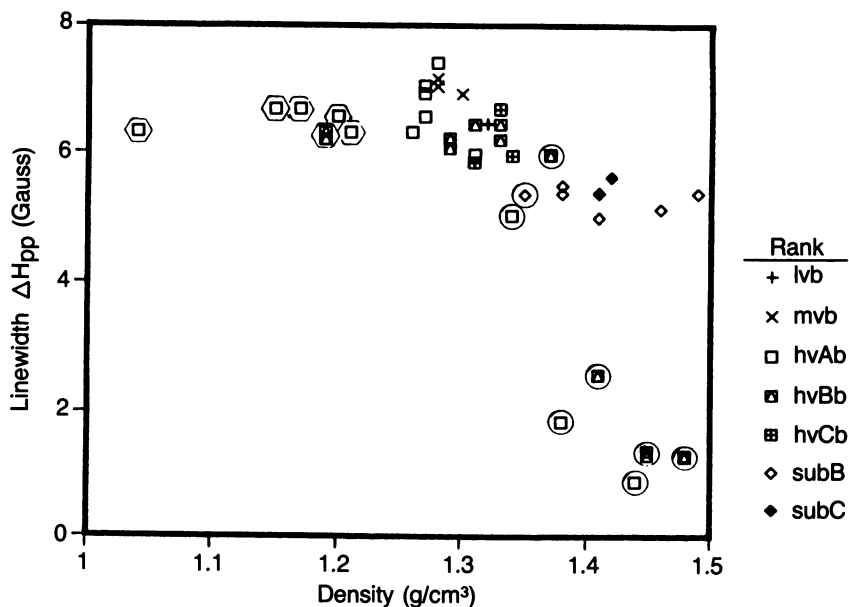


Figure 3. A linewidth, density plot distinguishes exinite (○), inertinite (○), and vitrinite (plain) maceral types.

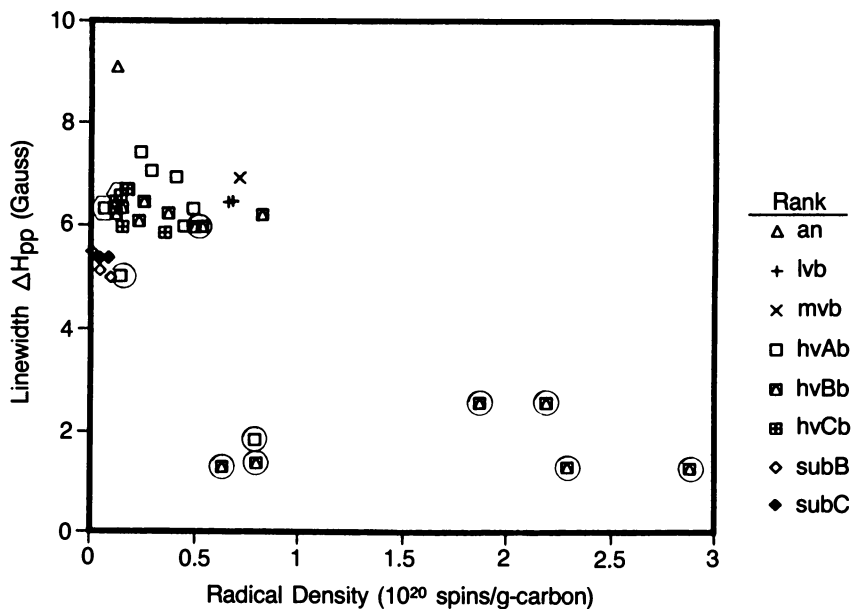


Figure 5. Linewidth increases with radical density for vitrinites but not for inertinites.

These conclusions are also supported by a quantitative analysis of the expected magnitudes of the linebroadening contributions. For low carbon radical densities, as in exinites and subbituminous-C coals, dipolar contributions should be relatively minor and the proton hyperfine broadening should be approximately proportional to the H/C ratio. This appears to be the case since, for exinites, $\Delta H_{pp} \sim 6.5$ gauss and H/C ~ 1.03 while for subbituminous-C coals, $\Delta H_{pp} \sim 5.4$ gauss and H/C ~ 0.88 . The exinite/sub-C linewidth ratio, ~ 1.20 , is similar to the ratio of H/C values 1.17. At higher radical densities a simple estimate of the dipolar interaction strength for the carbon radicals suggests that its contribution should be appreciable. A simple statistical calculation for randomly distributed radicals of density n radicals/cm³ yields the following estimate of the dipole contribution to the linewidth(11):

$$\delta \approx 3.8 \gamma h n \text{ (gauss)} \quad (2)$$

where γ is the electronic gyromagnetic factor and h is Planck's constant. For 10^{19} spins and a density of 1.2 g/cm^3 , appropriate for exinite, $\delta \sim 0.85$ gauss, appreciably smaller than the proton hyperfine contribution. For a high volatile bituminous coal

with 6×10^{19} spins/g and a density of 1.3 g/cm^3 , $\delta \sim 5.5\text{G}$ and appreciable broadening would be expected. The observed ΔH_{00} is not simply the sum of the hyperfine and dipolar contributions and depends on the form of the lineshapes.

An additional probe of the coupling of radicals to their environment is the study of microwave saturation. As outlined in Section I, at low microwave power levels the observed ESR intensity is proportional to the microwave field strength and the number of radicals. At high power levels, the response is no longer linear in microwave field strength, and it no longer reflects the number of radicals in the sample. A plot of Intensity/ \sqrt{P} vs P will be power-independent at low powers and will begin to fall with the onset of saturation. This behavior is shown for three of the macerals in Figure 6. The inertinite sample (from PSOC-106, hvBb) shows only a slight hint of saturation even at high power levels ($\sim 10^5 \mu\text{W}$). An exinite sample (also from PSOC-106) shows a fall-off at substantially lower levels ($\sim 10^3 \mu\text{W}$). The vitrinite sample, of a subbituminous B rank, (from PSOC-240, subB) shows saturation onset in the vicin-

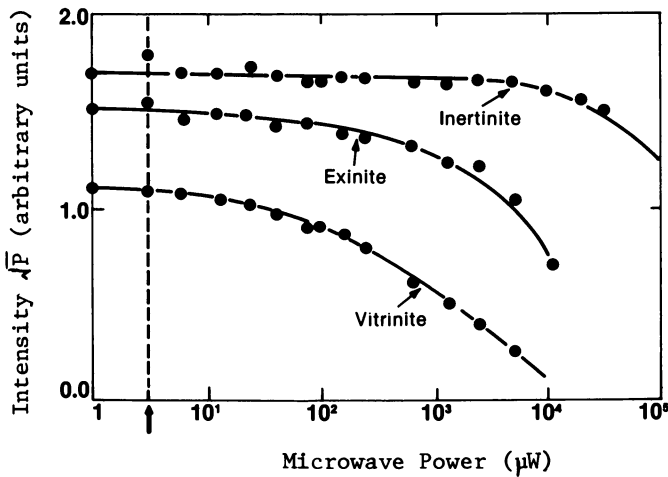


Figure 6: The various maceral types exhibit distinctly different microwave saturation properties.

ity of 10 μ W. Vitrinites of higher rank saturate at higher power levels, and the anthracite sample--the highest rank vitrinite in this sample suite, does not saturate at the highest microwave powers employed (200 mW). To insure a quantitative correlation between ESR intensity and carbon radical densities, all intensity determinations have been performed at 3 μ W, where saturation effects are minimal.

Chemical Correlations. The ESR g-values should provide a measure of heteroatom content of molecules bearing the carbon radical. It is spin-orbit-coupling of the radical electron with the heteroatom which produces the observed shift.⁽¹⁰⁾ It is of considerable interest to see the extent to which the g-value, a measure of the microscopic, molecular chemistry of the radical-bearing molecules, is related to more global measures of the chemistry of the organic species -- notably the elemental analyses. A comparison of g value with atomic O/C (Figure 7) reveals that inertinites and exinites are reasonably tightly clustered.

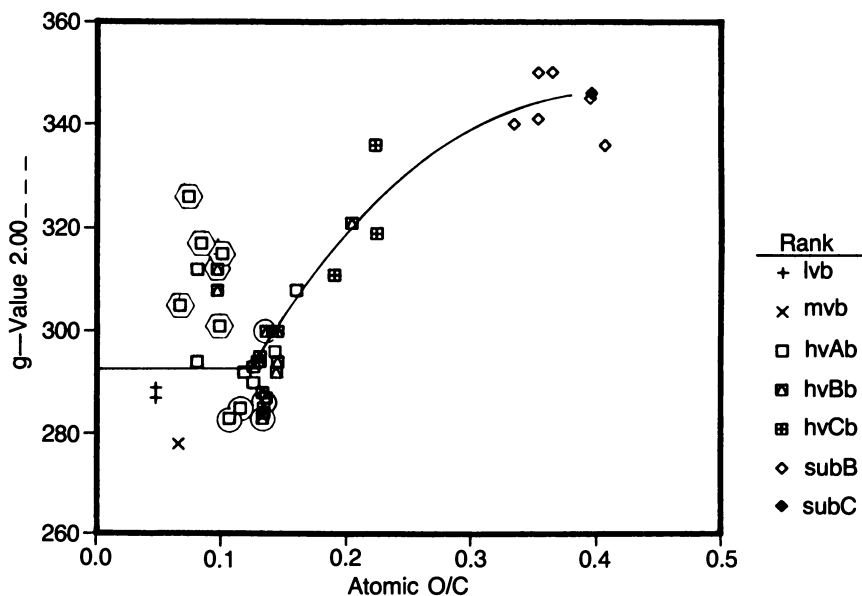


Figure 7. Systematic g-value, O/C variations are observed for vitrinites.

A g of 2.0029 for the inertinites reflects the aromatic character of the radicals and little, if any, heteroatom involvement. Exinites also are fairly tightly grouped, but g values of ~2.0031 are more typical of molecules containing nitrogen. By

contrast, vitrinites span a very broad range of g values, and the variation of g value is highly rank dependent. Subbituminous vitrinites have $g = 2.0034-5$, while the higher rank bituminous coals (lvb, mvb, hvAb) exhibit a value of 2.0029, appropriate for aromatic radicals. There is a pronounced increase in g above 2.0029 when the O/C value exceeds ≈ 0.15 and a limiting value of 2.0035 obtained for the highest O/C values ($\sim 0.34-0.40$). It appears that the oxygen which remains in higher rank

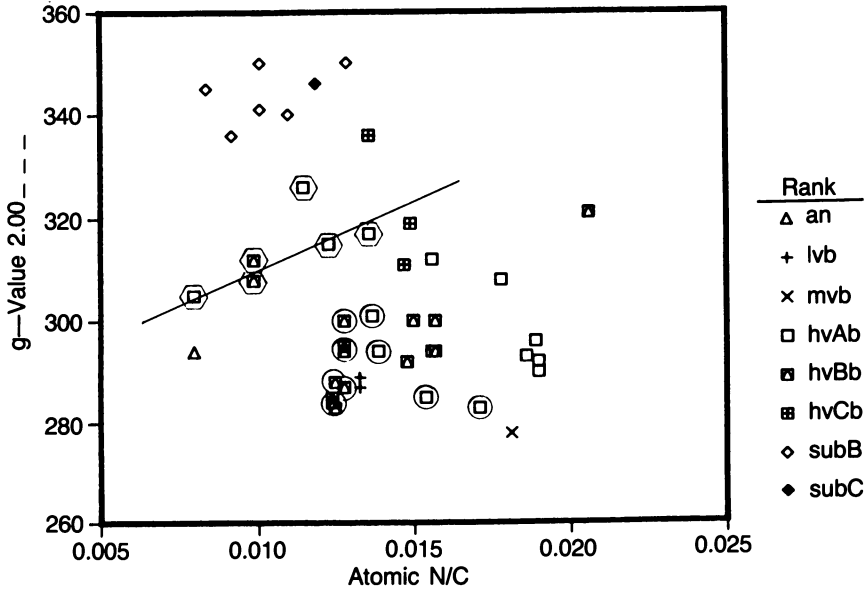


Figure 8. The g -value appears to track N/C for exinites.

coals does not shift the g value appreciably from that encountered in purely aromatic species. Conversely, substantial effects are seen in the lower rank coals. These may be associated with pendant phenolic or carboxylic species on the aromatic cores of the coal structure. A companion analysis of g vs N/C (Figure 8) shows little, if any, systematic variation for the vitrinites. However, with the exception of the one exinite sample which is known to be alginite, there does appear to be an increase of g with N/C for the exinite (sporinite) materials. This may suggest a different distribution of nitrogen forms in the organic precursors.

Carbon Radical Densities. The radical densities are the most variable of the quantities encountered, and perhaps the most

difficult to interpret, because of the many factors which play a role in determining the observed values. However, certain simple distinctions between radical properties in different maceral types and coal ranks can be gained by examining variations of radical density with the H/C value of the macerals (Figure 9). Exinites have relatively low radical densities, and there is not a great deal of variation from one exinite sample to the next. Similarly, subbituminous vitrinites also have radical densities conspicuously lower than their higher rank counterparts. The bituminous vitrinites have radical densities which vary over nearly an order-of-magnitude and as Figure 9 shows, the increase in radical density tracks increasing coal rank. By contrast, inertinites show wide ranges in radical density, which do not appear to be related to the physical quantities discussed here. The variation of radical density with H/C for the vitrinites

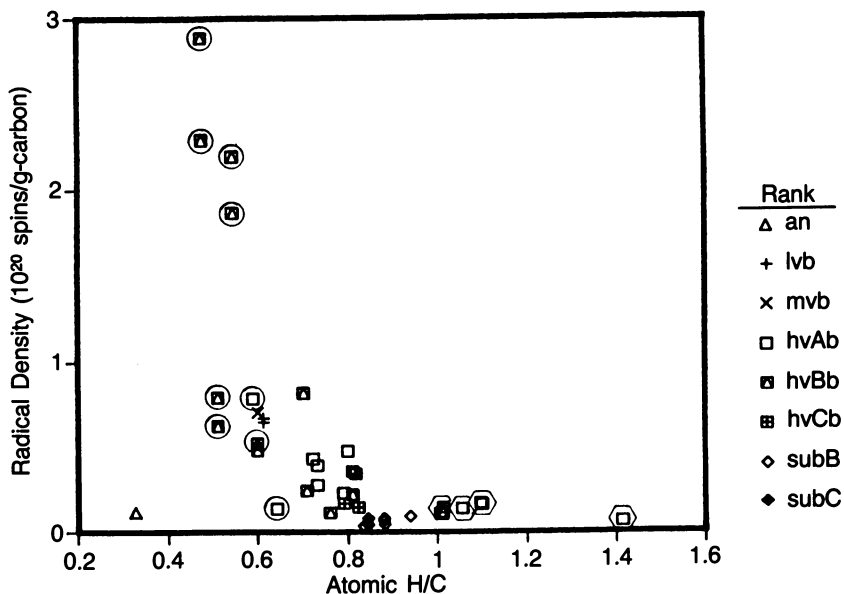


Figure 9. Vitrinite radical densities decrease roughly linearly with increasing H/C. Inertinite radical densities increase dramatically for H/C below 0.6.

shows a much more consistent and rank-dependent variation. Comparison of the inertinite data in the same format does not show the same consistency, suggesting that a variety of factors other than the chemistry of the organic have a strong influence on the carbon radical density in these macerals.

Discussion of ESR Results

ESR of Different Maceral Types. Each maceral type, with its different organic matter base, exhibits very different ESR properties. For exinites, the most important feature is the high degree of uniformity of radical type and density. There are relatively few radicals ($\sim 10^{19}$ spins/g - c) with very similar linewidths, lineshapes, and g values. The data suggest that nitrogen species are proximate to the host molecule -- a rather striking observation, since the N/C ratio of exinites is comparable to, or smaller than, for inertinite or vitrinite macerals. The relative g-value contributions from oxygen and nitrogen will be assessed in future variable frequency experiments. For inertinites, radicals appear associated with aromatic species, but the radical density, linewidth, and lineshape, are highly variable and do not appear directly correlated to chemical properties of the organic. Clearly, the details of the formation process of these inertinites are crucial determinants of the number and properties of these radicals.

ESR of Different Rank Vitrinites. The vitrinite samples provide the opportunity to study the systematics of radical chemistry as a function of the extent of coalification. Perhaps the most striking first observation is that the type of radical is different in subbituminous coals than it is for bituminous coals (with some intermediate behavior for high volatile C vitrinites), and that difference is associated with the substantially higher oxygen levels encountered. In light of this change in radical type, presumably associated with higher levels of pendant oxygen species, the nearly-linear increase in radical density with decreasing H/C is striking and suggests that the conditions associated with coalification of vitrinites are much more readily determined than in the inertinite case. ESR linewidths and lineshapes also vary systematically, with ΔH_{pp} increasing with coal rank.

Conclusions and Acknowledgments

The ability to examine individual coal macerals provides an opportunity for a detailed study of the roles of the chemistry of the starting organic material and the effect of coalification on the final materials. The different macerals exhibit distinct g-value, linewidth and radical density signatures which are related to their chemistry. The present overview will be extended to a qualitative analysis of the ESR properties and the behavior of these macerals under reaction conditions.

We express our appreciation to M. L. Gorbaty for his encouragement of his research activity and for many useful suggestions during the course of the work.

Literature Cited

1. H. L. Retcofsky, "Magnetic Resonance Studies of Coal" in Coal Science and Technology, Vol. 1 (M. L. Gorbaty, J. W. Larsen, I. Wender, eds.), (Academic, New York, 1982), p. 43.
2. D. E. G. Austen, D. J. E. Ingram, P. H. Given, C. R. Binder, and L. W. Hill in Coal Science (P. H. Given, ed.), ACS Advances in Chemistry Series, vol. 55, 1966, p. 344.
3. H. L. Retcofsky, G. P. Thompson, M. Hough, and R. A. Friedel, in Organic Chemistry of Coal (J. W. Larsen, ed.) ACS Symposium Series, vol. 71, 1978, p. 142.
4. G. R. Dyrkacz and E. P. Horwitz, Fuel 61, 3 (1982).
5. The fractional aromaticity observations were performed by the solid state ^{13}C NMR technique by Prof. R. Pugmire and co-workers at the University of Utah.
6. For a good general introduction to carbon radical ESR, see L. S. Singer, Proc. 5th Conf. Carbon, (Pergamon, New York, 1963), p. 37.
7. See, e.g. D. C. Nonhebel, J. M. Tedder, and J. C. Walton, Radicals (Cambridge Univ. Press, London, 1979), Ch. 3.
8. L. Petrakis and D. W. Grandy, Anal. Chem. 50, 303 (1978).
9. J. E. Wertz and J. R. Bolton, Electron Spin Resonance: Elemental Theory and Practical Applications, (McGraw-Hill, New York, 1972), Ch. 7.
10. See, e.g., G. Pake, Paramagnetic Resonance (Benjamin, New York, 1962), sec. 2-4.
11. P. W. Anderson, Physical Review 82, 342 (1951).
12. G. Pake, loc. cit., pp 61-67.
13. H. L. Retcofsky, G. P. Thompson, M. Hough, and R. A. Friedel, ACS Fuel Div. Preprints 22, 90 (1977).

RECEIVED January 26, 1984

Reactivity and Characterization of Coal Macerals

RANDALL E. WINANS, RYOICHI HAYATSU, ROBERT G. SCOTT, and
ROBERT L. MCBETH

Chemistry Division, Argonne National Laboratory, Argonne, IL 60439

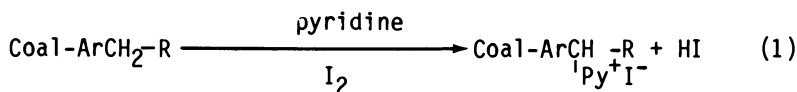
In a study of the organic structures in coals and their reactivity in chemical and thermal processes, it is desirable to reduce the complexity of the material by some sort of physical separation. One such approach is the separation of the coals into their maceral groups, which are the microscopically identifiable organic portions of coal which may have different origins, chemical and physical features, and reactivity. Two bituminous coals have been separated into their three main maceral groups: exinite, vitrinite, and inertinite, using a modified float-sink technique which uses analytical density gradient centrifugation (DGC) to determine the appropriate density ranges. The DGC technique, which also exploits the differences in densities, has just recently been reported (1,2). Also, several maceral samples were prepared by hand picking, including several vitrinites, a fusinite, and a resinite. An alginite sample was obtained from the DGC separation (1). The maceral purity of these samples was determined from petrographic examination. The techniques used for characterization and for studying reactivity have been developed using whole coals.

The chemistry of macerals separated by DGC, float-sink and hand picking has been investigated recently by several techniques including: solid ^{13}C nmr (3,4), oxidation (5,6), and mass spectrometry (5-12). Early work focused on chemical properties (13,14) and esr spectroscopy (15). The approach used in this study combines pyrolysis-mass spectrometry (Py-MS) for characterization, batch vacuum pyrolysis for structural and thermal reactivity information, and a two step degradation to examine chemically reactive sites.

The Py-MS technique has been used extensively to characterize synthetic polymers, biopolymers, and fossil fuels (5-8,10,11). In this work the technique has been modified by using a mass spectrometer which provides precise mass measurements directly upon pyrolysis. The advantage of this approach is two

fold. First, it enables the detection and identification of pyrolysis products having the same nominal mass but different molecular formulae and hence different precise masses. The results presented here demonstrate that this can be a significant advantage. Second, the technique provides a wealth of detailed information which can be conveniently sorted for comparisons between different samples. High resolution MS has been shown to be useful in the analysis of volatile compounds in petroleum and coal liquids (16-20). Aczel and co-workers (18-20) demonstrated that it can be a very useful quantitative tool. The emphasis in this study has been to compare the variations in the distribution of hydrogen deficiency (Z number) and heteroatoms between the different coal macerals in high volatile bituminous coals. In the batch vacuum pyrolysis reaction the maceral concentrates are pyrolyzed in a vacuum, the products collected and characterized by gas chromatography mass spectrometry and by GC microwave plasma emission spectroscopy (GCMPEs). The vacuum technique has been chosen over the typical on-line pyrolysis-GCMS method for two reasons. First, experiments in this laboratory have shown that with the vacuum technique, secondary reactions such as the aromatization of alicyclics are less likely to occur. Second, better pyrolysis yield data can be obtained with a batch type reaction scheme.

In addition to characterization of thermal products, the chemical reactivity of these concentrates has been studied. Reactive benzylic sites have been determined from the reaction of the macerals with pyridine and iodine to form pyridinium iodides:



It has been shown that the number of pyridinium iodides per 100 carbon atoms in the original coal decreases with increasing rank (21). Further studies have shown that these derivatized coals are activated toward oxidative solubilization using a reagent, alkaline silver oxide, which normally is quite ineffective in dissolving raw coals. In the results from the thermal and chemical reactions, similarities and differences have been noted which will be discussed later. Also, it should be emphasized that in this study we are examining maceral concentrates from the three main groups which are derived from the same coal. These coals have been chosen to be representative of bituminous coals and not include sapropelic coals where the chemistry may be more unusual due to the typically large exinite content.

Experimental

Samples. Two of the coals used in this study were obtained from the Penn State Coal Sample Bank, an HVA bituminous coal (PSOC 1103) from the Upper Elkhorn #3 seam in Eastern Kentucky and an HVA bituminous coal (PSOC 828) from the Brazil Block seam in Indiana. A third coal from which vitrinite and fusinite were hand picked was an Illinois No. 2 seam HVC bituminous coal from Northern Illinois. Also, resinite and vitrinite samples were hand picked from a Hiawatha seam bituminous coal from the King 6 mine in Utah. Finally, the alginite sample was obtained from an Ohio No. 5 seam (PSOC-297) coal by DGC (2,5). All of the elemental and petrographic analyses are presented in Table I. The details of the sink-float technique have been reported previously (1). Typically, a 3 micron particle size demineralized coal is centrifuged in aqueous CsCl_2 solution of the appropriate density with a small amount of surfactant added to disperse the coal particles. The exinites in the float are collected and the sink fraction is further separated into vitrinite and inertinite by repeating the procedure at a higher density. The process yielded gram quantities of coal concentrates. The density cutoff points were determined from analytical DGC of coals of similar origin and rank. The technique used for petrographic analysis has also been reported earlier (2).

Pyrolysis. In the pyrolysis experiment, typically 30 mg of sample was heated in a quartz tube at 400°C for 24 hrs at 2×10^{-6} torr. Tars were trapped at room temperature and the more volatile products at liquid nitrogen temperature. These two fractions were analyzed by GCMPEs (MPD-850) using a 25m x 0.25 mm i.d. OV-101 fused silica column and by GCMS (Kratos MS-25) using a 30m x 0.25 mm i.d. DB-5 column.

The Py-MS data was obtained on the MS-25 spectrometer using a direct heating probe designed in this laboratory. The maceral samples were deposited as a slurry onto a fine platinum grid which is heated with a computer controlled D.C. current. The linear heating rates were varied between $25\text{--}100^\circ\text{C}/\text{min}$. The spectrometer was operated in the precise mass measurement mode using perfluorokerosene as an internal standard. Preliminary data analysis and averaging was performed on the Kratos DS-55 data system. These data then were transferred to a VAX 11/780 for final sorting and plotting.

Chemical Reactions. The pyridinium iodide derivatized samples were prepared by refluxing 1 g of coal or maceral concentrate in 60 ml of pyridine with 4 g of iodine for 70 hrs (21). The reaction mixture was poured into 10% aqueous NaHSO_3 and the solution filtered. The derivatized coal was washed free of pyridine, dried, and analyzed. Portions of the activated coal

Table I. Analytical Data for the Separated Coal Macerals¹

Sample	Seam	Prep ²	% C	% H	% N	% S	% O	% Ash	% Vit.	% Exin.	% Inert.	
Vitrinites												
PSOC 828	Brazil Block	SF	76.4	5.6	1.5	0.9	15.6	<1.0	90	4	6	
PSOC 1103	Upper Elkhorn	SF	80.4	5.6	1.8	1.0	11.2	<1.0	93	2	5	
ILL	ILL No. 2	HP	73.9	5.3	1.1	1.6	18.1	<1.0	>95			
Exinites												
Sporinite (828)	Brazil Block	SF	78.6	7.5	1.1	1.6	11.2	<1.0	9	91	0	
Sporinite (1103)	Upper Elkhorn	SF	80.9	6.4	1.5	1.1	10.0	<1.0	46	50	5	
Alginite (297)	Ohio No. 5	DGC	81.6	9.8	0.7	7.9 ³		<1.0	5	95	0	
Resinite	Hiawatha	HP	83.8	10.6	0.1	4.7 ³		0.8	0	100	0	
Inertinites												
PSOC 828	Brazil Block	SF	77.1	5.0	1.3	0.7	15.9	<1.0	67	0	33	
PSOC 1103	Upper Elkhorn	SF	70.9	3.8	1.2	8.8	15.3	9.0	16	2	82	
Fusinite	ILL No. 2	HP	79.3	3.2	0.5	4.0	13.0	4.0	5	0	>95	

¹See text for further description of the source of the samples, all elemental analyses on a dmmf basis

²SF = sink-float; HP = hand-picked; and DGC = density gradient centrifugation

³%S + %O

were oxidized with freshly prepared silver oxide in refluxing aqueous NaOH. The oxidation products, which were soluble in alkaline solution, were acidified and then extracted with a series of organic solvents. The major products were soluble only in alkaline solution or polar solvents. The methanol soluble acidic products were methylated with diazomethane. Approximate molecular size distributions were determined by gel permeation chromatography using a set of three ultra-styragel columns with 100, 500, and 1000 Å nominal pore diameters. The samples were eluted with THF and detected by UV at 254 nm and 220 nm for the sporinite samples. The columns were calibrated using a set of esters of known molecular weight.

Results and Discussion

The Py-MS experiments have provided detailed information on the labile organic structures found in the maceral concentrates. The utility of being able to obtain precise mass measurements is demonstrated in Table II where a small selection of peaks from the pyrolysis of the Brazil Block seam sporinite is listed. Note that at nominal $m/z = 108$ and 122 there are actually three distinct peaks corresponding to a quinone, an alkyl-phenol and a hydrocarbon. Normally with nominal mass pyrolysis data these peaks would only be assigned to alkyl phenols. All three peaks have a significant abundance for this maceral and vary considerably in the other maceral samples. This variation is shown on the bar graph in Figure 1 for the peaks at $m/z = 108$. Also, it is possible to identify sulfur and nitrogen containing pyrolysis fragments. In Table II a portion of the alkyl thio-*phene* series can be seen at $m/z=112$ and 126 . These are just a few examples of the usefulness of being able to obtain precise mass measurements. More detailed discussion of the application of HRMS to analysis of volatile fossil fuel derived substances can be found in the literature (16-20).

The precise mass measurement Py-MS technique provides a wealth of information, but the data must be sorted in order to facilitate comparisons between different samples. Meuzelaar and others (8) have applied statistical analysis to low resolution data in order to make comparisons. With precise mass measurement data the approach can be much simpler. We have written a computer program which sorts the data according to Z number (hydrogen deficiency) and heteroatom content. Typically, in the range $m/z = 30-250$, peaks containing over 98% of the total ion current can be assigned a formula. In Figure 2 the peaks from an average scan for the 828 sporinite have been assigned to five groups: aliphatic hydrocarbons ($Z = 0-3$), aromatic hydrocarbons ($Z>3$), and three groups comprised of peaks containing heteroatoms oxygen, sulfur, and nitrogen. The polycyclic aromatic

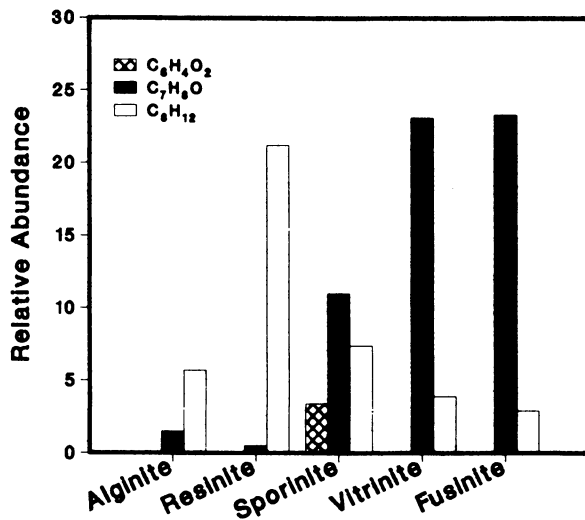


Figure 1. This bar graph shows the variation in the $m/z = 108$ peak components from Py-MS for a series of macerals. The sporinite and vitrinite are separated from the Brazil Block seam coal.

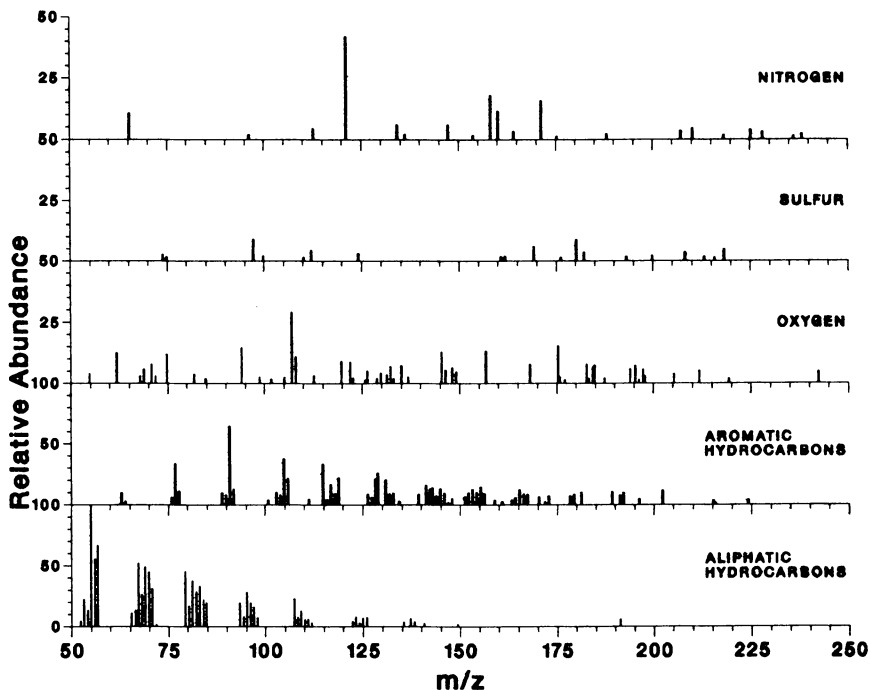


Figure 2. The sorted mass spectrum of the Brazil Block Seam sporinite.

Table II. Selected Peaks from Py-MS of a Sporinite

M/Z	Deviation Millimass Units	Relative Abundance	Formula
107.0474	-2.3	29.0	C ₇ H ₇ O
107.0832	-2.9	22.8	C ₈ H ₁₁
108.0152	-5.9	3.4	C ₆ H ₄ O ₂
108.0545	-3.0	11.0	C ₇ H ₈ O
108.0892	-4.7	7.4	C ₈ H ₁₂
112.0330	-1.7	4.4	C ₆ H ₈ S
113.1243	+3.9	4.3	C ₇ H ₁₅ N
115.0535	-1.2	33.3	C ₉ H ₇
116.0636	+1.0	4.3	C ₉ H ₈
117.0694	-1.0	16.4	C ₉ H ₉
122.0321	-4.6	2.2	C ₇ H ₆ O ₂
122.0772	+4.0	8.8	C ₈ H ₁₀ O
122.1090	-0.5	4.3	C ₉ H ₁₄
126.0413	-9.0	8.8	C ₇ H ₁₀ S

hydrocarbons and the heteroaromatics are depicted with open bars. To demonstrate the variability between the various maceral groups, the fusinite spectra is shown in Figure 3. The difference is readily seen qualitatively by just comparing the two spectra. The analysis has been extended to provide a more quantitative comparison between the two maceral groups.

A summary of the data as a percentage of the absolute intensities can be generated as a function of Z number and heteroatom content. An example of the summary for the 828 sporinite is shown in Table III. Several interesting features are seen in the plot of sum of absolute intensities as a function of Z-number (Figure 4). At lower Z number the exinite macerals show significant variations. The resinite yielded more pyrolysis fragments at Z = 3 and 4 even though approximately 90% of the carbons are aliphatic while the alginite which is also highly aliphatic yielded major fragments at Z = 0-3. These results demonstrate that the aliphatic structures in these two macerals vary considerably as one would expect when their

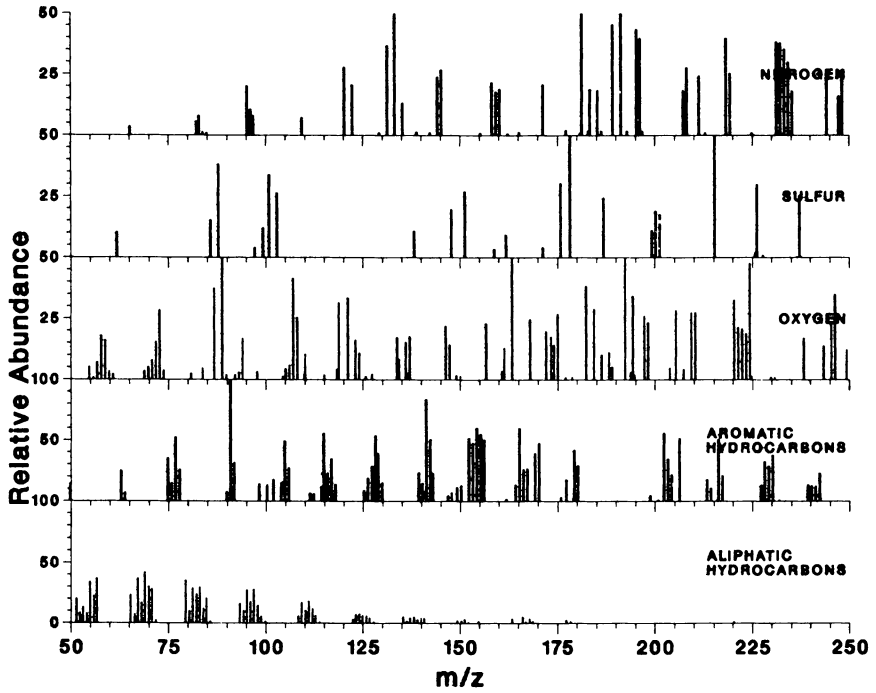


Figure 3. Sorted mass spectrum for the Illinois No. 2 fusinite sample.

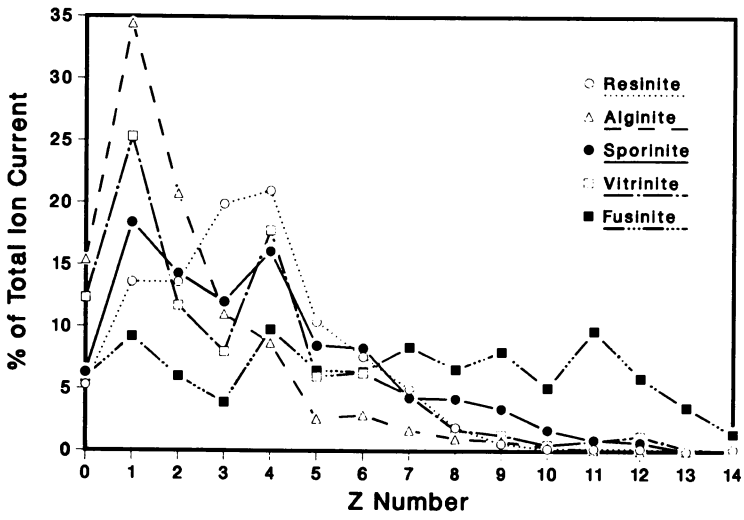


Figure 4. A comparison for 5 maceral samples of the variation of ion current with Z number for all peaks.

Table III. Distribution of the 828 Sporinities Total Ion Current Sorted by Z Number and Heteroatom Content (HC=hydrocarbons)

Z	HC	O	O ₂	O ₃	S	S ₂	N	NO	TOTAL (Z)
0	5.5			0.5			0.2		6.2
1	16.0	0.6	0.1	1.1	0.3	0.2	0.1		18.4
2	12.3	0.5	0.1	1.2	0.1	0.1			14.3
3	7.4	0.5		0.8	0.6	0.1	2.4	0.1	11.9
4	10.7	3.4		0.5	1.2		0.2	0.1	16.1
5	6.1	0.5	0.3	0.3	0.1		0.6	0.6	8.5
6	4.2	1.4	0.7	0.2	0.3		1.5		8.3
7	3.9						0.2	0.1	4.2
8	3.3	0.7	0.2						4.2
9	2.1	0.6					0.3	0.3	3.3
10	1.7								1.7
11	0.6	0.1						0.2	0.9
12	0.7								0.7
13									
14									
TOTAL	74.5	8.3	1.4	4.6	2.6	0.4	5.5	1.4	98.7

progenitors are considered. The resinite appears to be composed of highly alicyclic structures which are easily aromatized during the pyrolysis. In contrast, a major part of the alginites are probably macromolecules which contain mostly long chain methylene groups. This picture is in agreement with results obtained from oxidation of alginite (5). The sporinite Z number distribution falls in between resinite and alginite. Actually, the sporinite is more similar to the vitrinite. This conclusion is supported by heteroatom classification and the results from the batch vacuum pyrolysis which will be discussed later. The fusinite Z number distribution is very different from any of the other macerals and reflects its more aromatic nature, where fragments with high Z number are much more abundant.

The approximate distribution of the heteroatoms oxygen, nitrogen, and sulfur can be readily obtained from the Py-MS data. For example, an examination of Table III shows that for nitrogen containing species, heterocyclics, pyrroles (Z = 3) and indoles (Z = 6) predominate. In the case of a single oxygen compound, phenols (Z = 4) and benzofurans (Z = 6) are major families of pyrolysis fragments. The variations in the types of sulfur compounds for five maceral samples are depicted in the bar graph in Figure 5. Not surprisingly, the abundance of polycyclic sulfur compounds, which include benzothiophene,

dibenzothiophene, and larger ring number compounds, increases from the exinites to vitrinites to inertinites. Among the exinites the distributions vary considerably. With the alginite and resinite the major form is aliphatic while the sporinite has proportionally more thiophenols than all of the maceral samples. This is the first example of how sulfur compounds vary between various macerals of similar rank.

Of particular interest in this study is the nature of the non-aromatic structures in the three main maceral groups. It should be noted that the exinites in both the coals separated by float-sink are 90% sporinite. It has been theorized that small molecules, especially the aliphatics, are fairly mobile at some period during the formation of coal (5,6). The studies which support this theory were done on coals that are very rich in exinites and some contained alginite. Two of the coals chosen in the present work (PSOC 828 and 1103) have a more normal distribution of macerals and yet the pyrolysis results indicate that migration of molecules from the exinites to vitrinite and then incorporation into the macromolecular structure might have occurred.

Chromatograms from the GCMPEs carbon channel of the tar from two exinites and a vitrinite are shown in Figure 6 and the yields in Table IV. Long chain normal alkenes and alkanes dominate the compounds in the tar along with a series of triterpenes which are slightly altered hopanes. A general structure for hopane is shown in the upper right of the figure. Several points should be made concerning these results. First, we believe that these compounds are derived from the macromolecular structures in these macerals. During the preparation of the concentrates most of the soluble molecules are removed. Evidence for this is found from examination of the extracts of the whole, untreated coals. One of the major compounds isolated is the biomarker pristane which has been identified many times, previously, in extracts (22) and coal liquids (23). However, this compound is absent from the pyrolysis products, although it is stable under the conditions used. At least a portion of the macromolecular structures in the exinite and vitrinite could be similar. As one would expect, the yields of these aliphatic and alicyclic compounds are less in the vitrinites. The yields follow inversely the fraction of aromatic carbons (4) in these three maceral groups. The exinite concentrate for the Kentucky coal is quite impure (50% vitrinite) which is reflected in the pyrolysis yields.

Another similarity between vitrinite and the exinite is the pentacyclic triterpenes found in the pyrolysates. These compounds, which show the base peak at $m/z = 191$ in their mass

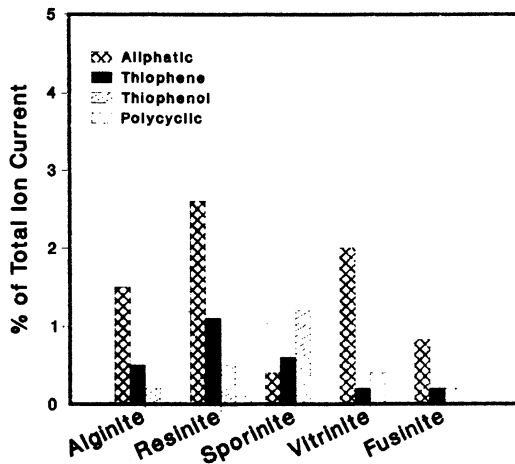


Figure 5. Distribution of sulfur compounds determined from Py-MS for five maceral samples. The vitrinite and sporinite are from the Brazil Block Seam coal.

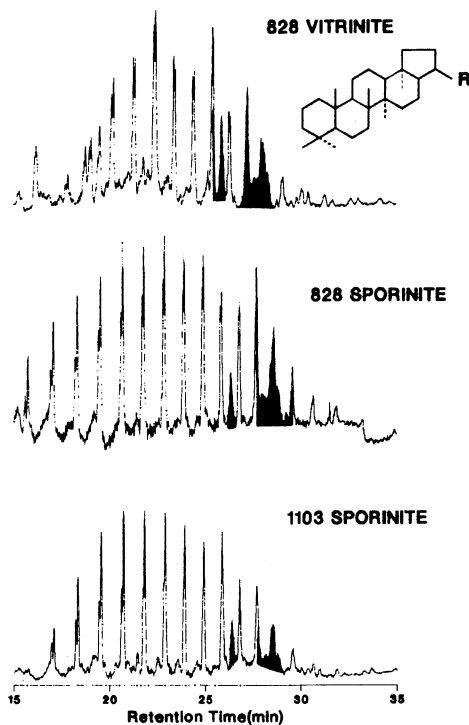


Figure 6. Partial gas chromatograms of vacuum pyrolysis tars. The shaded peaks are compounds derived from triterpenes.

Table IV. Yields from the Batch Vacuum Pyrolysis
Given in Weight %

Sample	% Volatiles	Tar	Char
Brazil Block			
828 Whole	29.6	8.4	62.0
Exinite	23.3	48.4	28.0
Vitrinite	16.3	16.9	67.8
Inertinite	16.9	13.4	69.7
Upper Elkhorn			
Whole	12.2	24.5	63.3
Exinite	14.8	35.2	50.0
Vitrinite	20.2	22.7	57.1
Inertinite	8.3	5.8	85.9
Illinois No. 2			
Fusinite	10.7	1.8	87.5

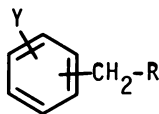
spectra, have been found in pyrolysis MS of alginite (5), and coals (24,25) coal and maceral extracts (6,9,12,26), and oil shales (27,28). From the GCMS it appears that only one of these peaks may represent a species containing one aromatized ring. Again these results suggest that there could have been a significant amount of molecular mobility during the early stages of the formation of this coal.

There was a much larger variation between pyrolysis products volatile fractions for the exinites and vitrinites. The sporinite yielded mostly normal alkanes and alkenes up to approximately C19 with C16 being the most abundant product. The very low molecular weight hydrocarbons such as methane and ethane were not analyzed. Also, benzene and phenol derivatives were found as minor products. The vitrinite products were dominated by aromatics such as alkylbenzenes, alkyl naphthalenes, phenols, and naphthols. The smaller alkane/alkenes were also found. These results are most consistent with what was found in pyrolysis MS of sporinites and vitrinites (5,7).

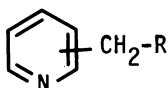
Pyrolysis results for the inertinite concentrates are fairly inconclusive due to the high concentration of vitrinite except for the Ill #2 fusinite which is quite unreactive. Pyrolysis MS of this fusinite shows mostly alkylated naphthalenes and phenanthrenes. What may be interesting is the Kentucky inertinite fraction which is thought to contain ~50% pseudo-vitrinite. This maceral which is usually categorized

with vitrinites is placed in the inertinite column due to its low reactivity both in pyrolysis and in the pyridine-iodine reaction.

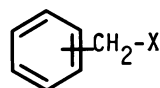
In studies of small molecules, it has been shown that only certain benzylic carbons are reactive enough to form pyridinium salts in refluxing pyridine and iodine (21). There are at least three modes of activating this carbon.



[1]



[2]



[3]

In the first case [1] Y can be either a hydroxy, alkoxy or nitro group. The first two groups are important but variable constituents in coals and the last is probably minor or non-existent. The second active class of species are the alkyl-pyridines [2]. The final case [3] includes substituents on the benzyl carbon where X can be an ether or carbonyl functional group. The general mechanism of this reaction is most probably the base catalyzed iodination of the benzyl carbon with subsequent displacement of the iodide by the pyridine to form the pyridinium salt. In all three modes of activation, the single aromatic ring can be replaced with polycyclic rings.

The yields of the reaction of maceral concentrates with pyridine and iodine show some interesting trends and are given in Table V. Unlike the results from the thermal reactions such as vacuum pyrolysis (Table IV) or short contact time liquefaction (29), the vitrinites are more reactive than the spornites. The inertinites are less reactive but the magnitude of the difference in the comparison with the other maceral groups from the Indiana and Kentucky coals is much less than what has been found for the yields from the thermal reactions.

Examination of the Py-MS results may provide some understanding of the variation observed between the different maceral types. A distribution pattern of the type shown in Table III has been determined for a select number of macerals which also have been reacted in the pyridine-iodine mixture. In examining the three different possible cases for activation of coal maceral benzylic groups, [1] and possibly [3] would appear to be the most important. From the Py-MS results alkyl pyridines have been found to be much less abundant than alkyl phenols which is not surprising considering the percentage of oxygen compared to

TABLE V. Yields from the Reaction of Maceral Concentrates in Pyridine/I₂

	Py ⁺ I ⁻ /100 Carbons	
	Observed	Calculated
Brazil Block		
Exinite	3.8	3.7
Vitrinite	4.2	4.4
Inertinite	3.4	1.3
Upper Elkhorn		
Exinite	3.5	2.2
Vitrinite	4.6	4.8
Inertinite	2.7	2.3
Illinois No. 2		
Vitrinite	3.8	
Fusinite	1.55	
Hiawatha		
Resinite	0.6	

¹Values calculated on a 100% maceral basis.

nitrogen in these samples. A likely candidate for [3] structures could be benzyl ethers, which along with [1] would yield phenol and alkyl phenol fragments in the Py-MS. Based on these arguments there should be a direct relationship between the relative intensities of all the phenolic fragments of a maceral and reactivity of that maceral toward pyridine and iodine. Figure 7 shows that for our small number of samples, there is a rough linear relationship. This result is important in that it supports the notion that Py-MS can be a useful tool for examining coal structure and that the information can be used to explain or predict chemical reactivity.

Coals derivatized with pyridine/I₂ have been found to be susceptible to mild oxidants (21). Alkaline silver oxide is too weak to solubilize untreated coals to any large extent, however, coal-pyridinium salts yield typically soluble but still high molecular weight products. The extent of solubilization depends on the number of pyridinium groups. This oxidant has been applied to several of these coal macerals yielding, as is found with whole coals, fairly high molecular weight products. Approximate molecular size distributions for the methyl esters of the products have been determined by gel permeation

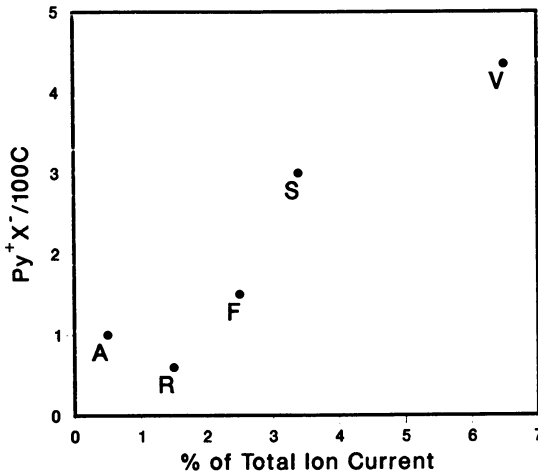


Figure 7. A plot which shows the correlation of number of Py^+X^- formed for a maceral sample with the summation of intensity from alkyl phenols in the Py-MS experiment. A - alginite, R - resinite, F - fusinite (Ill. No. 2) S - sporinite (PSOC 828), and V - vitrinite (PSOC 828)

chromatography. In Figure 8, the distributions for three different macerals are compared. Again, it should be emphasized that the molecular size scale is only approximate and that what is important is the comparison between the three chromatograms. All three samples have a peak at ~ 400 . While for the sporinite and vitrinite, the majority of the sample is found with molecular sizes greater than 400; the reverse is true for the inertinite. As has been seen in other results, vitrinites and their associated sporinites are generally similar. A significant variation is found for the inertinites. The vitrinite does vary from the sporinite in the existence of a peak at ~ 3000 which as yet is unexplained but is reproducible. The studies of these products are in the initial stages and are being continued.

Conclusions

This study has demonstrated that the Py-MS technique using precise mass measurements can be useful for characterizing macerals. Furthermore, the information derived from the technique can be used to understand the chemical and thermal reactivity of coal macerals. When the results from all three approaches described in this paper are compared for the different maceral types, several general conclusions can be

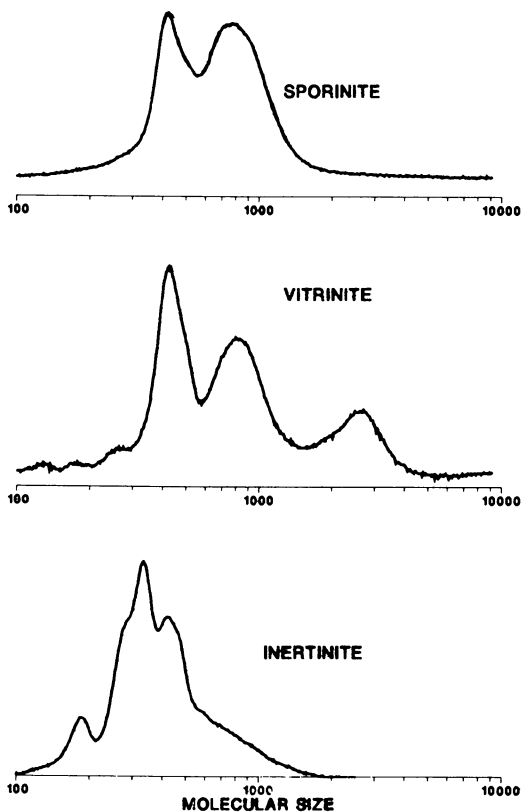


Figure 8. Gel permeation chromatograms for methylated oxidation products from Brazil Block Seam sporinite and vitrinite and the Upper Elkhorn Seam inertinite.

drawn. Chemical structures in the exinite group vary considerably with sporinite being much more similar to vitrinite than to the other exinite macerals. Alginite appears to be comprised of long chain aliphatics while resinite has a much more alicyclic structure. In contrast the inertinite, fusinite, is quite different even though only a minor slightly reactive portion can be examined.

Acknowledgments

This work was performed under the auspices of the Office of Basic Energy Sciences, Division of Chemical Sciences, U.S. DOE under contract W-31-109-ENG-38. The authors thank K.L. Stock for the maceral separations, G.R. Dyrkacz for the petrographic analysis and helpful discussion, and W. Spackman, Penn. State University for choosing and providing the coal samples.

Literature Cited

1. Dyrkacz, G.R.; Bloomquist, C.A.A.; Horwitz, E.P. Sep. Sci. Technol. 1981, 16, 1571.
2. Dyrkacz, G.R.; Horwitz, E.P. Fuel 1982 61, 3.
3. Zilm, K.W.; Pugmire, R.J.; Larter, S.R.; Allan, J.; Grant, D.M. Fuel 1981, 60, 717.
4. Pugmire, R.J.; Zilm, K.W.; Woolfenden, W.R.; Grant, D.M.; Dyrkacz, G.R.; Bloomquist, C.A.A.; Horwitz, E.P., J. Orgn. Geochem. 1982, 4, 79.
5. Winans, R.E.; Dyrkacz, G.R.; McBeth, R.L.; Scott, R.G.; Hayatsu, R., Proceedings Inter. Conf. Coal Sci. 1981 p. 22.
6. Allan, J.; Larter, S.R., "Advances in Organic Geochemistry 1981" Bjorøy, M., Ed., Wiley:Chichester, U.K., 1983, p. 534.
7. van Graas, G.; de Leeuw, J.W.; Schenck, P.A., in "Advances in Organic Geochemistry" 1979, Douglas, A.G.; Maxwell, J.R., Eds., Pergamon:Press, Oxford 1980, p. 485.
8. Meuzelaar, H.L.C.; Harper, A.M.; Pugmire, R.J. Preprint Div. of Fuel Chemistry, ACS. 1983, 28(1), 97.
9. Allan, J.; Bjorøy, M.; Douglas, A.G., in "Advances in Organic Geochemistry 1975"; Campos, R.; Goni, J., Eds.; Pergamon:Oxford, 1977; p. 633.
10. Larter, S.; Douglas, A.G., in "Environmental Biogeochemistry and Geomicrobiology"; Krumbein, W.E., Ed.; Ann Arbor, 1978; Vol. 1 p. 373.
11. Philp, R.D.; Russell, N.J., in "Advances in Organic Geochemistry 1979"; Douglas, A.G.; Maxwell, J.R., Eds., Pergamon:Oxford 1981; p. 653.
12. Philp, R.P.; Saxby, J.D., "Advances in Organic Geochemistry 1979"; Douglas, A.G.; Maxwell, J.R., Eds., Pergamon:Oxford 1981; p. 639.
13. Given, P.H.; Peaver, M.E.; Wyss, W.F., Fuel 1960, 39, 323.

14. Given, P.H.; Peaver, M.E.; Wyss, W.F., Fuel 1966, 44, 425.
15. Sharkey, A.G.; McCartney, J.T., in "Chemistry of Coal Utilization," Elliot, M.A., Ed., Wiley-Interscience: NY 1981, p. 241.
16. Schultz, J.L.; Kessler, T.; Friedel, R.A.; Sharkey, A.G., Fuel 1972, 51, 242.
17. Sharkey, A.G.; Schultz, J.L.; Kessler, T.; Friedel, R.A., in "Spectrometry of Fuels," Friedel, R.A., Ed., Plenum Press: NY 1970, p. 1.
18. Aczel, T., Rev. Anal. Chem. 1971, 1, 226.
19. Aczel, T.; Williams, R.B.; Brown, R.A.; Pancirov, R.J.; in "Analytical Methods for Coal and Coal Products," Karr, C., Ed., Academic Press: NY 1978, p. 499.
20. Aczel, T.; Lumpkin, H.E., in "Refining of Synthetic Crudes," Gorbaty, M.L.; Harney, B.M., Eds., Adv. in Chem. Series No. 79, ACS:Washington, 1979; p. 13.
21. Hayatsu, R.; Scott, R.G.; Winans, R.E.; McBeth, R.L.; Botto, R.E., "Proceedings International Conference on Coal Science, 1983, p. 322.
22. Hayatsu, R.; Winans, R.E.; Scott, R.G.; Moore, L.P.; Studier, M.H., Fuel 1978 57 541.
23. White, C.M.; Schultz, J.L.; Sharkey, A.G. Nature 1977, 268, 620.
24. Gallegos, E.J., J. Chromatog. Sci., 1981, 156.
25. Baset, Z.H.; Pancirov, R.J.; Ashe, T.R., "Advances in Organic Geochemistry, 1979"; Douglas, A.G.; Maxwell, J.R., Eds., Pergamon:Oxford, 1981; p. 619.
26. Jones, D.W.; Pakdel, H.; Bartle, K.D. Fuel 1982, 61, 44.
27. Seifert, W.K.; Moldowan, J.M., in "Advances in Organic Geochemistry, 1979"; Douglas, A.G.; Maxwell, J.R., Eds., Pergamon:Oxford 1981; p. 229.
28. Tissot, B.P.; Welte, D.H., "Petroleum Formation and Occurrence," Springer-Verlag: N.Y. 1978.
29. King, H.H.; Dyrkacz, G.R.; Winans, R.E. (Fuel, in press).

RECEIVED January 9, 1984

Aspects of the Hydrogen Atom Transfer Reactions of Macerals

CHOL-YOO CHOI and LEON M. STOCK

Department of Chemistry, The University of Chicago, Chicago, IL 60637

The influences of macerals from several bituminous coals on the hydrogen-deuterium exchange reaction between tetralin- d_{12} and diphenylmethane and on the reduction of fluorenone have been studied. The sporinite-rich exinites are more effective promoters of the exchange reaction than the corresponding vitrinites or alginite. The semifusinite-rich inertinites are even less effective promoters of the exchange reaction. More important, they are less selective in reactions with tetralin. The presence of sulfur containing compounds in the macerals has a notable influence on their reactivity in hydrogen transfer reactions.

The reactivity pattern for the reduction of fluorenone--sporinite > vitrinite > alginite > semifusinite > fusinite > resinite--defines a bell shaped dependence on the H/C ratio of the maceral and presumably reflects the quantity of readily oxidized hydroaromatic compounds in the maceral. The differences in the effectiveness of the macerals depends in part upon their ability to initiate the reduction of the ketone and in part upon the facility with which they undergo oxidation. As a consequence, there may be synergistic interactions between the components of the different macerals in oxidative hydrogen transfer processes.

The concept that free radical reactions are responsible for the initial fragmentation reactions of large coal molecules and for the essential hydrogen transfer reactions that occur during coal dissolution reactions is quite widely accepted (1). The in-

teractions between coals and labeled molecules such as tetralin- d_{12} have been examined in several laboratories to increase our understanding of these reactions (2-5). Recent findings concerning the selective and reversible abstraction reactions of hydrogen atoms from Tetralin by radicals formed during the thermal decomposition of Illinois No. 6 coal at 400°C (2) and other bituminous coals (3-5) are in accord with the formulation of the dissolution reaction as a free radical process. The fact that weak organic acids and bases have only a modest influence on the exchange reactions of aromatic, aliphatic, and benzylic hydrogen atoms under these conditions whereas compounds such as benzyl phenyl ether, benzyl phenyl sulfide, thiophenol, the BDPA radical, anthraquinone, anthrone, tetracene, and acridine actively promote the benzylic hydrogen atom transfer reactions suggests quite strongly that hydroaromatic compounds are especially reactive in the hydrogen transfer processes (2). In addition, benzyl phenyl sulfide and thiophenol significantly enhance the rate of dissolution of Illinois No. 6 coal (6). Other workers have investigated the dehydrogenation of coals with benzoquinone (7), iodine (8), sulfur (9), palladium on calcium carbonate (10), and benzophenone (11,12). Although the reactions of many coals with benzophenone occur rather slowly at 400°C, the reaction can be used to define their hydrogen donor capability quite conveniently because a single product, diphenylmethane, is formed in the reaction.

The hydrogen transfer reactions of macerals have received scant attention. Peover examined the dehydrogenation of five pure exinites and vitrinites from the same seam using benzoquinone in dimethylformamide at 153°C for several hours (7). His results suggest that exinites are usually somewhat better hydrogen donors than the corresponding vitrinites. Reggel and his coworkers studied the reaction using palladium on calcium carbonate to dehydrogenate four macerals from an hvA bituminous coal catalytically (13). They found that 31, 25, 18, and 5 hydrogen atoms were removed per 100 carbon atoms of exinite, vitrinite, micrinite, and fusinite, respectively. They also conclude that the exinites are generally more reactive.

Dyrkacz and his coworkers have recently described a new procedure for the separation of coals into macerals (14). The macerals can be obtained in pure form, but only in limited quantity. Inasmuch as many of the methods used for the study of coal require relatively large amounts of material, we have undertaken new work on the development of small scale reactions for the accurate determination of the differences in chemical reactivity of macerals. The hydrogen transfer reactions are discussed in this report. Preliminary work revealed that very reproducible results could be obtained when 25 mg of a representative maceral was used as a catalyst for the hydrogen exchange reaction between tetra-

lin-d₁₂ and diphenylmethane at 400°C and when 5 mg of a maceral was used as a reagent for the reduction of fluorenone at the same temperature. Consequently, these reactions have been employed to study the hydrogen atom transfer reactions of macerals from several different coals.

Experimental Part

Materials. The macerals used in this study were obtained from G.R. Dyrkacz and R.E. Winans of the Argonne National Laboratory. Some of the samples were separated from the whole coal by hand, others were prepared by density gradient centrifugation and others by float-sink techniques as described in Chapters 5 and 9. The resinite from the King 6 Mine of the Hiawatha Seam, the virinite and fusinite from the hvC Illinois No. 2 bituminous coal and the alginite from the hvA Ohio Lower Kittaning No. 5 bituminous coal (PSOC-297) contain only negligible amounts of other macerals. The petrographic information for the pure macerals from hvB Indiana No. 1 Block Seam bituminous coal (PSOC-106) has been reported previously (14). The compositions of the macerals separated from hvC Indiana Brazil Block Seam bituminous coal (PSOC-828) and hvA Kentucky Upper Elkhorn No. 3 Seam bituminous coal (PSOC-1103) were determined by G.R. Dyrkacz. The results are summarized in Tables I and II.

All of the samples prepared by centrifugation and the float-sink method were demineralized and milled to three micron diameter. The separations were conducted in the presence of a surface active agent, polyoxyethylene(23) lauryl ether, in cesium chloride solutions (14). The macerals were washed thoroughly to reduce the quantity of surfactant in the maceral to less than 500 ppm and the quantity of chloride ion in the wash water to below the limit detectable by precipitation with silver ion (14).

Promotion of Hydrogen Exchange. The influence of the macerals on the exchange of hydrogen between diphenylmethane and tetralin-d₁₂ was determined using degassed solutions of diphenylmethane (0.376 mmole) and tetralin-d₁₂ (0.376 mmole) and the macerals (25mg) in glass tubes in an argon atmosphere at 400°C. The products were isolated and analyzed using high field nmr spectroscopy as previously described (2). Certain macerals incorporate deuterium during the reaction and the change in the deuterium content of tetralin-d₁₂ is emphasized in this report rather than the degree of incorporation of this isotope into diphenylmethane. Control experiments indicate that neither polyoxyethylene(23) lauryl ether nor cesium chloride enhance the rate of the exchange reactions between tetralin-d₁₂ and diphenylmethane. The results for the pure macerals and the maceral concentrates are summarized in Tables III and IV.

Table I. Ultimate Analyses of Coals and Macerals Concentrates.^a

Coal	Concentrate	Composition (%)				
		C	H	N	O (diff)	S
PSOC-828	Demineralized whole	76.7	5.1	1.4	15.9	0.9
PSOC-828	Exinite	78.7	7.5	1.1	11.2	1.6
PSOC-828	Vitrinite	76.4	5.6	1.5	15.6	0.9
PSOC-828	Inertinite	77.1	5.0	1.4	15.8	0.7
PSOC-1103	Demineralized whole	78.1	5.3	1.2	12.0	2.4
PSOC-1103	Exinite	80.9	6.4	1.5	10.1	1.1
PSOC-1103	Vitrinite	80.4	5.6	1.8	11.2	1.0
PSOC-1103	Inertinite	70.9	3.8	1.2	15.3	8.8
Hiawatha King 6	Whole	69.3	5.5	1.1	14.6	N.D.
Hiawatha King 6	Resinite	83.9	10.6	0.1	4.4	N.D.
Illinois No. 2	Demineralized whole	73.1	5.3	1.3	18.1	2.2
Illinois No. 2	Vitrinite	71.6	5.1	1.1	17.6	0.5
Illinois No. 2	Demineralized vitrinite	73.9	5.3	1.1	18.1	1.6
Illinois No. 2	Demineralized fusinite	79.3	3.2	0.5	13.0	4.0

^aHiawatha King 6 whole coal contained 9.5% ash, Illinois No. 2 vitrinite contained 3.1% ash, and Illinois No. 2 demineralized fusinite contained 4.0% ash. All the other samples contained less than 1% ash.

Table II. Petrographic Analysis of Maceral Concentrates from PSOC-828 and PSOC-1103 Coals.

Coal	Concentrate	Composition (%)		
		Exinite	Vitrinite	Inertinite
PSOC-828	Exinite	91.0	9.0	0.0
PSOC-828	Vitrinite	4.0	89.8	6.2
PSOC-828	Inertinite	0.0	67.5	32.5
PSOC-1103	Exinite	45.5	49.6	4.9
PSOC-1103	Vitrinite	2.5	92.5	5.0
PSOC-1103	Inertinite	1.5	16.2	82.3

Maceral	Principal Macerals		
	PSOC-106 ^a	PSOC-828	PSOC-1103
Cutinite	0.3	0.6	0.2
Resinite	2.4	0.9	0.6
Sporinite	17.4	13.6	6.6
Total exinite	20.1	15.1	7.4
Vitrinite	35.2	61.8	74.2
Micrinite	3.2	4.9	5.6
Inertodetrinite	15.7	5.2	3.7
Semifusinite	20.7	9.9	6.5
Fusinite	5.7	3.1	2.6
Total inertinite	45.3	23.1	18.4

^aReference 14.

Table III. The Influences of Certain Coals and Pure Macerals on the Deuterium-Hydrogen Exchange Reaction of Tetralin- d_{12} and Diphenylmethane at 400°C.^a

Maceral (mg)	Deuterium Content of Tetralin (%)		
	Aromatic Positions	Benzylic Positions	Aliphatic Positions
Indiana No. 1 Block Seam hvB Bituminous Coal (PSOC-106) ^b			
None ^c	95(96)	92(97)	92(94)
Exinite, $\bar{\rho} = 1.176$, (25)	96	84	91
Exinite, $\bar{\rho} = 1.210$, (25)	95	80	89
Vitrinite, $\bar{\rho} = 1.291$, (26)	95	85	90
Vitrinite, $\bar{\rho} = 1.330$, (25)	95	84	90
Inertinite, $\bar{\rho} = 1.371$, (25)	95	87	89
Inertinite, $\bar{\rho} = 1.447$, (25)	95	87	89
Hiawatha King 6 Mine hvB Bituminous Coal			
None ^c	91(96)	91(97)	94(94)
Whole (25)	89	80	92
Resinite (25)	90	85	93
Illinois No. 2 hvC Bituminous Coal			
None ^c	94(96)	92(97)	93(94)
Whole (25)	93	74	89
Demineralized whole (26)	93	69	88
Vitrinite (25)	95	77	91
Demineralized vitrinite (25)	95	78	91
Demineralized fusinite (26)	87	72	87

^aDiphenylmethane (0.376 mmole) and tetralin- d_{12} (0.376 mmole) were reacted for 60 minutes in the presence of these materials.

^bThe density, $\bar{\rho}$, is noted for each maceral fraction, reference 14.

^cThe original isotopic composition of the Tetralin used in these experiments is given in parentheses. The isotopic composition of the Tetralin isolated from reactions carried out without coal materials is also shown.

Table IV. The Influence of Macerals from PSOC-828 and PSOC-1103 on the Deuterium-Hydrogen Exchange Reaction of Tetralin-d₁₂ and Diphenylmethane at 400°C.^{a,b}

Maceral (mg)	Deuterium Content of Tetralin(%)		
	Aromatic Positions	Benzylic Positions	Aliphatic Positions
Indiana Brazil Block Seam hvC Bituminous Coal (PSOC-828)			
None	95(96)	91(97)	93(94)
Demineralized whole (25)	94	83	91
Exinite (25)	94	76	91
Vitrinite (25)	94	80	91
Inertinite (25)	96	88	89
Kentucky Upper Elkhorn No. 3 Seam hvA Bituminous Coal (PSOC-1103)			
None	96(96)	92(97)	92(94)
Demineralized whole (25)	94	82	90
Exinite (25)	97	74	88
Vitrinite (25)	93	83	88
Inertinite (25)	95	75	90

^aThe observed experimental results for the macerals have been normalized to 100% maceral purity.

^bThe experiments were conducted as described in footnotes a and c of Table III.

Ketone Reduction. Pure samples of representative compounds were reacted with fluorenone to define the general pattern of reactivity. In a typical experiment, fluorenone (0.025 mmole), the hydroaromatic compound (0.025 mmole) and benzene (50 μ l) were reacted in an argon atmosphere in a glass vessel at 400°C for 60 minutes. The composition of the solution at the end of the reaction was determined by gas chromatography. The results for the seven compounds examined in this work are summarized in Table V.

The reduction of the macerals by fluorenone was also studied using degassed solutions of fluorenone (0.025 mmol) in benzene (50 μ l) and the maceral concentrate (5mg) in a glass vessel in an argon atmosphere at 400°C. Most reactions were carried out for 30 or 60 minutes. The entire reaction mixture was then filtered through a short column containing 100-200 mesh Florisil using methylene chloride as the eluting solvent. The extent of conversion of the ketone to fluorene was determined by gas chromatography of the eluent. The experimental results are summarized in Tables VI and VII.

Results

The hydrogen atom exchange reactions between Tetralin and diphenylmethane and the reduction of the ketones were studied in the presence of a selected group of raw whole coals, demineralized whole coals, and demineralized macerals. The macerals used in this work were obtained from two hvA bituminous coals, one from the Kentucky Upper Elkhorn No. 3 Seam (PSOC-1103) and one from the Ohio Lower Kittaning No. 5 Seam (PSOC-297); two hvB bituminous coals, one from the Indiana No. 1 Block Seam (PSOC-106) and one from the Hiawatha King 6 Mine; and two hvC bituminous coals, one from the Illinois No. 2 Seam and one from the Indiana Brazil Block Seam (PSOC-828).

The exchange reaction of tetralin-d₁₂ and diphenylmethane has previously been studied using as little as 50mg of material. Preliminary experiments with smaller quantities of some representative coals indicated that the reactions could not be conducted reproducibly at the desired level of accuracy, $\pm 2\%$, with less than 25mg of material. We therefore used this quantity of the coal material in the subsequent experiments. Only very small amounts of cesium chloride and Brij 35, the surface active agent employed in the density gradient separation, are retained in the macerals. Control experiments, in which as much as 25mg of these materials were added to the reaction system, established that these substances had no measurable influence on the exchange reaction. The coal macerals obtained from PSOC-106 hvB bituminous coal by centrifugation and from Hiawatha hvB and Illinois No. 2 hvC bituminous coals by hand selection were very pure. The extent to which these substances influence the exchange reaction is presented in Table III.

Table V. Dehydrogenation of Representative Hydrogen Donors by Fluorenone at 400°C

Hydrogen donor	Conversion to fluorene (%)
1,2,3,4-Tetrahydroquinoline	28
5,12-Dihydrotetracene	14
9,10-Dihydroanthracene	14
1,2,3,4,5,6,7,8-Octahydroanthracene	6
9,10-Dihydrophenanthrene	5
Tetralin	3
Decalin	0.4

^aFluorenone (0.025 mmole) and the H-donor (0.025 mmole) were reacted in argon at 400°C for 60 minutes.

Table VI. The Reduction of Fluorenone to Fluorene by Coals and Macerals at 400°C for 1 Hour in the Presence of Benzene.^a

Coal	Sample (mg)	Conversion to fluorene(%)
Hiawatha King 6	Whole (5.0)	39
Hiawatha King 6	Resinite (5.1)	15
Illinois No. 2	Whole (5.0)	43
Illinois No. 2	Demineralized whole (5.0)	49
Illinois No. 2	Vitrinite (5.0)	44
Illinois No. 2	Demineralized vitrinite (5.0)	42
Illinois No. 2	Demineralized fusinite (5.0)	19
PSOC-106 ^b	Exinite, $\bar{\rho} = 1.176$, (5.2)	67
PSOC-106 ^b	Exinite, $\bar{\rho} = 1.210$, (5.1)	67
PSOC-106 ^b	Vitrinite, $\bar{\rho} = 1.291$, (5.2)	46
PSOC-106 ^b	Vitrinite, $\bar{\rho} = 1.330$, (5.0)	38
PSOC-106 ^b	Inertinite, $\bar{\rho} = 1.371$, (5.1)	25
PSOC-106 ^b	Inertinite, $\bar{\rho} = 1.447$, (5.0)	16
PSOC-297	Alginite (5.0)	41

^aThese experiments were carried out with 0.025mmole of fluorenone in benzene (50 μ l).

^bThe average density of the different macerals is noted.

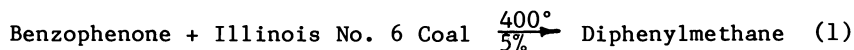
Table VII. The Reduction of Fluorenone to Fluorene by Maceral Concentrates from PSOC-1103 and PSOC-828 at 400°C for 1 Hour in the Presence of Benzene^a

Coal	Maceral (mg)	Conversion to fluorene (%)	
		Measured	Normalized
PSOC-1103	Exinite (5.0)	66	87
PSOC-1103	Vitrinite (5.0)	50	50
PSOC-1103	Inertinite (5.0)	33	29
PSOC-828	Exinite (5.0)	60	61
PSOC-828	Vitrinite (5.0)	46	47
PSOC-828	Inertinite (5.0)	41	30

^aThe experiments were carried out with 0.15 mmole of fluorenone in benzene (50 μ l).

The maceral concentrates obtained by float-sink methods from PSOC-828 and 1103 were somewhat less pure than the macerals obtained by hand or by centrifugation. For convenient comparison, the data obtained in the exchange reactions have been normalized to 100% maceral purity on the basis of the petrographic information presented in Table II using simultaneous linear equations. The normalized results are summarized in Table IV.

Benzophenone, as mentioned in the Introduction, has been used to assess the hydrogen donor capacity of coals (11, 12). Unfortunately, most coals react very slowly with this compound at 400°C, equation 1. For example, less than 5% of this ketone is converted to diphenylmethane by a vitrinite-rich sample of Illinois No. 6 coal in benzene in one hour at 400°C. Preliminary work revealed that the exinite, vitrinite, and inertinite isolated from PSOC-828 exhibit small, but apparently significant



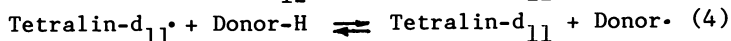
differences in reactivity. However, the extent of reaction was too small for accurate work. Consequently, we sought a more reactive ketone. Halogenated benzophenones are more reactive than the unsubstituted compound, but competitive dehalogenation reactions complicate the interpretation of the results. On the other hand, the reduction of fluorenone proceeds more than twice as rapidly as that of benzophenone to give a single product. Quite accurate results can be obtained when 5mg of the maceral are used in the reaction. In addition, the possible contaminants in the macerals, Brij 35 and cesium chloride, do not accelerate the reduction of fluorenone by Tetralin. Several representative compounds were examined to gain perspective on the relationship between the structure and reactivity of different hydroaromatic compounds, Table V. The encouraging results obtained in these experiments and in preliminary experiments with coals prompted study of the reactions of all the macerals with fluorenone. The results for the quite pure macerals from Illinois No. 2 coal, PSOC-106, and 297 and the Hiawatha King 6 Seam coal are presented in Table VI. The normalized results for the maceral concentrates obtained from PSOC-828 and 1103 are summarized in Table VII.

Several lines of evidence led us to conclude that most of the macerals contain compounds that are reactive in hydrogen transfer reactions, but that these materials are present in different amounts in the different macerals. This feature of the chemistry was examined by the study of the reactions of the

macerals from PSOC-828 at different time intervals as displayed in Figure 1.

Discussion

Promotion of Hydrogen Exchange. The radicals derived from the coal molecules by simple thermal homolyses and by molecule-induced homolyses initiate exchange reactions between tetralin-d₁₂ and the donors in the reaction system--principally diphenylmethane and the hydroaromatic compounds in the macerals (2). While it is clear that many different factors influence the exchange reactions, the simplified sequence of reactions shown in equations 2-5 illustrates the potential dependence of the exchange



process on the concentration and selectivity of the initiating radicals, R \cdot , derived from the coal molecules. The results for the macerals may be conveniently examined on the basis of this reaction sequence.

The highly purified macerals from the Indiana No. 1 coal, PSOC-106, all modestly enhance the exchange of hydrogen atoms tetralin-d₁₂ and diphenylmethane. The same pattern of reactivity--benzylic exchange > aliphatic exchange > aromatic exchange--is observed with each maceral. These findings are compatible with the results obtained in other studies of whole coals with labeled Tetralins (2-5). While the reactivities of the macerals from this coal do not differ appreciably, the low density exinites appear to be somewhat more effective agents for the promotion of the hydrogen transfer reaction.

The results obtained for the macerals from the Indiana Brazil Seam coal, PSOC-828, parallel the results for the macerals of the PSOC-106 coal in all respects except that the macerals from the PSOC-828 coal are significantly more effective catalysts for the exchange reaction. The macerals from the Kentucky Upper Elkhorn Seam, PSOC-1103, on the other hand, behave somewhat differently. The inertinite and exinite exhibit higher reactivity than the vitrinite. This alteration in behavior is almost certainly the consequence of the high sulfur content of the semifusinite-rich inertinite fraction, Table I. Although no information is available concerning the nature of the sulfur compounds in this maceral concentrate, it is known that sulfur compounds such as hydrogen sulfide, thiols, and certain thioethers are especially effective agents for the promotion of hydrogen exchange

reaction (6). The finding that the whole coals from the Illinois No. 2 Seam and the Kentucky No. 3 Seam are somewhat more reactive than anticipated on the basis of the reactivity of the individual macerals may also originate in the greater quantity of sulfur-containing compounds in the whole coals, Table II.

The difference in the extent of exchange at the benzylic and aliphatic positions of Tetralin is measurably less when the inertinites rather than the vitrinites from PSOC-106 and PSOC-828, are used to promote the reaction. Indeed, the inertinite obtained from PSOC-828 enhances the exchange reactions at the benzylic and aliphatic positions of Tetralin to a comparable degree. This decrease in selectivity suggests that the radicals formed in the initial fragmentation reactions of these semifusinite-rich macerals differ significantly in their behavior from the radicals produced from the other macerals.

The exinites isolated from PSOC-106, 828, and 1103 are relatively rich in sporinite, Table II. For comparison, we examined the resinite isolated from a Hiawatha coal. The exchange datum for this pure maceral, Table III, indicates that it is a significantly less effective agent for the promotion of the exchange reaction than the sporinite-rich macerals isolated from the other samples in spite of the fact that the whole Hiawatha coal is more reactive than the other whole coals.

In summary, all the macerals examined in this study enhance the hydrogen atom transfer reactions between tetralin-d₁₂ and the hydrogen atom donors in the reaction system. Although the range of reactivity is relatively narrow, the differences in reactivity are well beyond the limits of experimental error. The results indicate that the sporinite-rich exinites are significantly more reactive than the corresponding vitrinites and even other alginate-rich exinites. The semifusinite-rich inertinites, in contrast, are simultaneously less effective promoters of the exchange reaction and less selective in their reactions with Tetralin. It is pertinent, however, that reactive substances such as the sulfur compounds in the inertinite isolated from the Kentucky Upper Elkhorn coal can alter the reactivity pattern significantly. The available information strongly suggests that the different coal macerals and the initial products of their dissolution reactions in donor solvents decompose to form radicals at somewhat different rates and that the radicals formed in these processes exhibit different degrees of reactivity.

Ketone Reduction. The reduction of fluorenone to fluorene was adopted for the study of the donor capabilities of the macerals. The mechanism of this reaction, which apparently takes place in several steps, has not been defined and is currently under study in our laboratory.

The extent to which demineralization influences the reduction was examined by a comparison of several different portions of Illinois No. 2 coal. Very comparable results were obtained for the whole coal, the demineralized whole coal, the vitrinite and the demineralized vitrinite. These observations imply that the demineralization procedures used for the preparation of the macerals do not alter their reactivity as reducing agents importantly. These observations contrast with the results obtained in the study of the exchange reactions. The difference appears to be related to the degree to which these reactions are influenced by sulfur-containing molecules. This interpretation is supported by the fact that the reaction of fluorenone with Tetralin at 400°C is accelerated only modestly by the addition of benzyl phenyl sulfide. In contrast, the exchange reaction is greatly accelerated by the addition of this substance (2). For example, Tetralin (0.038 mmole) converts 4% of fluorenone (0.025 mmole) to fluorene. The addition of benzyl phenyl sulfide (6mg) to Tetralin and fluorenone increases the conversion to 12% whereas the addition of Illinois No. 6 coal (6mg) increases the conversion to 60%.

The macerals of the PSOC-828 coal react at similar rates during the initial stages of the reduction reaction, Figure 1. These results suggest that all the maceral concentrates obtained from this coal contain compounds that can readily transfer hydrogen to fluorenone and undergo aromatization, but that these reactive substances are present in different quantities in the different macerals. Although this suggestion must be tested more thoroughly by the examination of the macerals isolated from other coals, the observation suggests that there may be important synergistic interactions between the components of several macerals in some reactions.

The differences in the reactivities of the macerals become more apparent in the 30-60 minute reactions. The behavior of the macerals and the reference compounds are compared in Table VIII.

The reactivity pattern--sporinites > vitrinites > alginite > semifusinites > fusinite > resinite--established for the macerals in this reaction illustrates the very great differences in the reactivities of the coal molecules derived from different kinds of natural products. However, the sporinites, vitrinites, and semifusinites isolated from several different bituminous coals exhibit similar behavior. The relationship between the reactivity of the macerals and their atomic H/C ratio is shown in Figure 2. The pattern of reactivity suggests that there is a bell shaped relationship between the effectiveness of the maceral as a reducing agent and its H/C ratio. Such a relationship is plausible

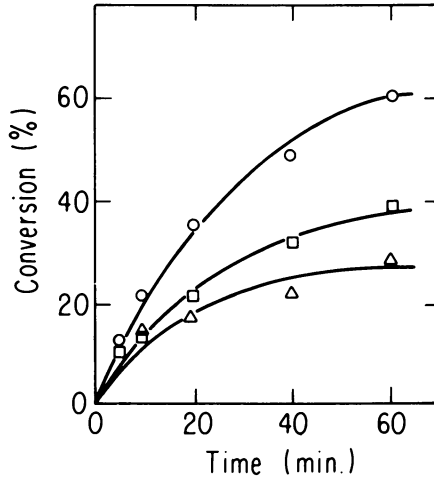


Figure 1. The extent of conversion of fluorenone to fluorene by the exinite (circles), vitrinite (squares), and inertinite (triangles) macerals isolated from PSOC-828.

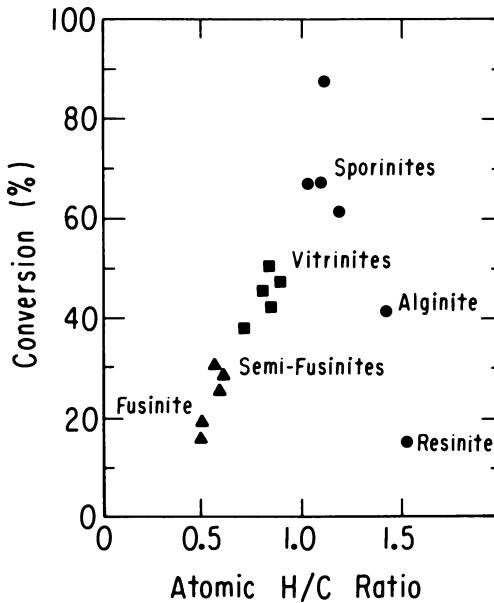


Figure 2. The relationship between the conversion of fluorenone to fluorene and the atomic H/C ratio for the macerals examined in this study.

Table VIII. The Reduction of Fluorenone by Macerals and Representative Hydrocarbons at 400°C in 60 Minutes

Maceral or reference compound	Conversion of fluorenone (%)
Sporinite-rich exinite (PSOC-1103)	87
Sporinite-rich exinite, ($\bar{\rho} = 1.176$, PSOC-106)	67
Sporinite-rich exinite, ($\bar{\rho} = 1.210$, PSOC-106)	67
Sporinite-rich exinite (PSOC-828)	61
Vitrinite (PSOC-1103)	50
Vitrinite (PSOC-828)	47
Vitrinite ($\bar{\rho} = 1.291$, PSOC-106)	46
Vitrinite (Ill. No. 2)	42
Alginite (PSOC-297)	41
Vitrinite ($\bar{\rho} = 1.330$, PSOC-106)	38
Semifusinite-rich inertinite (PSOC-828)	30
Semifusinite-rich inertinite (PSOC-1103)	29
1,2,3,4-Tetrahydroquinoline	28
Semifusinite-rich inertinite ($\bar{\rho} = 1.371$, PSOC-106)	25
Fusinite (Ill. No. 2)	19
Semifusinite-rich inertinite ($\bar{\rho} = 1.447$, PSOC-106)	16
Resinite (Hiawatha)	15
5,12-Dihydrotetracene	14
9,10-Dihydroanthracene	14
1,2,3,4,5,6,7,8-Octahydroanthracene	6
9,10-Dihydrophenanthrene	5
Tetralin	3
Decalin	<1

because the H/C ratios may reflect the quantities of aromatic hydroaromatic and saturated aliphatic compounds in the macerals. Presumably, the substances with the greatest concentration of hydroaromatic compounds are most readily oxidized.

All the macerals used in this investigation react with fluorenone much more readily than pure common hydroaromatic compounds such as 9,10-dihydroanthracene, 9,10-dihydrophenanthrene and Tetralin. This finding suggests that the dehydrogenation reaction requires initiation. To test this idea, we added small quantities of coal to mixtures of fluorenone and the hydroaromatic compounds. The acceleration of the reaction by the coal molecules is striking, Figure 3. In the presence of Illinois No. 6 coal, Tetralin and 9,10-dihydroanthracene are as readily dehydrogenated as the reactive sporinities. Thus, the differences in the reactivities of the macerals stem, in part, from the differences in the rates at which the coal molecules undergo decomposition to initiate hydrogen transfer reactions and, in part, from the differences in the quantities of suitably reactive hydroaromatic structural elements.

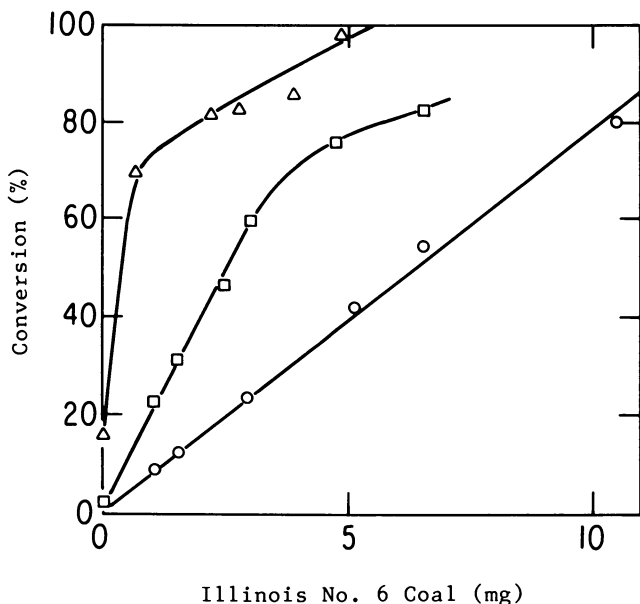


Figure 3. The extent of conversion of fluorenone to fluorene by Illinois No. 6 coal (circles), Tetralin (0.038 mmole) and Illinois No. 6 coal (squares), and dihydroanthracene (0.038 mmole) and Illinois No. 6 coal (triangles).

In summary, the macerals exhibit a broad range of reactivity in their ability to dehydrogenate fluorenone. Even more important, there appears to be a synergism between the structural elements capable of initiating the reaction and those elements capable of undergoing oxidation in the macerals.

Acknowledgment

We are indebted to G.R. Dyrkacz and his collaborators and to R.E. Winans and K.L. Stock for the preparation of the macerals used in this study. The research was supported by the Department of Energy. The whole coal samples were provided by W. Spackman from the Pennsylvania State University Coal Sample Bank.

Literature Cited

1. Whitehurst, D.D.; Mitchell, T.O.; Farcasiu, M. "Coal Liquefaction"; Academic Press: New York, 1980
2. King, H.H.; Stock, L.M. Fuel 1982, 61, 257-264
3. Cronauer, D.C.; McNeil, R.I.; Young, D.C.; Ruberto, R.G. Fuel 1982, 61, 610-9
4. Wilson, M.A.; Collin, P.J.; Barron, P.F.; Vassallo, A.M. Fuel Process. Technol. 1982, 5(3-4), 281-298
5. Skowronski, R.P.; Ratto, J.J.; Goldberg, I.B.; Heredy, L.A. Fuel 1983, 62, 000-000
6. Huang, C.B.; Stock, L.M. Am. Chem. Soc., Div. Fuel Chem., Preprints 1982, 27(3-4), 28-36
7. Peover, M.D. J. Chem. Soc. 1960, 5020-6
8. Mazumdar, B.K.; Choudhury, S.S.; Lahiri, A. Fuel 1960, 39, 179-182
9. Mazumdar, B.K.; Chakrabartty, S.K.; De, N.G.; Ganguly, S.; Lahiri, A. Fuel 1962, 41, 121-8
10. Reggel, L.; Wender, I.; Raymond, R. Fuel 1968, 47, 373-389
11. Raaen, V.F.; Roark, W.H. Fuel 1978, 57, 650-1
12. Whitehurst, D.D.; Mitchell, T.O.; Farcasiu, M. "Coal Liquefaction"; Academic Press: New York, 1980; Chap. 8-9
13. Reggel, L.; Wender, I.; Raymond, R. Fuel 1970, 49, 281-6
14. Dyrkacz, G.R.; Horwitz, E.P. Fuel 1982, 61 3-12
15. Pugmire, R.J.; Woofender, W.T.; Mayne, C.L.; Karas, J.; Grant, D.M. Am. Chem. Soc. Div. Fuel Chem., Preprints 1983, 28(1), 103-117

RECEIVED October 5, 1983

Author Index

- Andrejko, M. J., 21
Bensley, David F., 33
Bloomquist, C. A. A., 65,121
Brenner, Douglas, 47
Choi, Chol-yoo, 157
Cohen, A. D., 21
Crelling, John C., 1,33
Davis, Alan, 99
Dyrkacz, Gary R., 65,121
Gebhard, L. A., 121
Grant, David M., 79
Hayatsu, Ryoichi, 137
Horwitz, E. Philip, 65
Karas, Jirina, 79
Kuehn, Deborah W., 99
Mayne, Charles L., 79
McBeth, Robert, 137
Painter, Paul C., 99
Pugmire, Ronald J., 79
Ruscic, L., 65
Scott, Robert G., 137
Silbernagel, B. G., 121
Stock, Leon M., 157
Winans, Randall E., 1,137
Woolfenden, Warner R., 79

Subject Index

A

- Absorption bands
FTIR
rotated matrix of factor loadings
for components analysis
aliphatic stretching region in
vitrinite, 114t
and volatile matter in
vitrinite, 117t
aromatic out-of-plane bending
region in vitrinite, 115t
calorific value of
vitrinite, 116t
reflectance of vitrinite, 117t
Aldwarke Silkstone, density gradient
separation and carbon-13
NMR, 81-95
Alginite
aromaticities, 12t
reduction of fluorenone, 173t
Alginites, coal PSOC-2, PSOC-858, and
British maceral
concentrates, 83t,85t
Aliphatic absorbing region, in
vitrinite determined by IR
spectroscopy, 54-59
Aliphatic CH₂/CH index, Beluga River
Alaska lignite, 91-92
Aliphatic groups in vitrinite, FTIR
spectral area, 109-10
Aliphatic positions, deuterium-
hydrogen exchange reaction of
tetralin-d₁₂ and
diphenylmethane, 162t,163t
Aliphatic region due to methyls and
ethyls, CP/MAS and dipolar dephas-
ing data, 88f
Aliphatic stretching region in
vitrinite, rotated matrix of
factor loadings for components
analysis of FTIR absorption
bands, 114t
Aliphatic stretching, FTIR of
vitrinite, 103-12
Alkyl phenols, Py-MS, 153f
Analytical analyses of demineralized
coals, density fractions, 71t
Aromatic adjacent hydrogen in
vitrinite, FTIR spectral area vs.
reflectance, 109-13
Aromatic carbons, nonprotonated and
protonated, carbon
resonances, 84,86t
Aromatic character, in vitrinite
determined by IR
spectroscopy, 54-59
Aromatic out-of-plane bending region
in vitrinite, rotated matrix of
factor loadings for components
analysis of FTIR absorption
bands, 115t
Aromatic out-of-plane bending, FTIR of
vitrinite, 103-12
Aromatic positions, deuterium-hydrogen
exchange reaction of tetralin-d₁₂
and diphenylmethane, 162t,163t
Aromatic stretching, FTIR of
vitrinite, 103-12
Aromatic-to-aliphatic ratios,
carbon-13 NMR, 80-95
Aromaticity, 73
characterization, 11,12t
variation with density for
volatile bituminous coals,
73-77

Author Index

- Andrejko, M. J., 21
Bensley, David F., 33
Bloomquist, C. A. A., 65,121
Brenner, Douglas, 47
Choi, Chol-yoo, 157
Cohen, A. D., 21
Crelling, John C., 1,33
Davis, Alan, 99
Dyrkacz, Gary R., 65,121
Gebhard, L. A., 121
Grant, David M., 79
Hayatsu, Ryoichi, 137
Horwitz, E. Philip, 65
Karas, Jirina, 79
Kuehn, Deborah W., 99
Mayne, Charles L., 79
McBeth, Robert, 137
Painter, Paul C., 99
Pugmire, Ronald J., 79
Ruscic, L., 65
Scott, Robert G., 137
Silbernagel, B. G., 121
Stock, Leon M., 157
Winans, Randall E., 1,137
Woolfenden, Warner R., 79

Subject Index

- A
- Absorption bands
FTIR
rotated matrix of factor loadings
for components analysis
aliphatic stretching region in
vitrinite, 114t
and volatile matter in
vitrinite, 117t
aromatic out-of-plane bending
region in vitrinite, 115t
calorific value of
vitrinite, 116t
reflectance of vitrinite, 117t
Aldwarke Silkstone, density gradient
separation and carbon-13
NMR, 81-95
Alginite
aromaticities, 12t
reduction of fluorenone, 173t
Alginites, coal PSOC-2, PSOC-858, and
British maceral
concentrates, 83t,85t
Aliphatic absorbing region, in
vitrinite determined by IR
spectroscopy, 54-59
Aliphatic CH₂/CH index, Beluga River
Alaska lignite, 91-92
Aliphatic groups in vitrinite, FTIR
spectral area, 109-10
Aliphatic positions, deuterium-
hydrogen exchange reaction of
tetralin-d₁₂ and
diphenylmethane, 162t,163t
Aliphatic region due to methyls and
ethyls, CP/MAS and dipolar dephas-
ing data, 88f
Aliphatic stretching region in
vitrinite, rotated matrix of
factor loadings for components
analysis of FTIR absorption
bands, 114t
Aliphatic stretching, FTIR of
vitrinite, 103-12
Alkyl phenols, Py-MS, 153f
Analytical analyses of demineralized
coals, density fractions, 71t
Aromatic adjacent hydrogen in
vitrinite, FTIR spectral area vs.
reflectance, 109-13
Aromatic carbons, nonprotonated and
protonated, carbon
resonances, 84,86t
Aromatic character, in vitrinite
determined by IR
spectroscopy, 54-59
Aromatic out-of-plane bending region
in vitrinite, rotated matrix of
factor loadings for components
analysis of FTIR absorption
bands, 115t
Aromatic out-of-plane bending, FTIR of
vitrinite, 103-12
Aromatic positions, deuterium-hydrogen
exchange reaction of tetralin-d₁₂
and diphenylmethane, 162t,163t
Aromatic stretching, FTIR of
vitrinite, 103-12
Aromatic-to-aliphatic ratios,
carbon-13 NMR, 80-95
Aromaticity, 73
characterization, 11,12t
variation with density for
volatile bituminous coals,
73-77

Ash

content of vitrinites, exinites and inertinites, 140t

content of density fractions of demineralized coals, 71

Atomic ratios analyses of demineralized coals, density fractions, 71t

Atomic ratios with density, variation, volatile bituminous coals, 73-77

B

Beluga River Alaska lignite, 91-92

Benzophenone and Illinois No. 6 coal to diphenylmethane, 168

Benzyl carbons, pyridinium salts, 150

Benzyl positions, deuterium-hydrogen exchange reaction of tetralin-d₁₂ and diphenylmethane, 162t,163t

Birefringent organics in peat, 22,23,27f,29f

Bituminous coal

deuterium-hydrogen exchange reaction of tetralin-d₁₂ and diphenylmethane, 162t

high-volatile, distribution of hydrogen deficiency and heteroatoms, 138

volatile, variation of atomic ratios with density, 73-77

Bituminous coal macerals, distribution of organic sulfur, 14t

Bituminous rank, Elkhorn No. 3 seam Eastern Kentucky-hvA, photomicrographs, 6f-7f

Blue-light photomicrographs of lip-tinite macerals, 35,37f

Brazil block coal seam, spectral parameters of fluorescence spectra, 41t

Brazil Block Seam sporinite and vitrinite, gel permeation chromatograms for methylated oxidation products from, 153f

Brazil block Seam sporinite mass spectrum, 142d,142f

Brazil block batch vacuum pyrolysis yields, 149t reflectance and maceral content, 35-44

BTU analyses--See Heating value analyses

C

Calorific value of vitrinite, 116

rotated matrix of factor loadings for components analysis of FTIR absorption bands, 116t

Calorific value, vitrinite concentrates, 102t,108t

Carbon

coal PSOC-2, PSOC-858, and British maceral concentrates, 83t,85t

content of density fractions of demineralized coals, 71

vitrinite concentrates, 102t,108t

Carbon content of preinertinites, prephlobaphenites (and precorcollinites), and presclerotinites, 23-30

Carbon content of vitrinites, exinites and inertinites, 140t

Carbon radical densities, 132-34

Carbon radicals, determination of g-values, linewidths, radical densities and saturation properties of carbon radicals, 121-34

Carbon-13 cross-polarization/magic angle sample spinning nuclear magnetic resonance spectroscopy, multiple pulse techniques, 79-95

Carbons

benzyl, pyridinium salts, 150 nonprotonated and protonated, carbon resonances, 84,86t

Carboxylic acid peak, in vitrinite determined by IR spectroscopy, 54-59

Chain fern, microtome section, 30f

Char, batch vacuum pyrolysis

yields, 149t

Characterization

aromaticity, 11,12t

direct techniques, 14

electron spin resonance, 11,13

free radicals, 11,13

gas chromatography, 13

mass spectrometry, 13

organic structural analysis, 13

overview, 9-15

pyrolysis, 13

solid ¹³C NMR, 11,12t

Coal, rank, and maceral content, 2-3

Coalification value of vitrinite, 116

Color determination, content of peats, 23-30

Conversion processes, reactivity of macerals, 15

Corporcollinites, premaceral

contents, 28,30f

Cutinite

classification and origin, 4

coal PSOC-2, PSOC-858, and British maceral concentrates, 83t,85t

determined by fluorescence, 35-44

Cutinite content, PSOC-828 and

PSOC-1103, 161t

D

- Decalin
 dehydrogenation by
 fluorenone, 165t,173t
 reduction of fluorenone, 173t
 Dehydrogenation of hydrogen donors by
 fluorenone, 165t,173t
 Demineralized coal, density fractions,
 analytical and maceral
 analyses, 71-77
 Demineralized vitrinite and fusinite,
 deuterium-hydrogen exchange reac-
 tion of tetralin-d₁₂ and
 diphenylmethane, 162t
 Densities, carbon radical, 132-34
 Density fractions of demineralized
 coals, analytical and maceral
 analyses, 71-77
 Density gradient centrifugation of
 small coal particles in aqueous
 CsCl density gradient, 124-27
 Density gradient centrifugation
 separation, float-sink
 technique, 137-40
 Density gradient centrifugation,
 separation, 81-84
 Density gradient separation, 65-77
 Density variation, separation, 8-9
 Density, variation of atomic ratios
 with, 73-77
 Derivative spectroscopy, FTIR of
 vitrinite, 103-12
 Desmocollinite, classification, 4
 9,10-Dihydroanthracene
 dehydrogenation by
 fluorenone, 165t,173t
 reduction of fluorenone, 173t
 9,10-Dihydrophenanthrene
 dehydrogenation by
 fluorenone, 165t,173t
 reduction of fluorenone, 173t
 5,12-Dihydrotetracene
 dehydrogenation by
 fluorenone, 165t,173t
 reduction of fluorenone, 173t
 Dioxide, sporinites total ion
 current, 144t
 Diphenylmethane, hydrogen atom trans-
 fer reactions, 157-63
 Dipolar dephasing, carbon-13 NMR, 79

E

- Electron spin resonance of exinite,
 vitrinite, and inertinite,
 determination of g-values,
 linewidths, radical densities and
 saturation properties of carbon
 radicals, 121-34

- Electron spin resonance,
 characterization, 11,13
 Elemental analyses of demineralized
 coals, density fractions, 71t
 Elemental analysis, coal PSOC-2,
 PSOC-858, and British maceral
 concentrates, 83t,85t
 Elkhorn No. 3 seam Eastern
 Kentucky-hvA bituminous rank,
 photomicrographs, 6f,7f
 ESR absorption signal, explanation of
 intensity, 123
 ESR spectrum, explanation of width and
 shape, 123
 Ethyl groups in vitrinite, FTIR
 analysis, 110f
 Ethyl peak, in vitrinite determined by
 IR spectroscopy, 54-59
 Ethyls, aliphatic region due to,
 CP/MAS and dipolar dephasing
 data, 88f
 Exinite content, PSOC-828 and
 PSOC-1103, 161t
 Exinite
 analytical and maceral analysis
 of density fractions, 71t
 batch vacuum pyrolysis yields, 149t
 CP/MAS spectra, 86f
 determination of g-values,
 linewidths, radical densities
 and saturation properties of
 carbon radicals, 121-34
 fractograms for preparative DGC
 separation, 82f
 H/C and ring index values of coal
 macerals in PSOC-106, 73-77
 sporinite-rich, reduction of
 fluorenone, 173t
 Exinites
 elemental analysis, 140t
 N/C, 132f

F

- Float-sink technique, density gradient
 centrifugation separation, 137-40
 Fluorenone, reduction, hydrogen atom
 transfer reactions, 163-74
 Fluorescence spectra, of coal
 macerals, 33-44
 Fluorescence, root of woodwardia, 30f
 Fluorinite, white-light and fluores-
 cent light petrographic
 analyses, 35-44
 Fractions, density, analyses of
 demineralized coals, 71t
 Free radicals, characterization, 11,13
 FTIR spectra, selected parameters of
 coalification and organic struc-
 ture of vitrinite, 99-119

FTIR spectral area vs reflectance, for aromatic adjacent hydrogen in vitrinite, 109-13

FTIR spectral area, aliphatic groups in vitrinite, 109-10

Functional group analysis of vitrinite, FTIR, 99-119

Functional groups, in vitrinite determined by IR spectroscopy, 54-59

Fusinite

- aromaticities, 12t
- classification and origin, 5
- Elkhorn No. 3 seam Eastern Kentucky coal, 6f,7f
- Illinois No. 2, mass spectrum, 144f
- in coal samples, 91
- liquefaction, 15,16t
- PSOC-828 and PSOC-1103, 161t
- reduction of fluorenone, 173t
- white-light and fluorescent light petrographic analyses, 35-44

G

g-value, resonance, definition, 122

Gas chromatograms, vacuum pyrolysis tars, 148f

Gas chromatography mass spectrometry, distribution of hydrogen deficiency and heteroatoms, 138

Gas chromatography, characterization, 13

GC microwave plasma emission spectroscopy, distribution of hydrogen deficiency and heteroatoms, 138

Gel permeation chromatograms for methylated oxidation products, Brazil Block Seam sporinite and vitrinite and the Upper Elkhorn Seam inertinite, 153f

Georgia nymphaea peat, colors, 23-28

H

Heating value analyses, of peats, 22,28,31f

Herrin, reflectance and maceral content, 35-44

Hiawatha King 6 mine hvB bituminous coal, deuterium-hydrogen exchange reaction of tetralin-d₁₂ and diphenylmethane, 162t

Hiawatha King, reduction of fluorenone to fluorene, 166t

Hiawatha, reflectance and maceral content, 35-44

Hydrocarbons, sporinites total ion current, 144t

Hydrogen

- coal PSOC-2, PSOC-858, and British maceral concentrates, 83t,85t
- content of density fractions of demineralized coals, 71
- content of peats, 23-30
- vitrinite concentrates, 102t,108t

Hydrogen atom transfer reactions, tetralin-d₁₂ and diphenylmethane and reduction of fluorenone, 157-63

Hydrogen content of vitrinites, exinites and inertinites, 140t

Hydrogen deficiency and heteroatoms, distribution, 138

Hydrogen donors, dehydrogenation, by fluorenone, 165t,173t

Hydrogen in vitrinite, FTIR spectral area vs reflectance, 109-13

Hydrogen/carbon ratios, variation with density for volatile bituminous coals, 73-77

Hydroxyl peak, in vitrinite determined by IR spectroscopy, 54-59

I

Illinois basin coal, maceral content determined by fluorescence microscopy, 35-44

Illinois No. 2

- batch vacuum pyrolysis yields, 149t
- reduction of fluorenone to fluorene, 166t

Illinois No. 2 fusinite, mass spectrum, 144f

Illinois No. 2 hvC bituminous coal, deuterium-hydrogen exchange reaction of tetralin-d₁₂ and diphenylmethane, 162t

Illinois No. 6 coal

- IR spectroscopy
- liptinite in, 51-64
- vitrinite in, 51-64

Indiana Brazil Block seam hvC bituminous coal, deuterium-hydrogen exchange reaction of tetralin-d₁₂ and diphenylmethane, 163t

Indiana No. 1 Block Seam hvB bituminous coal, deuterium-hydrogen exchange reaction of tetralin-d₁₂ and diphenylmethane, 162t

Inertinite

- analytical and maceral analysis of density fractions, 71t
- aromaticities, 12t
- batch vacuum pyrolysis yields, 149t

Inertinite--Continued

- CP/MAS spectra, 86f
determination of g-values,
linewidths, radical densities
and saturation properties of
carbon radicals, 121-34
fractograms for preparative DGC
separation, 82f
H/C and ring index values of coal
macerals in PSOC-106, 73-77
PSOC-828 and PSOC-1103, 161t
semifusinite-rich, reduction of
fluorenone, 173t
Upper Elkhorn Seam, gel permeation
chromatograms for methylated
oxidation products form, 153f
- Inertinites**
elemental analysis, 140t
liquefaction, 15,16t
premaceral contents, 28,30f
- Inertinite macerals**
classification and origin, 5
elkhorn No. 3 seam Eastern Kentucky
coal, 6f,7f
- Inertinite radical densities, 133f**
- Inertodetrinite, PSOC-828 and
PSOC-1103, 161t**
- Iodine and pyridine to pyridinium,
maceral reaction, 138**
- IR analysis, Fourier transform,
organic structure of
vitrinite, 99-119**
- IR spectroscopy**
intensity of radiation transmitted
for various sample
thicknesses, 61,62f
preparation of samples, 49-51
- Isopycnic density gradient centrifuga-
tion of small coal particles in
aqueous CsCl density
gradient, 124-27**

K

- Kentucky Upper Elkhorn No. 3 seam hvA
bituminous coal, deuterium-
hydrogen exchange reaction of
tetralin-d₁₂ and
diphenylmethane, 163t**
- Ketone reduction, 164**

L

- Liptinite**
aromaticities, 12t
in Illinois No. 6 coal, IR
spectroscopy, 51-64
- Liptinites, coal PSOC-2, PSOC-858, and
British maceral
concentrates, 83t,85t**

Liptinite macerals

- blue-light photomicrographs, 35,37f
classification and origin, 4
determined by fluorescence, 35-44
white-light photomicrographs, 35,36f
Liquefaction of inertinites, 15,16t
Lower Kittanning seam, vitrinite
functional group analysis by
FTIR, 99-119

M

- Maceral reaction with pyridine and
iodine to pyridinium, 138**
- Macerals, definition, 1-2**
- Macrinite**
classification and origin, 5
in coal samples, 91
- Magic/angle sample spinning nuclear
magnetic resonance spectroscopy,
multiple pulse techniques, 79-95**
- Markham Main, density gradient separa-
tion and carbon-13 NMR, 81-95**
- Mass spectrometry**
characterization, 13
gas chromatography, distribution of
hydrogen deficiency and
heteroatoms, 138
- Mass spectrometry and vacuum
pyrolysis, 137-46**
- Mass spectrum**
Brazil block seam sporinite, 142f
Illinois No. 2 fusinite, 144f
- Methines, dephasing carbon-13 NMR, 84**
- Methyl groups in vitrinite, FTIR
analysis, 110f**
- Methyl index, Beluga River Alaska
lignite, 91-92**
- Methyl peak, in vitrinite determined
by IR spectroscopy, 54-59**
- Methylated oxidation products, Brazil
Block Seam sporinite and vitrinite
and the Upper Elkhorn Seam
inertinite, 153f**
- Methylenes, dephasing carbon-13
NMR, 84**
- Methyls, aliphatic region due to,
CP/MAS and dipolar dephasing
data, 88f**
- Micrinite**
aromaticities, 12t
in coal samples, 91
PSOC-828 and PSOC-1103, 161t
white-light and fluorescent light
petrographic analyses, 35-44
- Microscopic analysis of microtome thin
sections, of peat, 21-27**
- Microtome thin sections of peat,
microscopic analysis, 21-27**

Microwave plasma emission spectroscopy, distribution of hydrogen deficiency and heteroatoms, 138
 Microwave saturation properties, various maceral types, 130f
 Mineral matter content of coal before demineralization, coal PSOC-2, PSOC-858, and British maceral concentrates, 83t,85t
 Minnesota sphagnum peat, colors, 23-28
 Moisture, vitrinite concentrates, 102t,108t
 Multiple pulse techniques, carbon-13 cross-polarization/magic angle sample spinning nuclear magnetic resonance spectroscopy, 79-95

N

N/C for exinites, 132f
 Nitrogen
 coal PSOC-2, PSOC-858, and British maceral concentrates, 83t,85t
 content of density fractions of demineralized coals, 71
 Nitrogen content of vitrinites, exinites and inertinites, 140t
 Nitrogen oxide, sporinites total ion current, 144t
 NMR, solid ¹³C,
 characterization, 11,12t
 North Celymen, density gradient separation and carbon-13 NMR, 81-95
 Nuclear magnetic resonance spectroscopy, multiple pulse techniques, 79-95
 Nymphaea peat, Georgia, colors, 23-28

O

O/C variations for vitrinites, 131f
 1,2,3,4,5,6,7,8-Octahydroanthracene dehydrogenation by
 fluorenone, 165t,173t
 reduction of fluorenone, 173t
 Optical diagram, of
 microspectrophotometer, 52f
 Organic structural analysis,
 characterization, 13
 Organic structure of vitrinite, and selected parameters of coalification by FTIR spectra, 99-119
 Overview, separations, 5,8-9
 Oxidation products, Brazil Block Seam sporinite and vitrinite and the Upper Elkhorn Seam
 inertinite, 153f
 Oxides, sporinites total ion current, 144t

Oxygen

 coal PSOC-2, PSOC-858, and British maceral concentrates, 83t,85t
 content of density fractions of demineralized coals, 71
 content of peats, 23-30
 Oxygen content of vitrinites, exinites and inertinites, 140t
 Oxygen-containing functional groups, in vitrinite determined by IR spectroscopy, 54-59
 Oxygen/carbon ratios, variation with density for volatile bituminous coals, 73-77

P

Peats

 premaceral contents, 21-28
 proximate analyses, 22,28,31f
 ultimate analyses, 22,28,31f
 Petrographic analysis of maceral concentrates, PSOC-828 and PSOC-1103 coals, 161t
 Petrographic characterization, 3-5
 Phenols
 alkyl, Py-MS, 153f
 in vitrinite determined by IR spectroscopy, 54-59
 Phlobaphenites, premaceral contents, 28,30f
 Premaceral contents of peats, 21-28
 Previtrinite contents, correlated with volatile matter contents of peats, 23-30
 Proton decoupling, dephasing carbon-13 NMR, 84
 Proximate analyses of demineralized coals, density fractions, 71t
 Proximate analyses, of
 peats, 22,28,31f
 Pseudovitrinite
 Elkhorn No. 3 seam Eastern Kentucky coal, 6f,7f
 white-light and fluorescent light petrographic analyses, 35-44
 PSOC-106, -297, -1103, -828, reduction of fluorenone to fluorene, 166t
 PSOC-1103 coal, petrographic analysis of macerals concentrates, 161t
 PSOC-2 and PSOC-858, fractograms for preparative DGC separation, 82f
 PSOC-828 coal, petrographic analysis of maceral concentrates, 161t
 Py-MS, peaks, sporinite, 143t
 Pyridine and iodine to pyridinium, maceral reaction with, 138
 Pyridinium salts, benzylic carbons, 150
 Pyridinium, iodine and pyridine to, maceral reaction, 138

Pyrolysis, characterization, 13
 Pyrolysis-mass spectrometry and vacuum
 pyrolysis, 137-46

R

Rank of coal, and maceral content, 2-3
 Reactivity of macerals, conversion
 processes, 15
 Red/green quotient,
 fluorescence, 35,41t
 Reduction of fluorenone, hydrogen atom
 transfer reactions, 163-74
 Reflectance
 vitrinite, coal PSOC-2, PSOC-858,
 and British maceral
 concentrates, 83t,85t
 white-light and fluorescent light
 petrographic analyses, 35-44
 Reflectance in oil, vitrinite
 concentrates, 102t,108t
 Reflectance of vitrinite, rotated
 matrix of factor loadings for com-
 ponents analysis of FTIR absorp-
 tion bands, 117t
 Reflectance vs FTIR spectral area, for
 aromatic adjacent hydrogen in
 vitrinite, 109-13
 Resinite
 coal PSOC-2, PSOC-858, and British
 maceral concentrates, 83t,85t
 determined by fluorescence, 35-44
 reduction of fluorenone, 173t
 Resinite content, PSOC-828 and
 PSOC-1103, 161t
 Resinite macerals, classification and
 origin,4-5
 Resonance g-value, definition, 122
 Ring index, 73
 variation with density for volatile
 bituminous coals, 73-77
 Ring protonation index, Beluga River
 Alaska lignite, 91-92

S

Saturation behavior of carbon
 radical, 123-24
 Sclerotinites, premaceral
 contents, 28,30f
 Semifusinite
 classification and origin, 5
 Elkhorn No. 3 seam Eastern Kentucky
 coal, 6f,7f
 in coal samples, 91
 liquefaction, 15,16t
 PSOC-828 and PSOC-1103, 161t
 white-light and fluorescent light
 petrographic analyses, 35-44
 Semifusinite-rich inertinite, reduc-
 tion of fluorenone, 173t

Semimacrinite, classification and
 origin, 5

Separation

density gradient
 centrifugation, 81-84
 density gradient, 65-77
 density variation, 8-9
 Separations, overview, 5,8-9
 Solid ¹³C NMR,
 characterization, 11,12t
 Spectra, fluorescence, of coal
 macerals, 33-44
 Spectrophotometer, micro, optical
 diagram, 52f
 Spectroscopy, IR, Fourier transform,
 organic structure of
 vitrinite, 99-119
 Sphagnum peat, Minnesota,
 colors, 23-28
 Sporinite
 aromaticities, 12t
 Brazil block seam sporinite, mass
 spectrum, 142f
 Brazil Block Seam, gel permeation
 chromatograms for methylated
 oxidation products from, 153f
 classification and origin, 4
 CP/MAS spectra, 86f
 determined by fluorescence, 35-44
 fractograms for preparative DGC
 separation, 82f
 peaks from Py-MS, 143t
 Sporinite content, PSOC-828 and
 PSOC-1103, 161t
 Sporinite-rich exinite, reduction of
 fluorenone, 173t
 Sporinites total ion current, 146t
 Structural parameters of coals and
 coal macerals, 89t,90t
 Sulfides, sporinites total ion current
 sorted by Z number and heteroatoms
 contents, 144t
 Sulfur compound distribution,
 Py-MS, 148f
 Sulfur content of vitrinites, exinites
 and inertinites, 140t
 Sulfur
 coal PSOC-2, PSOC-858, and British
 maceral concentrates, 83t,85t
 content of density fractions of
 demineralized coals, 71
 distribution of organic, bituminous
 coal macerals, 14t

T

Tar, batch vacuum pyrolysis
 yields, 149t
 Telecollinite, classification, 4

1,2,3,4-Tetrahydroquinoline
 dehydrogenation by
 fluorenone, 165t,173t
 reduction of fluorenone, 173t

Tetralin
 dehydrogenation by
 fluorenone, 165t,173t
 reduction of fluorenone, 173t

Tetralin-d₁₂, hydrogen atom transfer
 reactions, 157-63

Terversal Dunsill, density gradient
 separation and carbon-13
 NMR, 81-95

Thicknesses, IR spectroscopy intensity
 of radiation transmitted for
 various, 61,62f

Trioxide, sporinites total ion
 current, 144t

Two dimensional, carbon-13 NMR, 79

U

Ultimate analyses of demineralized
 coals, density fractions, 71t

Ultimate analyses of peats, 22,28,31f

Upper Elkhorn Seam inertinite, gel
 permeation chromatograms for
 methylated oxidation products
 from, 153f

Upper Elkhorn, batch vacuum pyrolysis
 yields, 149t

V

Vacuum pyrolysis and pyrolysis-mass
 spectrometry, 137-46

van Krevelen plot, distribution for
 three main maceral groups, 9,10f

Vitrinite macerals, classification, 4

Vitrinite radical densities, 133f

Vitrinite reflectance, coal PSOC-2,
 PSOC-858, and British maceral
 concentrates, 83t,85t

Vitrinite
 aliphatic groups, 109-10
 analytical and maceral analysis of
 density fractions, 71t
 aromatic adjacent hydrogen in, FTIR
 spectral area vs
 reflectance, 109-13
 aromaticities, 12t

Vitrinite--Continued
 batch vacuum pyrolysis yields, 149t
 CP/MAS spectra, 86f
 determination of g-values,
 linewidths, radical densities
 and saturation properties of
 carbon radicals, 121-34

Elkhorn No. 3 seam Eastern Kentucky
 coal, 6f,7f

fractograms for preparative DGC
 separation, 82f

H/C and ring index values of coal
 macerals in PSOC-106, 73-77

in Illinois No. 6 coal, IR
 spectroscopy, 51-64

organic structure, and selected
 parameters of coalification by
 FTIR spectra, 99-119

PSOC-828 and PSOC-1103, 161t
 reduction of fluorenone, 173t

Vitrinites
 elemental analysis, 140t
 O/C variations, 131f

Volatile bituminous coals, variation
 of atomic ratios with
 density, 73-77

Volatile matter in vitrinite, rotated
 matrix of factor loadings for com-
 ponents analysis of FTIR absorp-
 tion bands, 117t

Volatile matter
 content of peats, 23-30
 vitrinite concentrates, 102t,108t

Volatiles, batch vacuum pyrolysis
 yields, 149t

W

White-light photomicrographs, of
 liptinite macerals, 35,36f

Woodwardiavirginica, microtome
 section, 30f

Woolley Wheatley Lime, density
 gradient separation and carbon-13
 NMR, 81-95

Z

Z number and heteroatom content,
 sporinites total ion current, 144t